

ICT-Emissions

Deliverable D.3.2.1: Report on the Development and Use of the Vehicle Energy/Emission Simulator

SEVENTH FRAMEWORK PROGRAMME

FP7-ICT-2011-7

COLLABORATIVE PROJECT – GRANT AGREEMENT N°: 288568

Deliverable number (D.3.2.1)

Version number: 1.3

Author(s): Christian Vock¹, Johannes Hubel¹, Dimitrios Tsokolis², Christos Samaras², Leonidas Ntziachristos², Robert Tola³, Claudio Ricci³, and Zissis Samaras²

Author'(s) affiliation (Partner short name): ¹AVL, ²LAT/AUTH, ³CRF



Document Control Page

Title	Report on the development and use of the vehicle energy/emission simulator.		
Creator	Christian Vock		
Editor	Christian Vock		
Brief Description	Description of how the models for the micro energy and emission simulator have been produced and perform and how the macro energy and emission modelling has been adapted to the needs of this project.		
Publisher	ICT-EMISSIONS Consortium		
Contributors	Christian Vock, Johannes Hubel, Dimitrios Tsokolis, Christos Samaras, Leonidas Ntziachristos, Robert Tola, Claudio Ricci, and Zissis Samaras		
Type (Deliverable/Milestone)	Deliverable		
Format	Report		
Creation date	24 July 2013		
Version number	1.3		
Version date	November 20, 2014		
Last modified by			
Rights	Copyright "ICT-EMISSIONS Consortium". During the drafting process, access is generally limited to the ICT-EMISSIONS Partners.		
Audience	<input type="checkbox"/> internal <input checked="" type="checkbox"/> public <input type="checkbox"/> restricted, access granted to: EU Commission		
Action requested	<input type="checkbox"/> to be revised by Partners involved in the preparation of the deliverable <input type="checkbox"/> for approval of the WP Manager <input type="checkbox"/> for approval of the Internal Reviewer (if required) <input type="checkbox"/> for approval of the Project Co-ordinator		
Deadline for approval			
Version	Date	Modified by	Comments

0.1	July 24, 2013	Christian Vock	Structure and TOC
0.2	Sept 17, 2013	Johannes Hubel	Advanced vehicle modes
0.3	Oct 9, 2013	Leonidas Ntziachristos	Conventional models and macro
0.4	October 23, 2013	Christian Vock	Final version
1.0	November 4, 2013	Zissis Samaras	Final approval
1.1	January 7, 2014	Christian Vock	Update Advanced Vehicles
1.2	February 27, 2014	Christian Vock, Christos Samaras, Leonidas Ntziachristos	Turin validation of macro model and Prius III plugin
1.2b	October 30, 2014	Dimitris Tsokolis and Leonidas Ntziachristos	WLTP/NEDC experience included. Turin and Rome real world validation
1.3	November 20, 2014	Zissis Samaras	Final approval

Contents

EXECUTIVE SUMMARY	x
Background	x
Methods and Results	xi
1 Micro Emission Models	1
1.1. General Considerations	1
1.2. Conventional vehicles	1
1.2.1. Collection of Vehicle Characteristics	4
1.3. Advanced vehicles	14
1.3.1. Operating Strategies	14
1.3.2. Hybrid Topologies	19
1.3.3. Vehicle Models	20
2 Macro Emission Models	61
2.1. General considerations	61
2.2. Validation of the macro emission approach	61
2.2.1. General scheme followed	61
2.2.2. Traffic conditions used for the validation	63
2.2.3. COPERT calculations	65
2.2.4. Comparison with measured values	66
2.2.5. Micro simulations	68
2.3. Results of the validation exercise	69
2.3.1. Turin traffic data – gasoline vehicle	69
2.3.2. Turin traffic data – diesel vehicle	71
2.3.3. Madrid traffic data – gasoline vehicle	72
2.3.4. Madrid traffic data – diesel vehicle	74
2.3.5. Extra case study – Turin traffic data (diesel vehicle)	74
2.4. Discussion	80
3 Model validation by chassis dynamometer measurements	83
3.1. Introduction	83
3.2. Vehicle validation	83
3.3. Results of Validation	86
3.3.1. Peugeot 308 NEDC	87

3.3.2. Peugeot 308 Artemis Road.....	88
3.3.3. BMW X1 NEDC	89
3.3.4. BMW X1 Artemis Road.....	90
3.3.5. Volkswagen Golf NEDC.....	91
3.3.6. Volkswagen Golf Artemis Road	92
3.3.7. Toyota Avensis NEDC	93
3.3.8. Toyota Avensis Artemis Road.....	94
3.3.9. Toyota Prius III Plugin	95
3.4. Overall Picture of Chassis Dynamometer Validation Results	102
4 Model validation by real-world on-board measurements.....	103
4.1. Introduction.....	103
4.1.1. Vehicles.....	103
4.1.2. Measurement Locations	104
4.2. On Board Measurements.....	105
4.2.1. Vehicle 1 - Fiat Punto 1.3 Diesel.....	106
4.2.2. Vehicle 2 - Fiat Punto 1.3 Gasoline.....	107
References	109
Abbreviations.....	110

List of tables

Table 1: Essential specifications for the fuel consumption modelling in AVL CRUISE.	5
Table 2: Mini cars (A') registrations and weighted-average specifications.	6
Table 3: Small cars (B') registrations and weighted average specifications.	6
Table 4: Medium cars (C') registrations and weighted average specifications.	7
Table 5: Executive cars (D') registrations and weighted average specifications.	7
Table 6: Jeeps and SUVs (E') registrations and weighted average specifications.	8
Table 7: Vehicle specifications for Tier 2 vehicles (10 bins).	9
Table 8: Overview Advanced Vehicle Models.	21
Table 9: Calculated traffic characteristics from Turin measurements.	64
Table 10: Calculated traffic characteristics from Madrid M30 highway simulation.	64
Table 11: FIAT Punto 1.2 gasoline specifications.	103
Table 12: FIAT Punto 1.3 diesel specifications.	104

List of figures

Figure 1: Vehicle segments selected for the micro simulation of conventional vehicles.	2
Figure 2: Evolution of CO ₂ emissions from new passenger cars [2].	3
Figure 3: Schematic of the structure of the 30 conventional vehicle micro-models.	4
Figure 4: AVL CRUISE model for a front wheel drive conventional vehicle.	5
Figure 5: Generic petrol and diesel full load curves.	8
Figure 6: Simulation and segment average CO ₂ emissions for petrol vehicles (work is still in progress, revised numbers may be expected).	11
Figure 7: Simulation and segment average CO ₂ emissions for diesel vehicles (work is still in progress, revised numbers may be expected).	12
Figure 8: Cumulative CO ₂ difference between three Tiers of diesel executive vehicles.	13
Figure 9: CO ₂ emissions for the (left) petrol and (right) diesel vehicles over the NEDC.	13
Figure 10: Operating Strategy – Start & Stop.	14
Figure 11: Operating Strategy – E-Drive.	15
Figure 12: Operating Strategy – Load Point Moving.	16
Figure 13: Operating Strategy – Engine Alone.	16
Figure 14: Operating Strategy – E-Boost.	17
Figure 15: Operating Strategy – Regenerative Braking.	18
Figure 16: Operating Strategy – Range Extender Operation – Optimum Operating Line.	18
Figure 17: Operating Strategy – Battery Assistance.	19
Figure 18: Operating Strategies used in different Hybrid Topologies.	20
Figure 19: Coverage of advanced vehicles within possible combinations of vehicle segment and hybrid topology.	22
Figure 20: Hybrid Topology – Mitsubishi iMieV.	22
Figure 21: AVL CRUISE Model Mitsubishi iMieV.	23
Figure 22: EV Control Logic Mitsubishi iMieV.	24
Figure 23: Simulation Input Data Mitsubishi iMieV.	24
Figure 24: Validation Result Mitsubishi iMieV.	25
Figure 25: Hybrid Topology – SMART Fortwo Coupe 52kW mhd.	25
Figure 26: AVL CRUISE Model SMART Fortwo Coupe 52kW mhd.	26
Figure 27: Simulation Input Data SMART Fortwo Coupe 52kW mhd.	26
Figure 28: Validation Result SMART Fortwo Coupe 52kW mhd.	27
Figure 29: Hybrid Topology – Audi A1 etron.	27
Figure 30: AVL CRUISE Model Audi A1 etron.	28
Figure 31: Simulation Input Data Audi A1 etron.	29
Figure 32: Simulation model validation results Audi A1 etron.	30
Figure 33: Hybrid Topology – Audi A3 1.4 TFSI.	30
Figure 34: AVL CRUISE Model Audi A3 1.4 TFSI.	31

Figure 35: Simulation Input Data Audi A3 1.4 TFSI	32
Figure 36: Validation Result Audi A3 1.4 TFSI	32
Figure 37: Hybrid Topology – BMW 116i.....	33
Figure 38: AVL CRUISE Model BMW 116i.....	33
Figure 39: Simulation Input Data BMW 116i.....	34
Figure 40: Validation Result BMW 116i	34
Figure 41: Hybrid Topology – Honda Civic Hybrid.....	35
Figure 42: AVL CRUISE Model Honda Civic Hybrid including HCU control logic	36
Figure 43: Simulation Input Data Honda Civic Hybrid.....	36
Figure 44: Validation Result Honda Civic Hybrid	37
Figure 45: Hybrid Topology – Toyota Prius III	37
Figure 46: AVL CRUISE Model including Hybrid Control Logic of Toyota Prius III	38
Figure 47: Simulation Input Data Toyota Prius III	39
Figure 48: Validation Results Toyota Prius III.....	39
Figure 49: Hybrid Topology – Volvo C30 T5.....	40
Figure 50: AVL CRUISE Model Volvo C30 T5.....	41
Figure 51: Simulation Input Data Volvo C30 T5.....	41
Figure 52: Validation Result Volvo C30 T5	42
Figure 53: Hybrid Topology – VW Golf 1.4L TSI.....	42
Figure 54: AVL CRUISE Model VW Golf 1.4L TSI.....	43
Figure 55: Simulation Input Data VW Golf 1.4L TSI.....	43
Figure 56: Validation Result VW Golf 1.4L TSI	44
Figure 57: Hybrid Topology – Volvo S60 D5.....	44
Figure 58: AVL CRUISE Model Volvo S60 D5.....	45
Figure 59: Simulation Input Data Volvo S60 D5	45
Figure 60: Model Validation Volvo S60 D5	46
Figure 61: Hybrid Topology – Audi A6 3.0L TFSI quattro	46
Figure 62: AVL CRUISE Model Audi A6 3.0L TFSI quattro	47
Figure 63: Simulation Input Data Audi A6 3.0L TFSI quattro	47
Figure 64: Validation Result Audi A6 3.0L TFSI quattro	48
Figure 65: Hybrid Topology – Fisker Karma	48
Figure 66: AVL CRUISE Model Fisker Karma	49
Figure 67: AVL CRUISE HCU Model Fisker Karma.....	49
Figure 68: Simulation Input Data Fisker Karma	50
Figure 69: Validation Results Vehicle Fisker Karma.....	50
Figure 70: Hybrid Topology – Mercedes Benz S400 Hybrid.....	51
Figure 71: AVL CRUISE Model Mercedes Benz S400 Hybrid	52
Figure 72: Hybrid Control Logic implemented in AVL CRUSIE.....	52
Figure 73: Simulation Input Data Mercedes Benz S400 Hybrid	53
Figure 74: Validation Results Mercedes Benz S400 Hybrid	53
Figure 75: Hybrid Topology – BMW X1 2.0d sDrive	54
Figure 76: AVL CRUISE Model BMW X1 2.0d sDrive	55
Figure 77: Simulation Input Data BMW X1 2.0d sDrive	55
Figure 78: Validation Results BMW X1 2.0d sDrive.....	56
Figure 79: Hybrid Topology – Nissan Pathfinder 3.5L CVT	56
Figure 80: AVL CRUISE Model Nissan Pathfinder 3.5L CVT	57
Figure 81: Simulation Input Data Nissan Pathfinder 3.5L CVT	58
Figure 82: Validation Results Nissan Pathfinder 3.5L CVT.....	58
Figure 83: CRUISE Model validation results.....	59
Figure 84: Summary of simulation results.....	60
Figure 85: Flowchart of fuel consumption comparison.....	62

Figure 86: Schematic representation and map of the M30 Madrid section simulated with PTV VISUM.	63
Figure 87: Effect of UTC implementation on average speed profiles during a saturated traffic condition (Turin). ..	65
Figure 88: Speed profiles for different saturation levels on a section of the M30 urban highway (Madrid).	65
Figure 89: Inserting average speeds in COPERT and calculating fuel consumption.	66
Figure 90: Available fuel consumption measurements in the ARTEMIS database for Euro 3 gasoline passenger cars < 1.4 l as a function of the average speed of the cycle.	67
Figure 91: Available fuel consumption measurements in the ARTEMIS database for Euro 3 diesel passenger cars < 2.0 l as a function of the average speed of the cycle.	67
Figure 92: Relative comparison of the available driving cycles in the ARTEMIS database with one of the monitored conditions (example shown: urban saturated condition – UTC OFF)	68
Figure 93: Calculated gasoline fuel consumption with COPERT for UTC on (left) and off (right).	69
Figure 94: Comparison of driving characteristics and COPERT fuel consumption for saturated over normal conditions; UTC ON (left), UTC OFF (right).	69
Figure 95: Absolute (left) and relative over COPERT (right) fuel consumption for all driving conditions.	70
Figure 96: Effect of saturation level and UTC condition on fuel consumption estimated with all available methods.	70
Figure 97: Relative impact of the calculation method on fuel consumption for different conditions.	70
Figure 98: Absolute (left) and relative over COPERT (right) fuel consumption for all driving conditions.	71
Figure 99: Effect of saturation level and UTC condition on fuel consumption estimated with all available methods.	71
Figure 100: Relative impact of the calculation method on fuel consumption for different conditions.	72
Figure 101: Fuel consumption estimated with COPERT for different saturation levels in the Madrid highway as a function of speed (left) and saturation level (right).	72
Figure 102: Impact of saturation level on the parameters of the driving.	73
Figure 103: Absolute (left) and relative over COPERT (right) fuel consumption for all driving conditions.	73
Figure 104: Effect of saturation level on fuel consumption calculated with all the available methods (left). Relative fuel consumption at 10% saturation as reference (right).	73
Figure 105: Absolute (left) and relative over COPERT (right) fuel consumption for all driving conditions.	74
Figure 106: Effect of saturation level on fuel consumption calculated with all the available methods (left). Using fuel consumption at 10% saturation as reference (right).	74
Figure 107: Schematic representation and map of an urban road in Turin simulated with AIMSUN.	75
Figure 108: Average speed vs. saturation of the 6 sections of the simulated urban road in Turin based on selected 9 vehicles (left) and the 3 average vehicles (right).	76
Figure 109: Fuel consumption calculated with both CRUISE and COPERT based on driving profiles of the selected 9 vehicles (left) and the 3 average vehicles (right).	76
Figure 110: Relative fuel consumption differences calculated with both CRUISE and COPERT based on driving profiles of the selected 9 vehicles (up) and the 3 average vehicles (down). The calculated fuel consumption in normal traffic conditions was used as the 100% basis in both software tools.	77
Figure 111: Average speed vs. saturation of the simulated urban road in Turin based on selected 9 vehicles (left) and the 3 average vehicles (right); impact of road length.	78
Figure 112: Relative fuel consumption differences calculated with both CRUISE and COPERT based on driving profiles of the selected 9 vehicles (up) and the 3 average vehicles (down). The calculated fuel consumption in normal traffic conditions were used as basis in both software; impact of road length	79
Figure 113: Impact of saturation and road length on ratio of relative fuel consumption calculated with both CRUISE and COPERT.	80
Figure 114: LAT experimental setup.	83
Figure 115: Experimental driving cycles.	84
Figure 116: Overview of the process to create engine maps from chassis dyno tests	85
Figure 117: Simulation validation overview.	86
Figure 118: Hybrid Topology – Toyota Prius III Plugin.	95
Figure 119: Schematic of the test protocol of the Toyota Prius III Plugin.	95
Figure 120: Schematic of the test protocol of the Toyota Prius III Plugin.	96
Figure 121: AVL CRUISE Model including Hybrid Control Logic of Toyota Prius III Plugin	97
Figure 122: Simulation Input Data Toyota Prius III Plugin	97

Figure 123: Simulation-Measurement Comparison Toyota Prius III Plugin - NEDC	98
Figure 124: Simulation-Measurement Comparison Toyota Prius III Plugin - WLTC	99
Figure 125: Simulation-Measurement Comparison Toyota Prius III Plugin – Artemis Urban.....	100
Figure 126: Simulation-Measurement Comparison Toyota Prius III Plugin – Artemis Road.....	101
Figure 127: Validation Results Toyota Prius III Plugin	102
Figure 128: Madrid section and VMS panel.....	104
Figure 129: Simulation vs. real consumption	106
Figure 130: Cumulative frequency	107
Figure 131: Vehicle speed	Fehler! Textmarke nicht definiert.
Figure 132: Cumulative fuel consumption.....	Fehler! Textmarke nicht definiert.
Figure 133: Simulation behavior still under investigation	Fehler! Textmarke nicht definiert.

EXECUTIVE SUMMARY

BACKGROUND

The main objective of this WP is to develop and validate the fundamental elements for energy and CO₂ emission simulation at micro and macro scale. This means that based on velocity profiles (micro simulation) or average velocity profiles (macro simulation) fuel consumption and CO₂ emission data is generated. While the simulation software already exists (see D3.1), main task of this WP is to generate vehicle models and make extensions to the software so that it is capable to achieve the goals of the project.

The emission simulation takes over velocity profiles generated in WP2 and WP4 to validate that the models generated show a correct behavior with real life profiles and with profiles from traffic simulation. This is important especially for hybrid controls, which due to their complexity may show incorrect behavior on specific driving situations. Of course such checks are preliminary since additional driving situations may occur.

In the overall context of ICT emissions emission simulation will be a follow-up task after traffic simulation to determine the influence of different ITS measures resulting in different velocity profiles on CO₂ emission. Consequently the models generated in WP3 will be used in WP5 for the integration and testing of the methodology developed in ICT emissions and in WP6 for the application of the methodology on different ITS scenarios.

WP3 is split into 5 different tasks:

- Task 1. Modeling of 'conventional' passenger cars at micro scale: Conventional passenger cars are vehicles which are not equipped with special electric systems in order to reduce fuel consumption.
- Task 2. Modeling of advanced technology passenger cars at micro scale: Advanced technology passenger cars are in the context of the project vehicles which are equipped with future technologies such as Start&Stop, Hybrids, Range Extender, or Electric vehicles.
- Task 3. Modeling of all vehicle types at macro-scale: The COPERT macro scale models is validated and compared with micro emission simulation results in real-world test cases.
- Task 4. Validation of the energy and emission modeling by chassis dynamometer: Measurements of single vehicles are done on the chassis dynamometer. Results of these measurements are compared with simulation results of the same vehicles in the micro simulation.
- Task 5. Validation of the energy and emission modeling by real-world tests: During WP2, fuel consumption measurements of vehicles on test sites were performed (Turin, Madrid). Results of these measurements are compared with simulation results of the same vehicles in the micro simulation.

METHODS AND RESULTS

The project created generalized vehicle models which are representative for a large share of the vehicles on the market. As it is not possible to generate one representative vehicle only because of the different vehicle sizes, fuel types, and efficiency levels, it was decided to generate one generalized vehicle for each of the combinations.

The project investigated in total 5 different vehicle sizes (A' to E'), 2 fuel types (gasoline, diesel), and 3 efficiency levels (approximate efficiency status of model years 2008, 2012, 2015). This gave 30 generalized vehicles in total. Basis of the vehicle data is efficiency level 2012 as for this level most vehicle data are currently available. Efficiency levels 2008 and 2015 were created based on 2012 using assumptions about efficiency increase/decrease and other changes in the specifications of the generalized vehicle models. A comparison for average fuel consumption data between simulations and published values shows a reasonable agreement for all classes. The work benefitted from the simulation activities performed by LAT in the framework of the WLTP/NEDC correlation activity since the finalization of the conventional vehicles within ICT-Emissions took advantage of the latest developments on modelling performed within the WLTP correlation project.

For the advanced vehicle models the situation is different. Since only a few vehicles on the market are equipped with advanced technologies such as hybrids a generalization similar to the one for conventional vehicles is not possible. An additional problem is also in the different hybrid topologies which result in very different influence on the emissions. Even when considering only the 6 advanced powertrain topologies (Start&Stop, Micro Hybrid, Mild Hybrid, Full Hybrid, Range Extender, Electric Vehicle) and removing the efficiency level 2008, this would result in 120 generalized vehicles, where for most of them no data would be available since not a single vehicle in the respective bin exists.

Instead, 15 specific vehicles equipped with different hybrid topologies and covering different vehicle categories were modeled. Data for the models were taken mainly from public data sources such as official homepages or vehicle test reports. These vehicles were one by one compared with published data or AVL internal measurements, where available. Maximum error between simulation and published data is 7% however starting from a low basis of 2.2 l/100km in the NEDC cycle. Average error is 3%. Considering the data on which the vehicle models are based upon this is a very good agreement. Specifically information such as fuel consumption maps or the hybrid control strategy is typically not available from public sources both having a significant influence on the fuel consumption.

Since the market share of vehicles equipped with advanced technologies is small at the moment, the influence of this group on the overall results of the project will be small. However the models generated shall give a good basis for future extensions with additional models when the market share of advanced vehicles rises.

The main work for the macro emission modeling was to check whether the results achieved with the average speed model introduced by COPERT fulfill the needs of the project. For the validation of the COPERT estimates, a comparison with simulated data using micro simulation (CRUISE) and alternative measured emissions data from the FP5 ARTEMIS project database was performed.

Generally COPERT estimates can predict the change in fuel consumption, in case ITS measures (e.g. UTC) are turned on or off or with satisfactory precision for macro-scale modelling (fleet wide modelling). In all cases examined in Madrid urban highway and in Turin

urban corridor, both the trends in emissions and the level of change were satisfactorily predicted. However, it also became obvious that for high saturation levels (e.g. >80%) and/or for very short road segments (e.g. <400 m) the average speed model is not capable to correctly predict changes in the fuel consumption. In such cases, the level of link aggregation will have to increase in the actual simulations to be performed in WP6, so that the minimum distance for each link is at a few hundred meters. Moreover, the simulation of congested conditions at a macro scale should be seen under the prism of the modelling limitations.

For the micro-simulation model validation, 4 different vehicles were measured on the chassis dynamometer. The vehicles cover different vehicle categories (2 C', 1 D', 1 E') and fuel types (2 gasoline, 2 diesel). Measurements were performed on an instantaneous basis, which allows also creation of fuel consumption maps. Measurements and micro emission simulations were done for different velocity profiles (NEDC, Artemis). The average error over all vehicles and driving cycles is 2.8% or 0.2 l/100km.

Additional model validation via real-world on board measurements was performed on 3 test sites: Madrid, Turin and Rome. In Madrid measurements were performed on 2 different vehicles, one diesel, and one gasoline, in Turin in one gasoline car and in Rome in one diesel car. The measurements were performed with cars equipped with a special OBDKey to retrieve second by second data on vehicle operation (e.g. engine speed, vehicle speed, fuel consumption). These data were used for comparison of the measurements with simulation results of vehicle models generated in CRUISE. Simulation results are typically within a +/-5% margin of the measurements which is in line with what is expected considering that fuel consumption was collected through the CAN-Bus and the 'general purpose' nature of the data used to feed the Cruise model.

1 Micro Emission Models

1.1. GENERAL CONSIDERATIONS

One of the most important parameter for the micro emissions modelling is the development of a sufficient number of vehicle classes, representing a range of vehicle technologies that will be able to realistically represent the range of CO₂ emissions and fuel consumption impacts that an ICT measure can lead to. For modelling purposes, the fleet of passenger cars can be generally split into two categories: (i) conventional vehicles, i.e. those that are basically equipped with an internal combustion engine, and (ii) advanced vehicles, i.e. those equipped with an advanced engine and different degrees of hybridisation and electric vehicles. Because of the different control logic in each case, the impact of an ICT measure may vary.

We have selected to model only diesel and petrol fuelled cars as ‘conventional’ vehicles. Other fuels which are or may become popular in the future were not modelled. For example, bi-fuelled vehicles, such as CNG/Gasoline or biofuelled vehicles, such as flexi-fuel E85 ones may increase their share in the future. However, including such vehicles in our sample would not offer new insights. All of the alternatively fuelled vehicles share the same basic technology with either gasoline (spark-ignition) or diesel (compression-ignition) vehicles. Hence, the relative impact of an ICT measure on tailpipe CO₂ emissions for alternatively fuelled vehicles would be the same with their corresponding conventional fossil fuel counterparts. In other words, the efficiency improvement is expected to be the same between a gasoline and an E85 fuelled vehicle (or between a biodiesel and a diesel vehicle), e.g. if UTC is enabled in an urban corridor. Of course the impact on total fossil-related CO₂ emission would be different if the corridor was used primarily by E85 or neat gasoline vehicles. However, calculating the impact in each case is only a matter of a post-processing by estimating what percentage of the total traffic is represented by E85 vehicles and assigning the efficiency improvement on their fossil CO₂ emissions only. But a separate micro-model would not be necessary in this case.

However, the impact of ICT measures on conventional vehicles will, further to the fuel used, depend on the size of the vehicle and its overall efficiency. We have opted to simulate the latter as an effect of the registration year of the car, assuming general trends imposed by EU Regulation 443/2009. The following sections better clarify the rationale and the approach in choosing the conventional vehicle types.

In the case of advanced vehicles, the objective was to cover the widest possible range of state-of-the-art technologies (e.g. start/stop, regenerative breaking, hybrid vehicles, and electrified vehicles) that are currently used or scheduled for mass production by automotive manufacturers. In this case, selecting a ‘typical’ vehicle of each type is not possible because there are only very few vehicles of each type available on the market today. Hence, we have chosen to identify single vehicle models which are today available and simulate these as representative examples of each technology category.

1.2. CONVENTIONAL VEHICLES

The first distinction for conventional (gasoline, diesel) vehicles was according to their size. In order to distinguish vehicles we have selected to classify them according to their market

segment – i.e. using the Letter-based characterisation (Segment A, B, C, ...). There is no universally agreed market segmentation system. The automotive industry classifies vehicles to the different segments based on the general characteristics of the vehicles, including their size, cost, performance, etc. Often, new market segments are created to lump vehicles that are differentiated from other vehicles in the stock. In order to take into account the vehicle characteristics that are mostly relevant in terms of CO₂ emissions, we have decided to distinguish vehicles according to a more compact segments list than usually considered. This is shown in Figure 1 which demonstrates the correspondence of the usually used car segment list with the condensed list that has been used in the framework of the ICT-Emissions project. The latter is consistent with earlier studies aiming to parameterize CO₂ emissions from cars [1]. The condensed list does not include sport coupe vehicles that, in any case, correspond to only a very small fraction of total car activity and condenses in one the segments D, E, F due to the rather similar overall characteristics of these vehicles. Therefore, the target would be to identify an ‘average’ or ‘generalized’ vehicle for each segment and fuel that should be simulated.

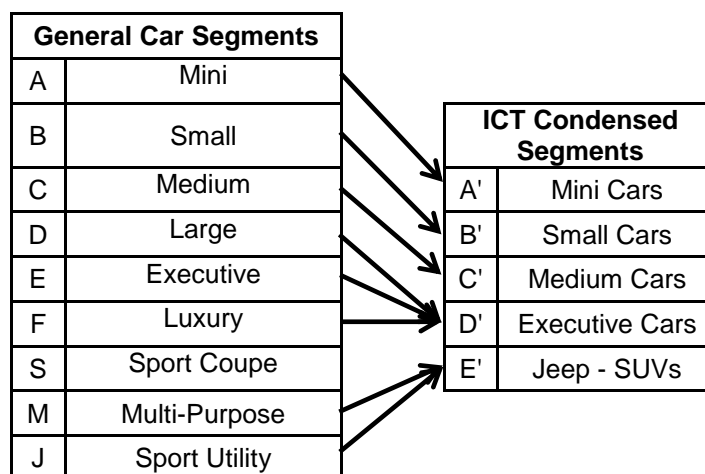


Figure 1: Vehicle segments selected for the micro simulation of conventional vehicles

The third distinction of the vehicles (further to their size and fuel) has to do with their overall efficiency. EU Regulation 443/2009 for passenger cars requests significant efficiency improvements to meet CO₂ targets. Because of this, vehicles being marketed each year are overall more efficient than in the previous year. The trend in terms of type-approval CO₂ emissions for new cars sold each year in Europe is shown in Figure 2. However, the efficiency improvement shown is under ideal type-approval conditions and several reports suggest that this is not reflected in the real-world [1, 3].

Therefore, in order to simulate vehicle types which reflect reality to the extent possible, we decided to define three overall efficiency tiers:

- Tier 1: The first tier reflects somewhat older vehicles, e.g. overall efficiencies represented by vehicles registered in year 2008. These have been Euro 4 vehicles where fuel efficiency improvements were mostly observable by aerodynamic drag reduction and engine combustion improvements.

- Tier 2: Vehicles representing efficiency levels of year 2012. These are Euro 5 vehicles where efficiency improvement are materialized with weight reduction, further efficiency improvement, low resistance tyres, and additional auxiliaries, such as start and stop.
- Tier 3: Vehicles representing efficiency levels of year 2015. This is required to be able to model ICT impacts on the near future vehicle fleet. These are going to be Euro 6 vehicles with further efficiency improvements based on in-cylinder measures (e.g. cylinder deactivation, downsizing, downspeeding) and more light weight construction.

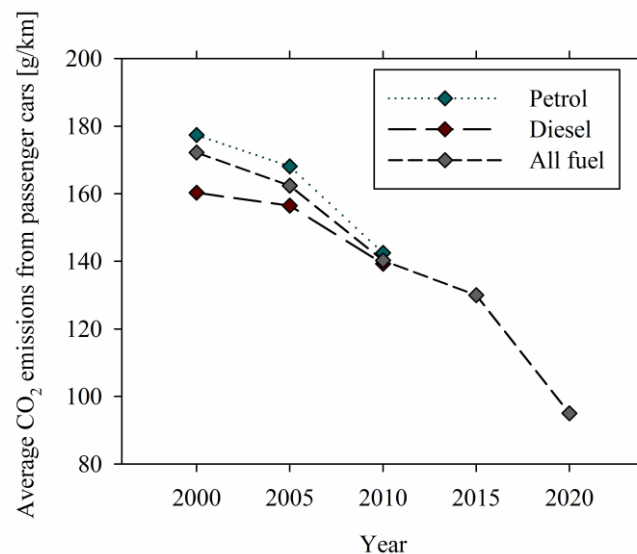


Figure 2: Evolution of CO₂ emissions from new passenger cars [2].

Based on these considerations 30 individual conventional generalized vehicle models have been developed and simulated to be used in ICT-Emissions. Each generalized vehicle corresponds to an individual vehicle 'bin'. The overall structure of the bins (generalized vehicle models) is shown in Figure 3. By using different proportions of vehicles in the different bins, it is considered that the entire passenger car fleet in each member state can be satisfactorily simulated in terms of its CO₂ emissions.

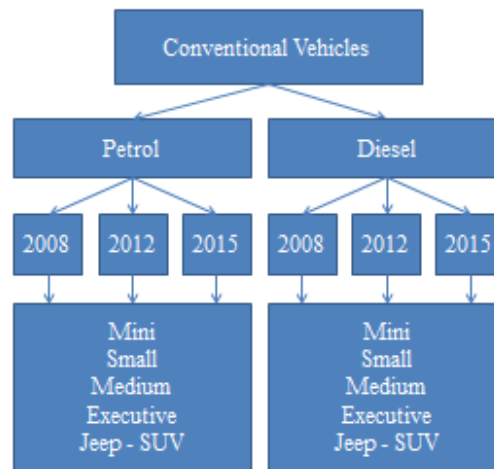


Figure 3: Schematic of the structure of the 30 conventional vehicle micro-models.

1.2.1. COLLECTION OF VEHICLE CHARACTERISTICS

The schematic of a generalized vehicle model developed within the AVL CRUISE environment is shown in Figure 4, with the example of a front wheel drive segment D' vehicle with a 6-gear manual gearbox. Similar generalized models were developed for each of the vehicles in the 30 bins. In general, for the mini, small, medium and executive cars segment a front wheel drive vehicle has been modelled, while for the jeeps and SUVs a four wheel drive model was assumed. For segments A', B', and C' a 5-speed gearbox has been used, while for the executive cars and the jeeps and SUVs a 6-speed manual gear box was implemented.

For each bin, detailed vehicle specifications are required to feed the model. The most important components for the modelling can be seen in Table 1. In order to collect this information, we explored the most popular vehicle models per bin, which are included in the CO₂ monitoring database [2]. The 2012 version of the database was analysed and based on that, Table 2 to Table 6 show the most popular models per segment. The percentage of total registrations that the selected models correspond to is also given in each of these tables. By summing up the percentages, the 32 in total shown vehicle models correspond to 52% of all new car registrations in 2012. Therefore, weighted-average specifications that are derived from these models are expected to closely reflect the corresponding stock characteristics.

In order to derive these weighted average characteristics, the specifications requested in Table 1 were collected for the models in Table 2 through Table 6. Manufacturer web-pages, model brochures and internet databases were consulted to produce this information. For several of the specifications (e.g. capacity, power) average values were produced by weighing with the number of registrations of the particular model. For other specifications (e.g. gear ratios) weighing average would not produce reasonable results. In these cases, engineering assessment of the typical gearbox ratios used in each vehicle segment was used. Based on these considerations, Table 7 shows the detailed vehicle specifications selected for each bin.

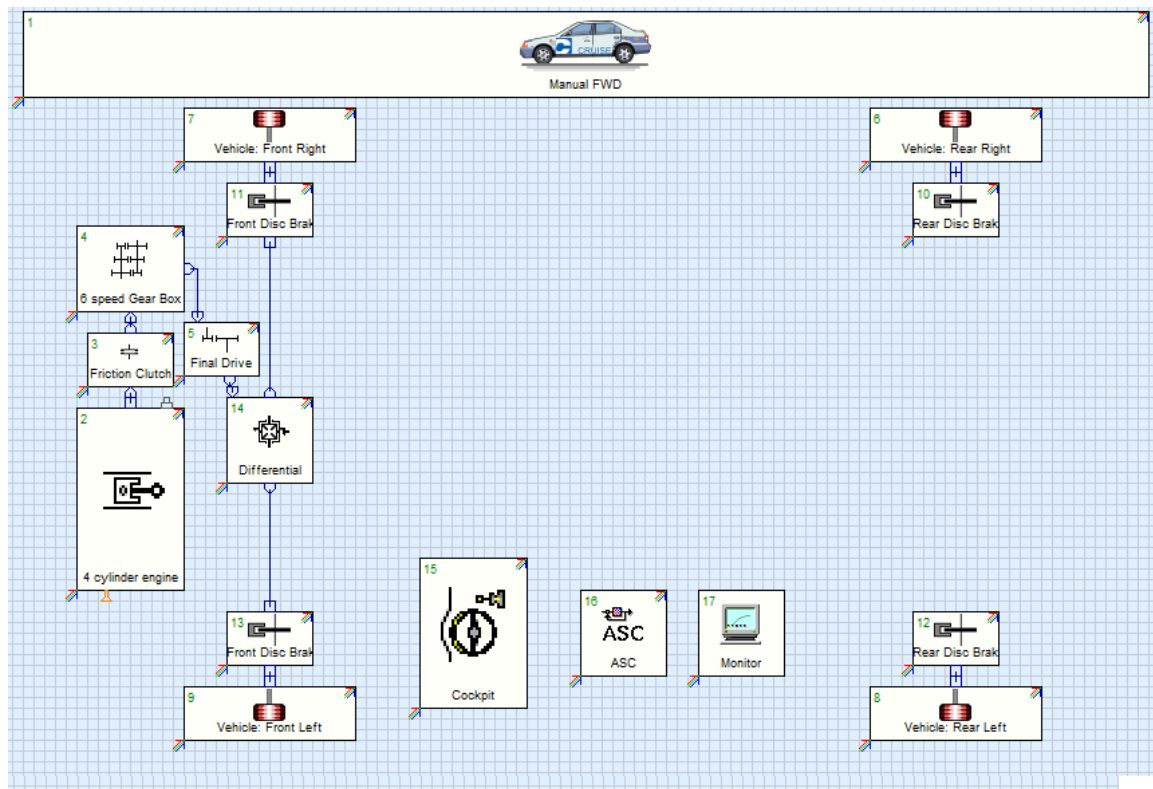


Figure 4: AVL CRUISE model for a front wheel drive conventional vehicle.

Table 1: Essential specifications for the fuel consumption modelling in AVL CRUISE.

Component	Modelling parameter
Chassis	Weight
	Driving resistance (frontal area, drag)
Engine	Displacement
	Number of cylinders
	Number of strokes
	Max power/RPM
	ICE full load curve
	Fuel type and density
	Fuel consumption map
Gearbox	All gear ratios
	Efficiency
Final Drive	Transmission ratio
	Efficiency
Wheels	Dynamic rolling radius

Table 2: Mini cars (A') registrations and weighted-average specifications.

Manufacturer	Model	Number Registrations	Percentage of total annual registrations across the segments	
Fiat	Panda	182542		
Peugeot	107	68447		
Renault	Twingo	92152		
Hyundai	i10	57047		
Total		400188	5%	
Fuel Type	CO ₂ (g/km)	Mass (kg)	Capacity (cm ³)	Power (PS)
Gasoline	111	972	1146	76
Diesel	103	1086	1348	75

Table 3: Small cars (B') registrations and weighted average specifications.

Manufacturer	Model	Registrations	Percentage of total annual registrations across the segments	
Citroen	C3	210711		
Fiat	Punto	131204		
Ford	Fiesta	301104		
Opel	Corsa	259714		
Renault	Clio	240395		
Seat	Ibiza	115289		
Toyota	Yaris	164175		
Volkswagen	Polo	279510		
Total		1702102	20%	
Fuel Type	CO ₂ (g/km)	Mass (kg)	Capacity (cm ³)	Power (PS)
Gasoline	127	1114	1250	80
Diesel	104	1196	1422	82

Table 4: Medium cars (C') registrations and weighted average specifications.

Manufacturer	Model	Registrations	Percentage of total annual registrations across the segments	
Citroen	C4	197103		
Ford	Focus	233124		
Ford	Mondeo	66702		
Opel	Astra	232418		
Peugeot	308	116176		
Renault	Megane	312533		
Seat	Altea	27073		
Toyota	Avensis	49604		
Volkswagen	Golf	472368		
Volkswagen	Passat	187398		
Total		1894499	22%	
Fuel Type	CO ₂ (g/km)	Mass (kg)	Capacity (cm ³)	Power (PS)
Gasoline	143	1381	1423	109
Diesel	120	1487	1686	107

Table 5: Executive cars (D') registrations and weighted average specifications.

Manufacturer	Model	Registrations	Percentage of total annual registrations across the segments	
Audi	A6	102714		
Mercedes	E220	21375		
Opel	Insignia	92184		
Volvo	S60	14577		
Total		230850	3%	
Fuel Type	CO ₂ (g/km)	Mass (kg)	Capacity (cm ³)	Power (PS)
Gasoline	164	1656	1995	137
Diesel	142	1773	2311	139

Table 6: Jeeps and SUVs (E') registrations and weighted average specifications.

Manufacturer	Model	Registrations	Percentage of total annual registrations across the segments	
BMW	X5	16104		
Hyundai	Tucson	36376		
Land Rover	Discovery	11846		
Land Rover	Range Rover	65908		
Mitsubishi	Outlander	12671		
Suzuki	Grand Vitara	11309		
Total		154214	2%	
Fuel Type	CO ₂ (g/km)	Mass (kg)	Capacity (cm ³)	Power (PS)
Gasoline	201	1688	2259	183
Diesel	183	2023	2463	175

In Table 7 the vehicle curb weight, the engine displacement and the maximum power were extracted from the CO₂ monitoring database for all segments and fuels. In addition to the curb mass, a 100 kg weight is added which represents the driver and the fuel. The European inertia class is then selected from the sum of the vehicle's curb mass, the fuel and the driver. The overall drag coefficients used have been calculated for each segment using average weighing factors from the refined sample. The same method has been applied for the calculation of the dynamic rolling radius, the width and height. The product of width and height along with an empirical factor of 0.84 resulted in the calculation of the frontal area. From the total vehicle's weight, the frontal area and the drag coefficient the driving resistance can then be calculated. Finally, characteristic full load curves that have been used dimensionless for each bin are shown in Figure 5.

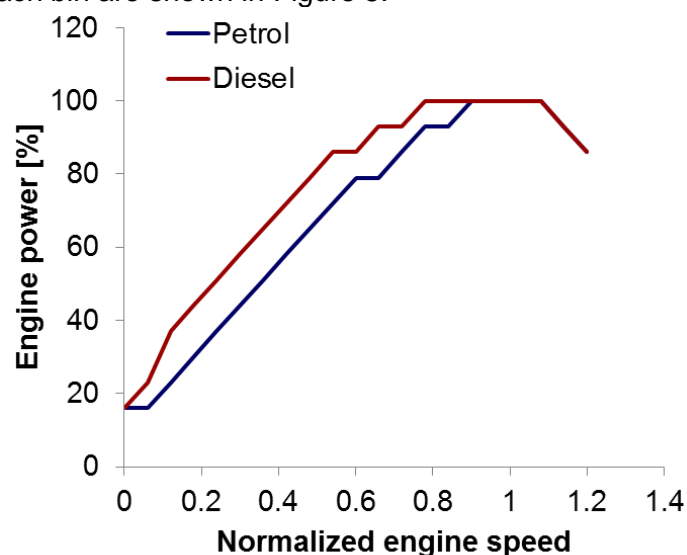


Figure 5: Generic petrol and diesel full load curves.

Table 7: Vehicle specifications for Tier 2 vehicles (10 bins).

Component	Specification	Mini		Small		Medium		Executive		Jeeps and SUVs	
		Gasoline	Diesel	Gasoline	Diesel	Gasoline	Diesel	Gasoline	Diesel	Gasoline	Diesel
Chassis	Weight [kg]	972	1086	1114	1196	1381	1487	1656	1773	1688	2023
	Inertia class [kg]	1020	1130	1250	1250	1470	1590	1700	1930	1810	2150
	Drag Coefficient	0.327		0.333		0.311		0.283		0.355	
	Frontal Area [m ²]	2.04		2.14		2.22		2.32		2.87	
Engine	Inertia	0.14	0.17	0.16	0.19	0.19	0.23	0.27	0.29	0.29	0.3
	Displacement [cc]	1146	1348	1250	1422	1423	1686	1995	2311	2259	2463
	Number of cylinders	4	4	4	4	4	4	4	4	4	4
	Max Power [kW] / Speed [RPM]	57/5800	56/4000	60/5800	61/4000	81/5800	80/4000	102/5800	104/4000	136/5800	130/4000
	Maximum Speed [RPM]	6500	5000	6500	5000	6500	5000	6500	5000	6200	5000
	Idle Speed [RPM]	950	750	950	750	950	750	950	750	950	750
Gearbox	1st gear	3.79	3.81	3.68	3.53	3.61	3.72	4.09	4.06	4.19	4.26
	2nd gear	2.08	2.07	2.00	1.93	1.98	1.99	2.25	2.16	2.69	2.55
	3rd gear	1.41	1.29	1.34	1.29	1.34	1.25	1.43	1.35	1.79	1.68
	4th gear	1.05	0.94	1.00	0.94	1.01	0.89	1.04	0.98	1.41	1.30
	5th gear	0.84	0.72	0.80	0.76	0.80	0.68	0.88	0.77	1.10	1.03
	6th gear	-	-	-	-	-	-	0.74	0.63	0.66	0.82
	Efficiency	0.96		0.96		0.96		0.96		0.96	
Final Drive	Transmission Ratio	3.825	3.382	3.871	3.200	4.167	3.648	3.754	3.462	4.056	3.796
	Efficiency	0.99		0.99		0.99		0.99		0.99	
Wheels	Dynamic Rolling Radius [mm]	286		300		317		337		371	
	Inertia [kg*m ²]	0.7		0.77		0.9		1.0		1.2	

The results of the simulation compared to the type-approval NEDC CO₂ values are shown in Figure 6 for the 5 gasoline Tier 2 models and in Figure 7 for the 5 diesel Tier 2 models.

The final results presented below were updated with the latest model developments using to the new evidence derived from the correlation work within the WLTP/NEDC correlation activity. In this activity, precise simulated vehicle models are being developed with the aim to be able to predict the impact of the changing driving cycle on new vehicle CO₂ targets. These models are based on confidential information provided by the manufacturers on the performance of several powertrain subsystems. Although confidential information cannot be used within ICT-Emissions, still the advanced knowledge collected in that activity concerning simulation details (gear change simulation, driver foresight simulation, fuel shut off strategies, etc.) will be of great benefit to ICT-Emissions as well..

Although the new models are up-to-date with the latest developments from the WLTP/NEDC correlation exercise, deviations from the CO₂ monitoring database average values still exist and range from 2 to 12%. Only the gasoline Jeep-SUV segment is associated with a higher error (calculated to be 21%) and thus can be neglected, since in addition this is the category with the largest variability of the average CO₂ value. For example in this segment both the BMW X1 with 175 g/km and BMW X3 with 236 g/km coexist, with an absolute CO₂ difference of 61 g/km.

One important parameter for the deviation from the values of the CO₂ monitoring database is the selected road load coefficients and inertia masses. The coefficients used from the automotive industry are significantly lower than the ones observed in real world driving [1]. Thus, no physical model for the driving resistance could be used. To deal with this issue, we located a representative vehicle for segment C' that emits approximately its segment's average CO₂ value and is as close as possible to the average fleet characteristics (frontal area, drag coefficient, weight, displacement, engine power). This vehicle was used as reference, and each segment's road load characteristic was calculated from Cruise's built-in function as shown below:

$$F = \frac{m}{m_{ref}} F_0 + \frac{m}{m_{ref}} F_1 V + \frac{C_d A}{C_{dref} A_{ref}} F_2 V^2$$

where F_0 , F_1 , F_2 the road load coefficients of the selected vehicle and A_{ref} , C_{dref} , m_{ref} its frontal area, drag coefficient and reference weight respectively and A , C_d , m each segment's average characteristics shown in **Fehler! Verweisquelle konnte nicht gefunden werden.** It can be realised that the exact force attributed to a single vehicle cannot be exactly calculated by this empirical formula and smaller or larger deviations are expected.

Another parameter that should be taken into account is the type approval procedure. During the measurement, the driver is taking advantage of the +/- 2 km/h speed limits given by the legislation, following a more fuel efficient driving trace through less aggressive accelerations and cruising in smaller speeds. In addition, for a single vehicle in a type approval test the maximum allowed deviation from the declared value is 4%. For example, assuming that the manufacturer brings a new vehicle for type approval measurement and declares that its vehicle emits 100 g/km, if in the test the measured CO₂ is below 104 g/km (up to 4% higher than the declared value), then the official value that is assigned is the 100 g/km. In these series of simulations, this was not taken into account.

What should also be taken into account is the infiltration of the Start & Stop technology to the passenger car fleet. The results of Figure 6 and Figure 7 do not consider the Start & Stop gain which may be up to 20 g/km in the Jeep-SUV segment. Finally, the cold start effect accounts for an extra 10% to the hot start emissions over the NEDC for all categories. This difference is rather an empirical approximation which provides satisfactory results for fast estimations of the cold start effect over the NEDC for both gasoline and diesel fuel vehicles.

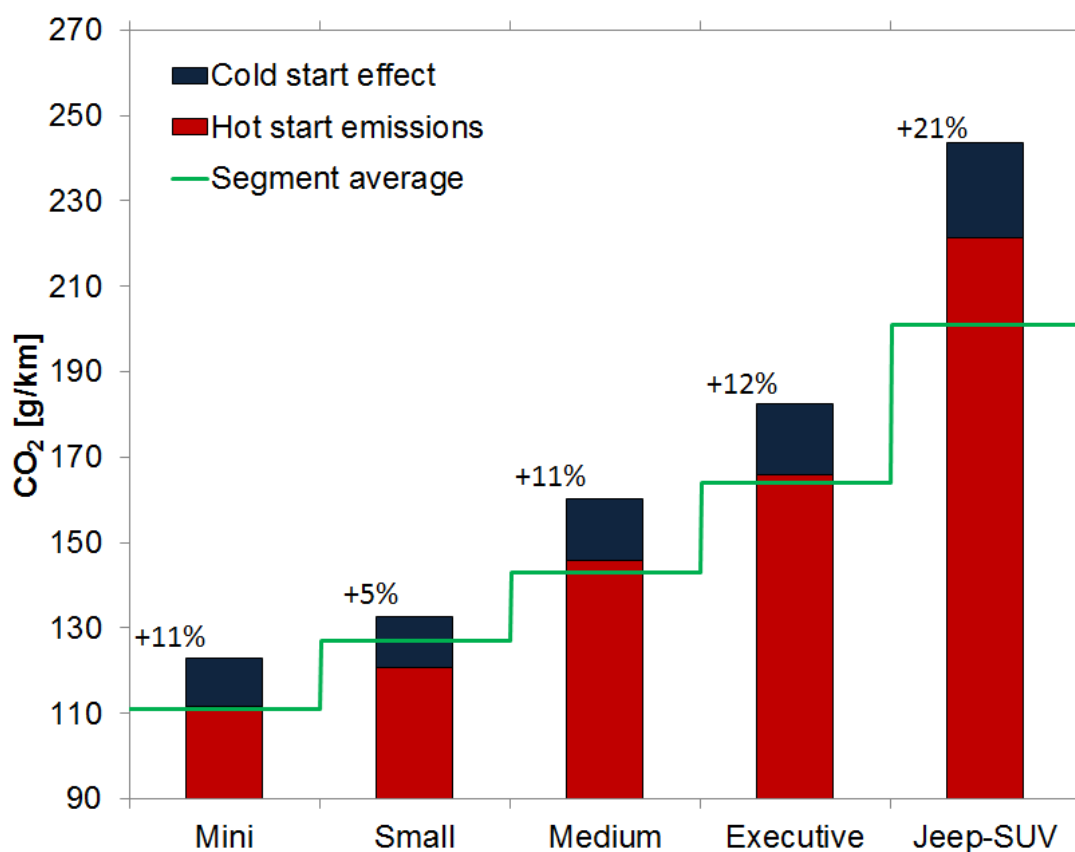


Figure 6: Simulation and segment average CO₂ emissions for petrol vehicles.

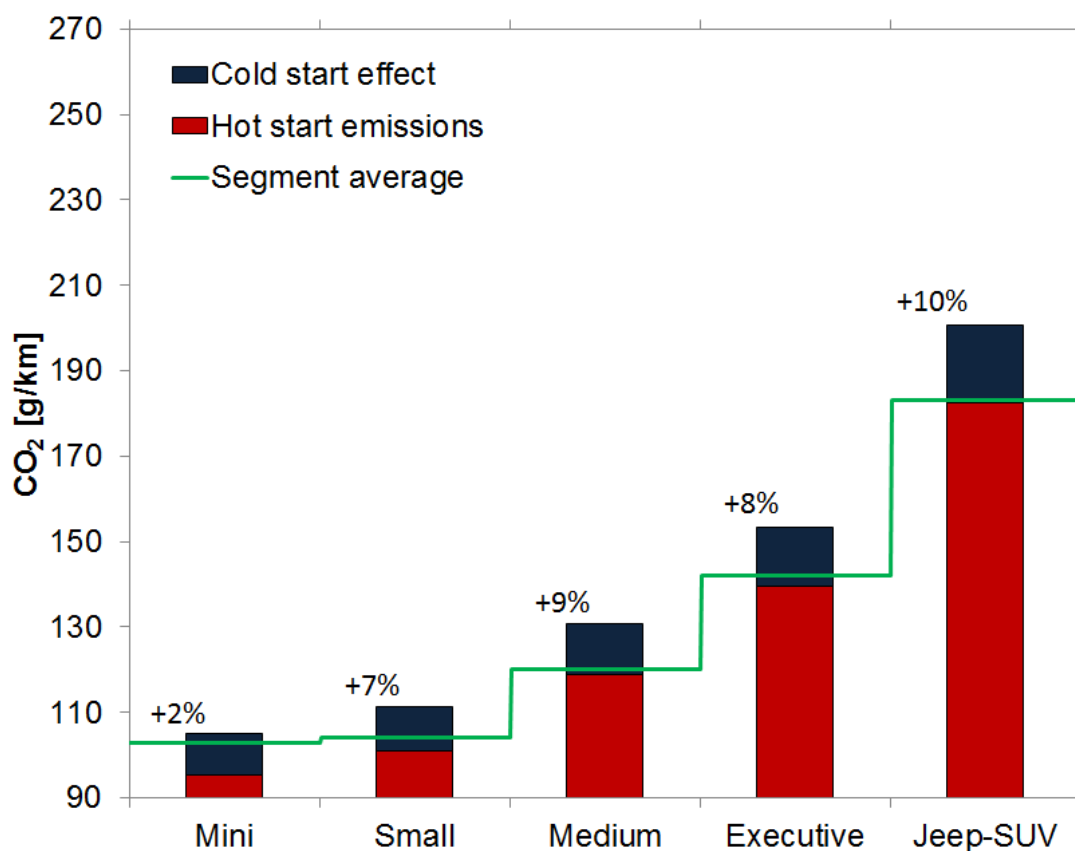


Figure 7: Simulation and segment average CO₂ emissions for diesel vehicles.

The Tier 1 and Tier 3 vehicles were based on the Tier 2 ones. The parameters that were altered to build these vehicles included the weight, the maximum engine power, the drag coefficient and the engine efficiency. In other words, we expect that these parameters are mostly responsible for the differentiation in the fuel consumption between the three vehicle Tiers.

The range of variation of these parameters between the different Tiers was based on observation of their change for popular models within each bin. Tier 1 vehicles were thus considered to weigh 5% more, have an overall 5% worse engine efficiency and 5% lower maximum engine power compared to corresponding Tier 2 vehicles. Tier 3 were considered to weigh 5% less, have a 5% more efficient engine and have 5% higher maximum engine power compared to Tier 2 (Figure 8). The drag coefficient for the three Tier categories is also expected to only slightly change between segments A', B' and C'. This is therefore considered not to change from 2008 to 2015, while for segments D' and E' this is considered to be 0.01 higher for Tier 1 and 0.02 lower for Tier 3 in absolute terms. An example of the result of the simulation is seen in Figure 8. Also Figure 9 shows the overall differences in CO₂ emissions between the three Tiers over the NEDC.

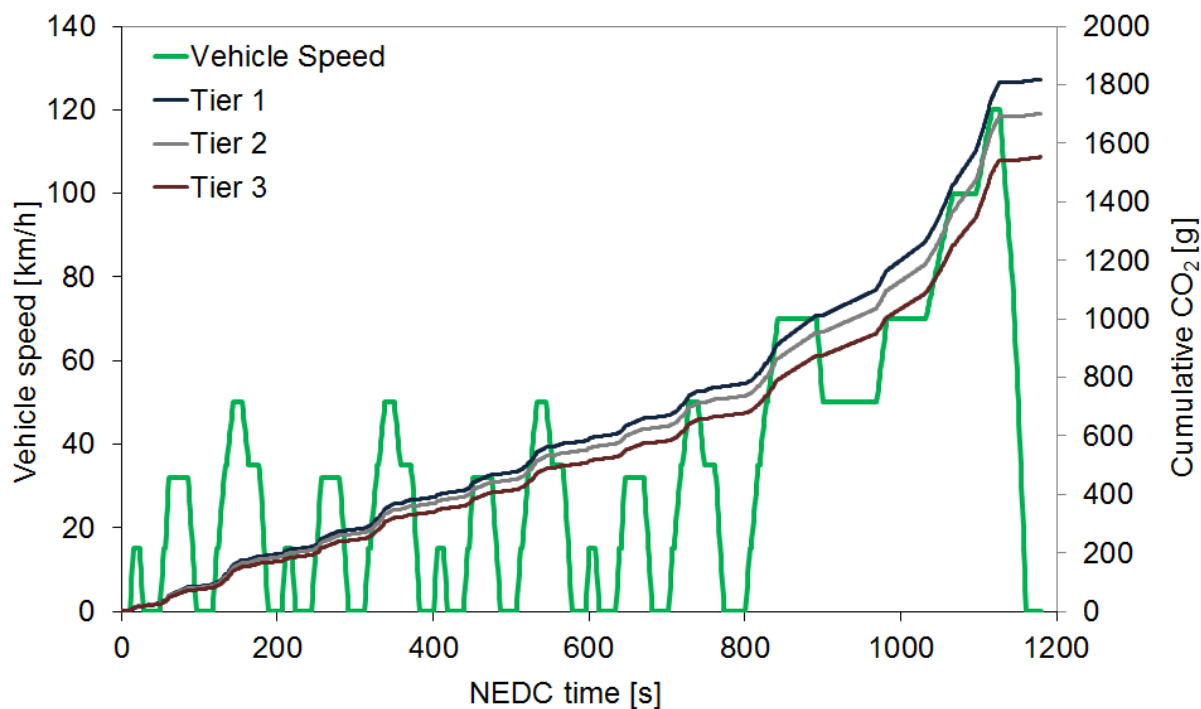


Figure 8: Cumulative CO₂ difference between three Tiers of diesel executive vehicles.

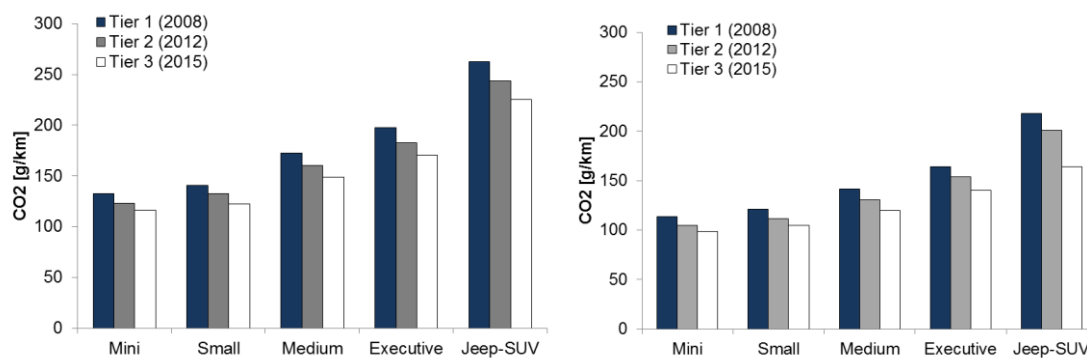


Figure 9: CO₂ emissions for the (left) petrol and (right) diesel vehicles over the NEDC.

1.3. ADVANCED VEHICLES

1.3.1. OPERATING STRATEGIES

Operating strategies describe different strategies a hybrid vehicle is capable of performing. Operating strategy means in this context in which form combustion engine and electric motor work together to e.g. charge the battery or boost the acceleration of the vehicle.

Which strategy is possible depends on the hybrid topology. The operating strategy is the main distinctive feature for the different hybrid topologies.

1.3.1.1. Start & Stop

The engine is switched-off in case of stationary vehicle (vehicle velocity below defined border when decelerating, no gear). The Start & Stop feature is active if the ICE temperature is above a defined limit and in case of no State of Charge (SOC) constraint. Battery charging during Internal Combustion Engine (ICE) idling is neglected.

Start & Stop helps to reduce fuel consumption and emissions during long phases of standing still, e.g. in traffic jam. It is mainly effective in urban driving conditions or highly saturated traffic with lots of stop and go conditions but less effective in extra urban or highway conditions.

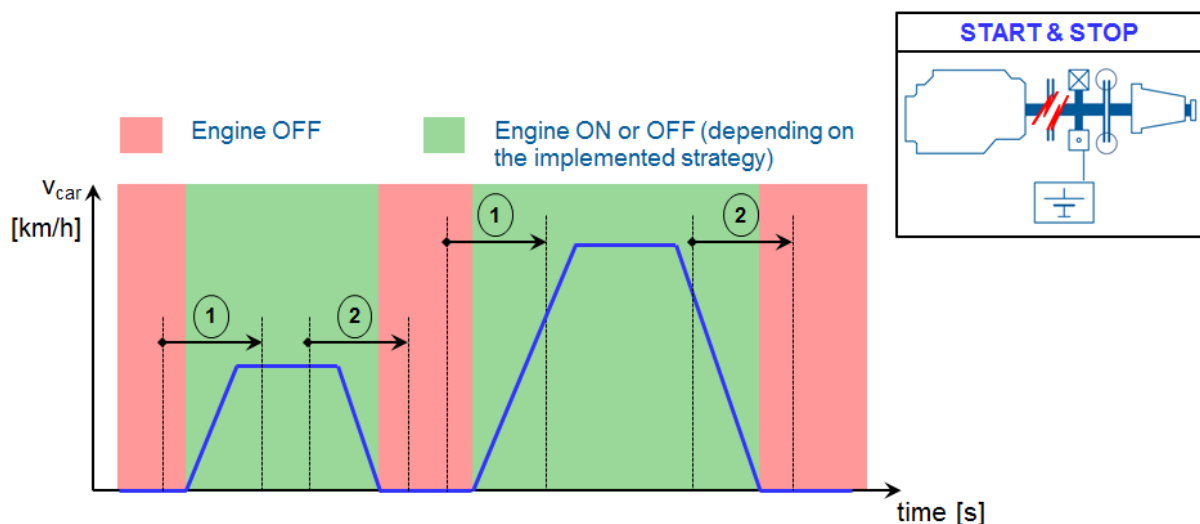


Figure 10: Operating Strategy – Start & Stop

1.3.1.2. E-Drive

E-Drive means that only the electric motor drives the vehicle. The ICE is turned off entirely. The e-Drive is operated, in case of available battery energy, to avoid low-efficiency ICE operating points (area 2 in Figure 11). This is the area where the fuel consumption of the ICE is very high. The e-Drive is activated in case of:

- 1) low vehicle speed + vehicle launch, or

- 2) required traction torque lower than a certain threshold

E-Drive is active mainly in urban driving conditions or highly saturated traffic with lots of stop and go conditions. In extra urban or highway conditions E-Drive is active only for pure electric vehicles or hybrid vehicles with high battery charge.

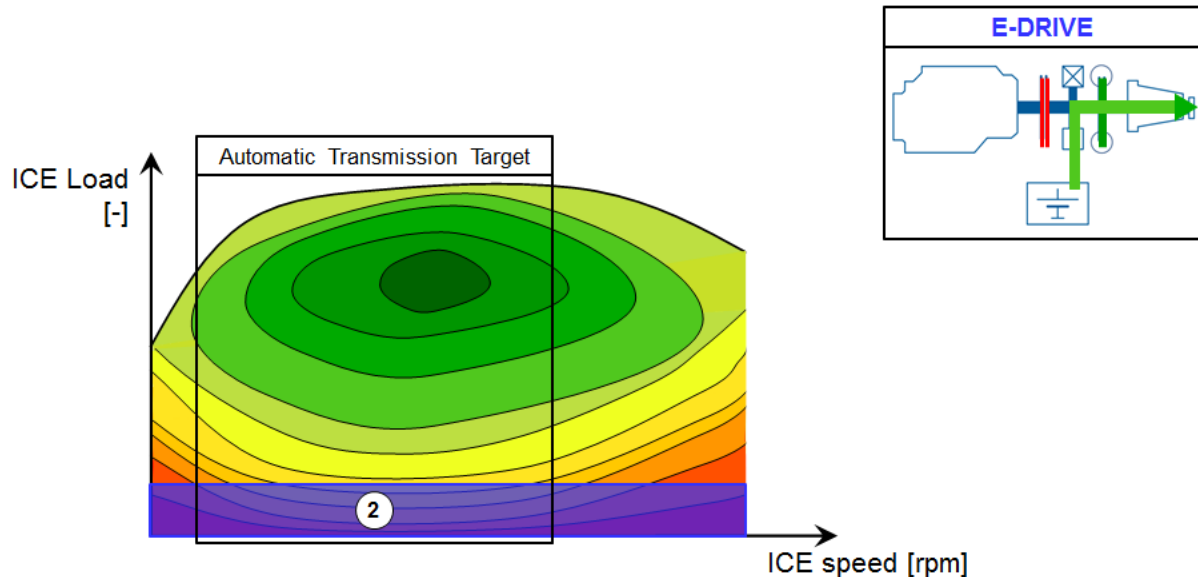


Figure 11: Operating Strategy – E-Drive

1.3.1.3. Load Point Moving

The Engine Load Point Moving (LPM) can be applied to shift the ICE operation towards better efficiency conditions. Load Point moving can work in both directions. Either the electric motor provides additional power to reduce the load of the ICE, or it acts as generator to increase the load of the internal combustion engine and at the same time recharge the battery. Which way the LPM is active depends on the load point of the ICE and the available battery charge.

The engine LPM function is activated in case of:

- 1) *e-Drive disabled* **and** *the required traction torque lower than a certain threshold*
- 2) The engine torque is defined by: $T_{q_{ICE}} = T_{q_{req}} + DT_{LPM}$

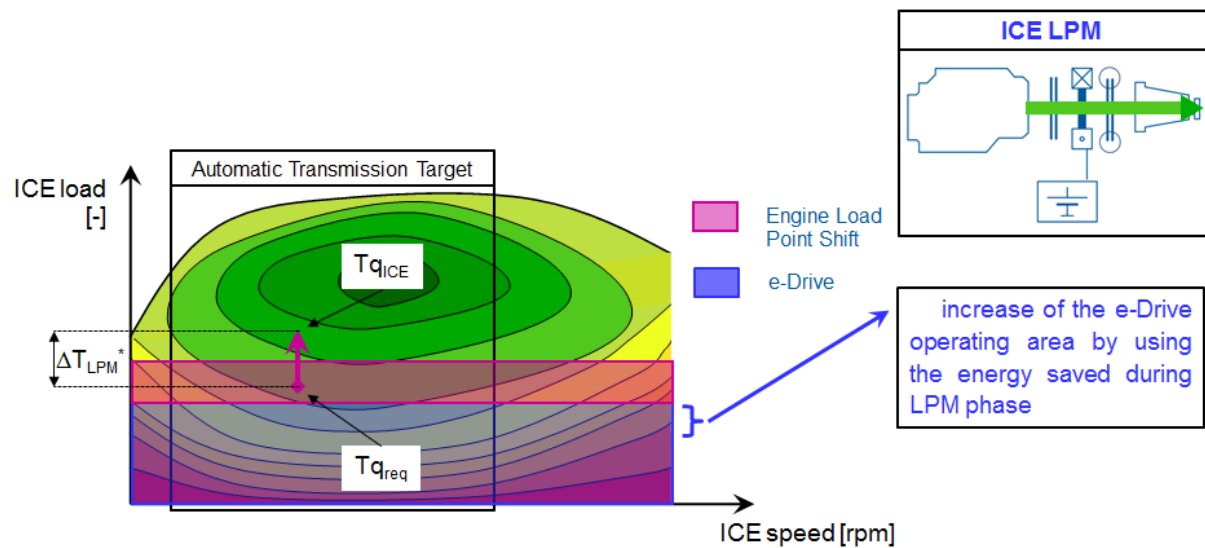


Figure 12: Operating Strategy – Load Point Moving

1.3.1.4. Engine Alone

The Engine Alone is applied when the ICE works at low specific fuel consumption. For range extender operation this is used in order to by-pass the battery losses: the range extender supplies exactly the required electric load. Engine alone condition is for hybrid vehicles equivalent to conventional vehicle driving conditions. This means that the same efficiency is reached. For range extender operation some efficiency is lost by converting the power of the ICE into electric energy.

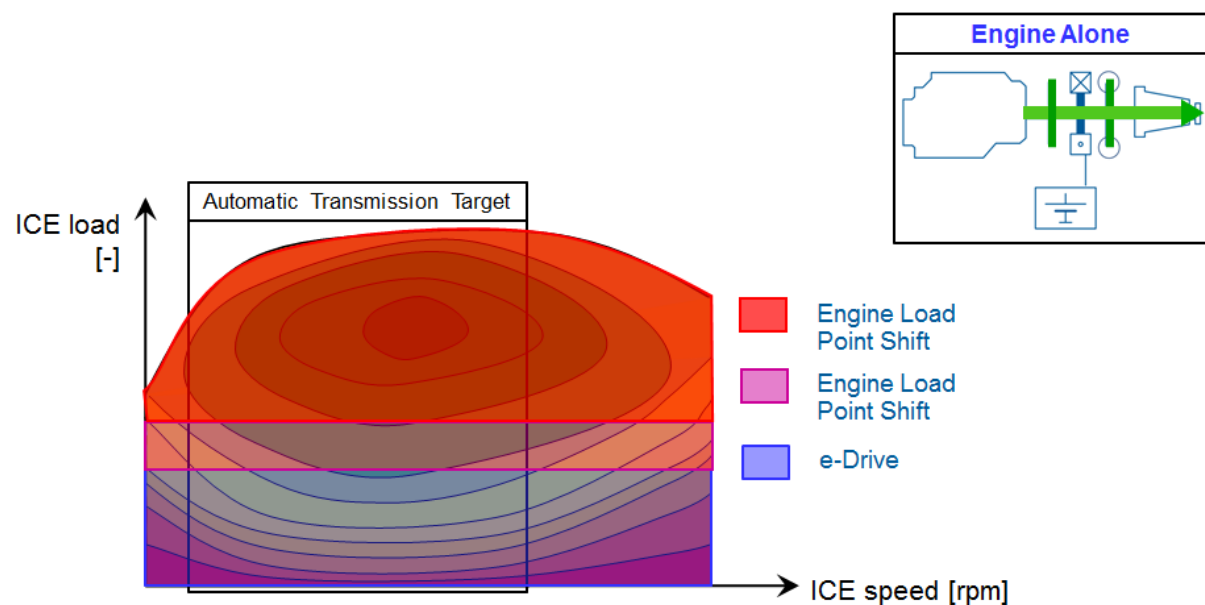


Figure 13: Operating Strategy – Engine Alone

1.3.1.5. E-Boost

The e-Boost is applied, in case of available battery energy, to improve full load performance. The e-Boost is linearly increased from 0 to 100 % starting from an APP limit. This function is not active during the NEDC.

With E-Boost additional short term power is supplied, which is mainly required during acceleration phases. Due to the additional power the size of the ICE can be reduced, which helps to reduce fuel consumption. E-Boost is also used to reduce fuel consumption during acceleration phases by moving the load point of the ICE into areas with lower fuel consumption (see Chapter 1.3.1.3).

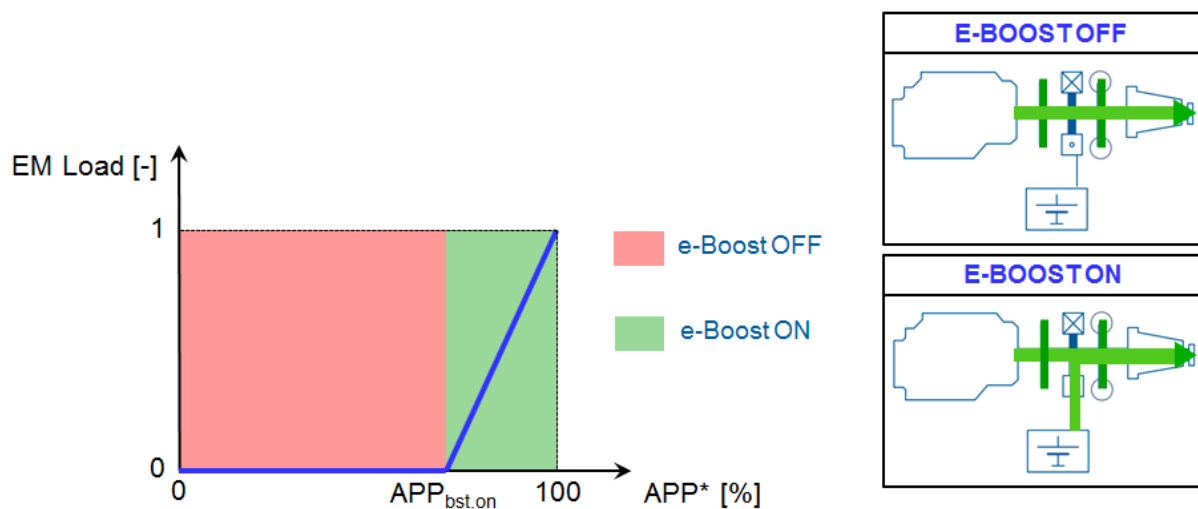


Figure 14: Operating Strategy – E-Boost

1.3.1.6. Regenerative Braking

The Regenerative Braking is applied in case of negative traction. During braking phases the engine is disengaged (by opening its clutch) and switched-off, if in warm state. For safety & comfort, traditional brakes are enabled during severe decelerations (no limitation during the NEDC). Two parameters define the linear transition between only regenerative braking and only traditional brakes.

During regenerative braking the electric motor acts as generator and charges the battery, so that a part of the kinetic energy lost during braking is recovered. Regenerative braking is applied for all hybrid vehicles as it extends the range the vehicle can drive on electric energy from the battery significantly.

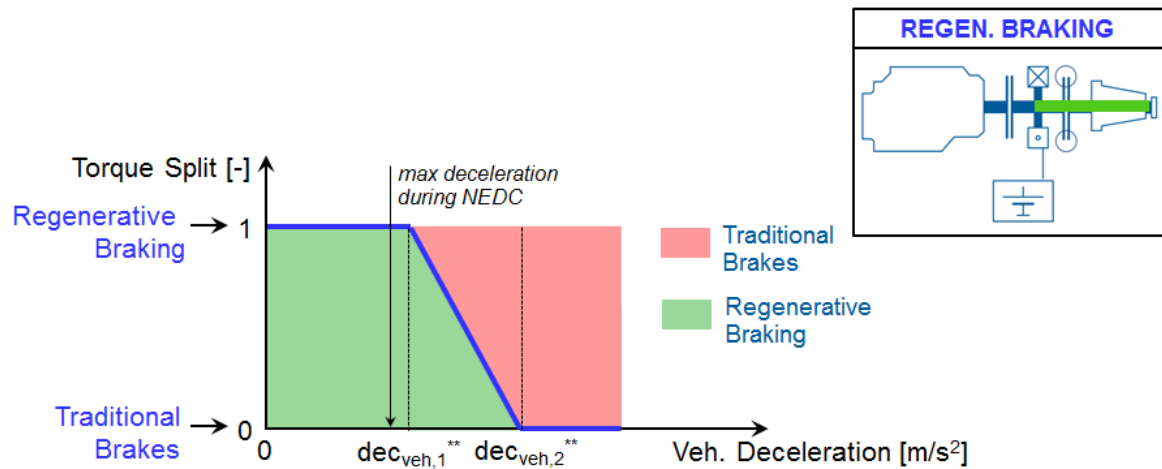


Figure 15: Operating Strategy – Regenerative Braking

1.3.1.7. Range Extender Operation - Optimum Operating Line

Optimum Operating Line is an operating strategy which can only be used in range extender operation. This is due to the fact that in the range extender architecture ICE and electric generator are working in series and are independent from the electric motor driving the wheels. Therefore for each power requirement of the ICE the most effective speed can be selected which provides the required power with the highest efficiency (lowest fuel consumption).

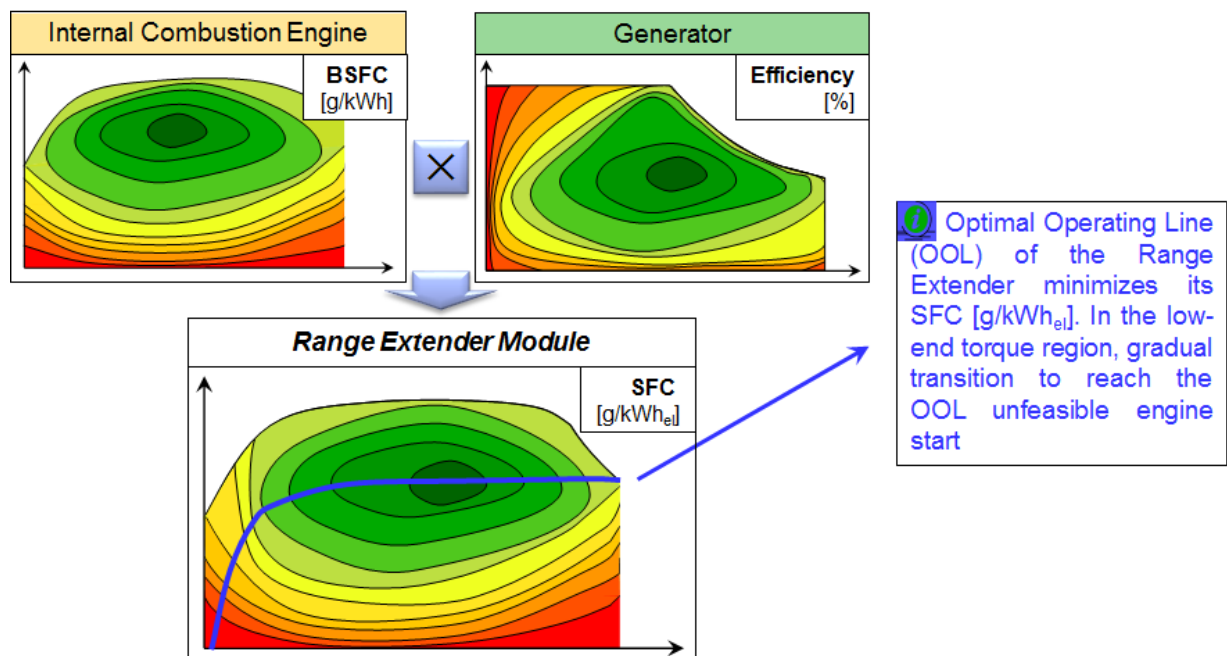


Figure 16: Operating Strategy – Range Extender Operation – Optimum Operating Line

1.3.1.8. Battery Assistance

It is applied in case of available battery energy, to supply the required electric power at full load conditions. This function is expected not to be active during the NEDC.

Battery assistance is a similar operating condition to E-Boost, but active also for constant speed driving conditions and is not limited to full load acceleration.

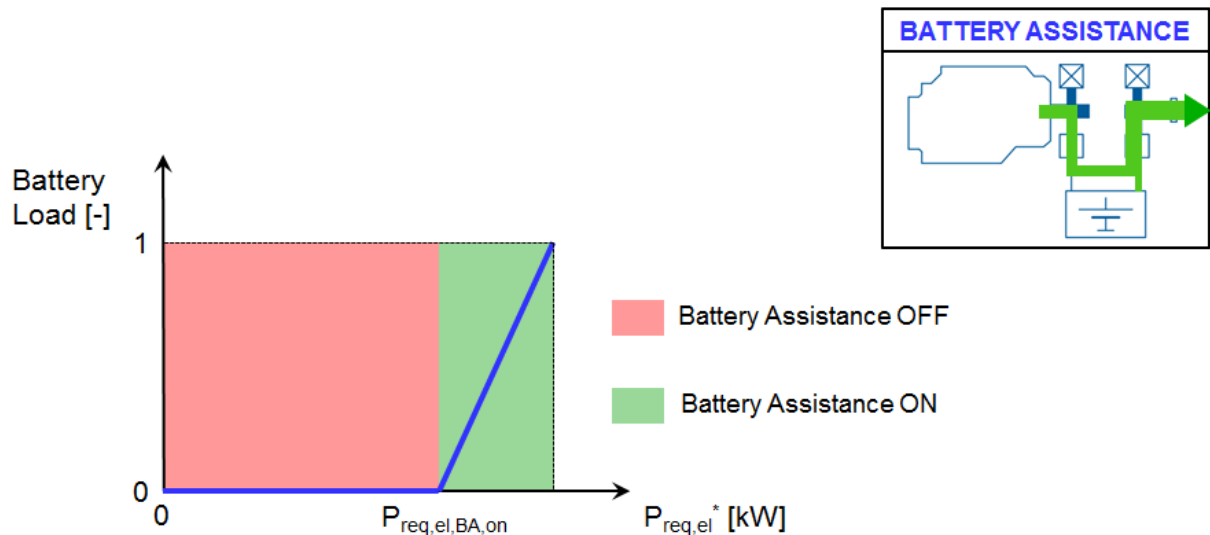


Figure 17: Operating Strategy – Battery Assistance

1.3.2. HYBRID TOPOLOGIES

For advanced vehicles the categorization is, besides the market segment, also based on the hybrid technology the vehicle is equipped with. The technologies are typically separated by how much they support and/or replace the internal combustion engine (ICE).

Depending on the hybrid topology different operating strategies may be used. Figure 18 gives an overview about the operating strategies used in different hybrid topologies.

Full HEV vehicles are typically additionally separated into standard HEVs and Plug-in HEVs. The main difference is that for Plug-in HEVs the battery can be charged at an electric power charger outside of the vehicle, for standard HEVs charging of the battery is done only by regenerative braking or via the ICE.

		Operating Strategy							
		Start & Stop	E-Drive	Load Point Moving	ICE Alone	E-Boost	Regenerative Braking	Optimum Operating Line	Battery Assistance
Hybrid Topology	Baseline								
	Micro HEV								
	Mild Hybrid								
	Full HEV								
	REX								
	EV								

HEV ... Hybrid Electric Vehicle
 REX ... Range Extender
 EV ... Electric Vehicle

Figure 18: Operating Strategies used in different Hybrid Topologies

1.3.3. VEHICLE MODELS

Sixteen different advanced vehicle models were generated using the simulation tool AVL CRUISE. Those models cover 7 different vehicle classes (A, B, C, D, E, F and J), as well as different transmission types (manual transmission MT, automated manual transmission AMT, automatic transmission AT and continuously variable transmission CVT) and hybrid topologies (Mild & Full Hybrid Electric Vehicle, full electric vehicle EV, range extender electric vehicle REX). The table below shows the vehicle models generated and validated. The first 15 models were mainly validated against type approval tests or if available by internal tests carried out at AVL.

For the 16th model (Toyota Prius III Plugin) an extensive measurement campaign on the chassis dyno as well as real lift tests were carried out at LAT. Based on this information a reverse engineering of the vehicle model in CRUISE was carried out. This vehicle is described in chapter 3.3.9.

Table 8: Overview Advanced Vehicle Models

Nr	Vehicle	Vehicle Class	ICE Type	Transmission	Hybrid Topology
1	Mitsubishi i MiEV	A	-	-	EV
2	SMART Fortwo coupe 52 kW mhd	A	Gasoline	AMT	Baseline
3	Audi A1 etron	B	Rotary	-	REX
4	Audi A3 1.4 TFSi	C	Gasoline	MT	Baseline
5	BMW 116i	C	Gasoline	MT	Baseline
6	Honda Civic Hybrid	C	Gasoline	m-CVT	Full HEV
7	Toyota Prius III	C	Gasoline	e-CVT	Full HEV
8	Volvo C30 T5	C	Gasoline	AT	Baseline
9	VW Golf 1.4L TSi	C	Gasoline	MT	Micro HEV
10	Volvo S60 D5	D	Diesel	AMT	Baseline
11	AUDI A6 3.0 TFSi quattro	E	Gasoline	DCT	Baseline
12	Fisker Karma	E	Gasoline	-	REX
13	Mercedes Benz S 400 HYBRID	F	Gasoline	AT	Mild Hybrid
14	BMW X1 20d sDrive	J	Diesel	MT	Micro HEV
15	Nissan Pathfinder 3.0L CVT	J	Gasoline	m-CVT	Baseline
16	Toyota Prius III Plugin	C	Gasoline	e-CVT	Plugin HEV

The vehicle classes are defined as shown in the General Car Segments column in Figure 1

All vehicle models, including their validation results, are specified in detail in the following chapters.

The data for the advanced simulation models are mainly taken from public data sources such as official homepages or vehicle test reports. Data not available at such sources are assessed based on AVL internal data base or are derived from comparable vehicles.

The validation of the different advanced vehicle models is done against published data, mainly the fuel consumption of the legislative test cycles (e.g. NEDC or FTP).

Since in ICT-Emissions it is planned to simulate also real world cycles, all advanced vehicle models are already basically tested for the supplied WLTP driving cycles.

The control logic required e.g. for the hybrid vehicles is realized in c-code directly within the CRUISE model or in Matlab Simulink. The controllers are initially optimized for the NEDC.

The selected vehicles of course cover only a small fraction of all possible combinations of vehicle segment and hybrid topology (see Figure 19), especially when considering additionally the transmission type. However especially for the advanced vehicles currently not all hybrid topologies exist in all vehicle segments (especially Diesel equipped cars) and sometimes only a single vehicle exists in one category. Therefore a generalization like for the conventional vehicles is not possible yet. This may be possible in the future when more and more hybrid vehicles exist on the market.

				Gasoline					Diesel					Electric Vehicle
				Baseline	Micro HEV	Mild Hybrid	Full HEV	REX	Baseline	Micro HEV	Mild Hybrid	Full HEV	REX	
Vehicle Segment	A	ICT Condensed Segments	A'	X										X
	B		B'					X						
	C		C'	X	X		X							
	D		D'						X					
	E			X				X						
	F					X								
	S			not covered in ICT Emissions										
	M		E'											
	J			X						X				

Figure 19: Coverage of advanced vehicles within possible combinations of vehicle segment and hybrid topology

1.3.3.1. Vehicle 1 – Mitsubishi iMiEV

The Mitsubishi iMiEV is a rear wheel driven (RWD) pure electric vehicle (EV). Only a limited number of different operating strategies are possible for electric vehicles (see Figure 20).

Hybrid Topology	Operating Strategy							
	Start & Stop	E-Drive	Load Point Moving	ICE Alone	E-Boost	Regenerative Braking	Optimum Operating Line	Battery Assistance
EV		X				X		

Figure 20: Hybrid Topology – Mitsubishi iMiEV

1.3.3.1.1. AVL CRUISE Model Layout

The vehicle layout in CRUISE is shown in Figure 21. It consists of the main parts of the drivetrain (electric motor, single transmission step, differential, brakes, rear wheels), additional vehicle parts such as the vehicle itself and the front wheels with their brakes and parts of the electric system such as the battery and electrical consumers. Compared to a conventional vehicle the ICE and the gear box are missing and are replaced by the electric motor which drives the rear wheels. Auxiliaries like heating are driven electrically and are considered by an electric consumer.

The control logic is defined as macro in the main vehicle model. The content of the control logic is shown in Figure 22. Different characteristic maps and functions are used to provide the operating strategies for e-Drive and regenerative braking. The information from the control logic is supplied via data bus channels to the electric motor and the brakes.

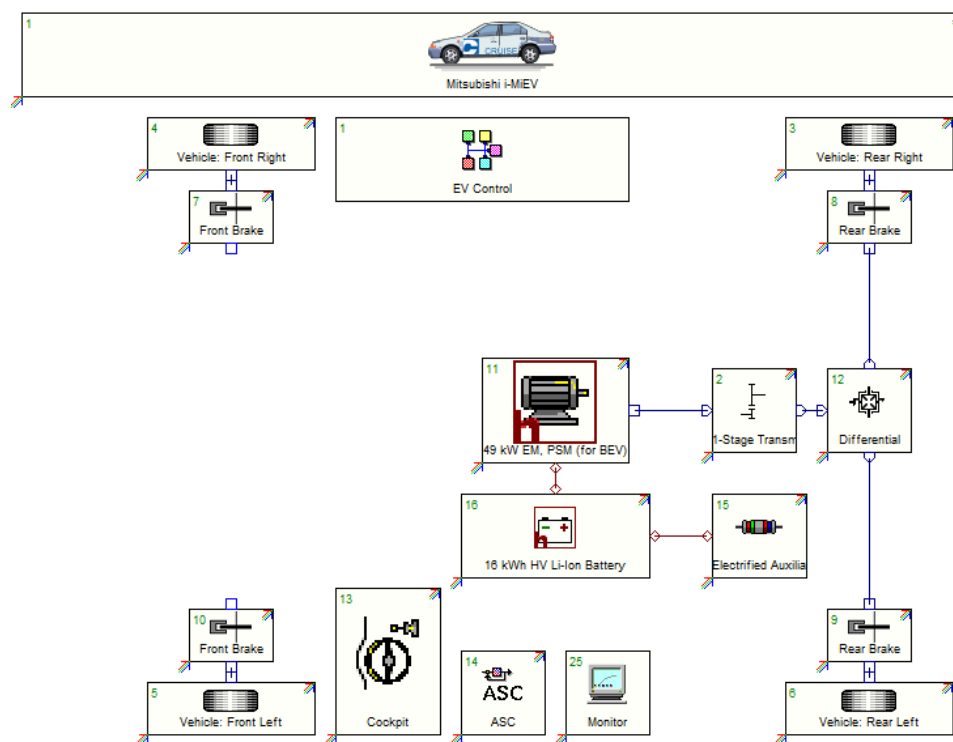


Figure 21: AVL CRUISE Model Mitsubishi iMieV

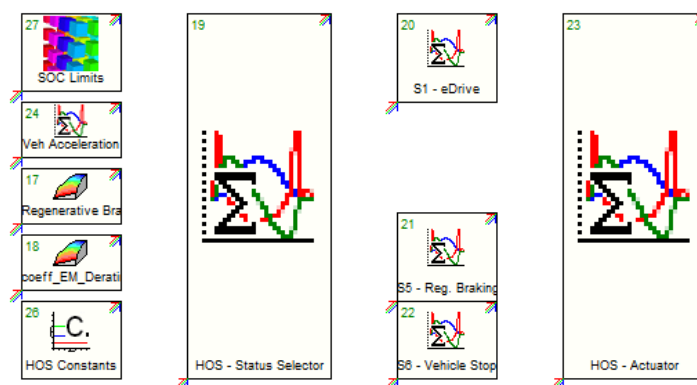


Figure 22: EV Control Logic Mitsubishi iMieV

1.3.3.1.2. Simulation Input Data

Some of the main characteristic input data of the vehicle model is listed in Figure 23.


Vehicle 1		Combustion Engine	
OEM	Mitsubishi	Type	-
Model	iMiEV	Displacement	- L
Model Year	2010	Max. Power	- kW @ rpm
Class	A	Max. Torque	- Nm @ rpm
Powertrain	EV, RWD	Transmission	
		Type	-
		No. of Gears	-
		Tire	
		Size	175/55R15
		E-Machine	
		Max. Power	49 / 2500-8000 kW / rpm
		Max. Torque	180 / 0-2000 Nm / rpm
		Battery	
		Capacity	16 kWh

Figure 23: Simulation Input Data Mitsubishi iMieV

1.3.3.1.3. CRUISE Model Validation Results

The AVL CRUISE simulation model is validated against the published All Electric Range (AER) of 150 km in NEDC cycle.

The deviation between published and simulated AER is within the expected error margin considering the accuracy and availability of the input data.

Detailed validation results are shown in Figure 24.


Vehicle 1 Mitsubishi iMieV		
NEDC AER		
published	150	km
simulated	142.5	km
Deviation	5%	

Figure 24: Validation Result Mitsubishi iMieV

1.3.3.2. Vehicle 2 – SMART Fortwo Coupe 52kW mhd

The SMART Fortwo Coupe 52kW mhd is a rear wheel driven (RWD) conventional vehicle with start stop system. Only a limited number of different operating strategies are possible for this vehicle (see Figure 25).

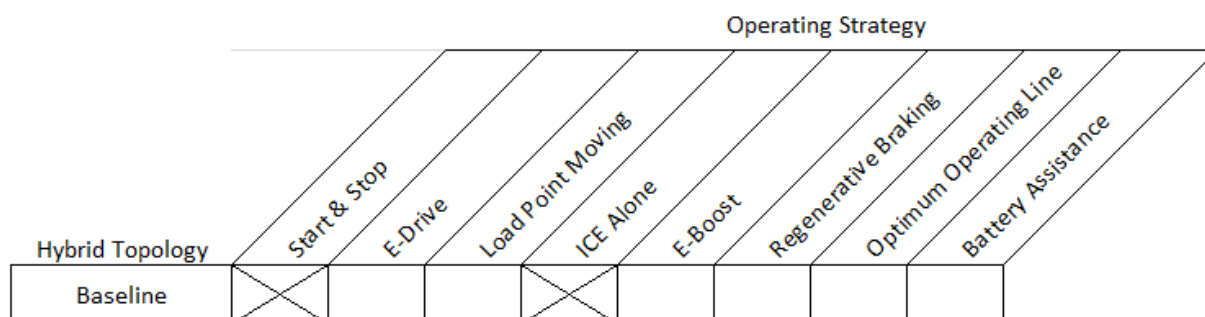


Figure 25: Hybrid Topology – SMART Fortwo Coupe 52kW mhd

1.3.3.2.1. AVL CRUISE Model Layout

The vehicle layout in CRUISE is shown in Figure 26. It consists of the main parts of the drivetrain (ICE, clutch, gear box, final drive, brakes, rear wheels), additional vehicle parts such as the vehicle itself and the front wheels with their brakes and control systems. Auxiliaries such as the alternator are considered by a mechanical consumer.

Since the SMART Fortwo is equipped with an automated manual transmission (AMT), the controls include shifting controls for the AMT as well as a control when the gear box switches into idle and the start-stop control. For most of these controls separate control elements exist within CRUISE which are used for this purpose.

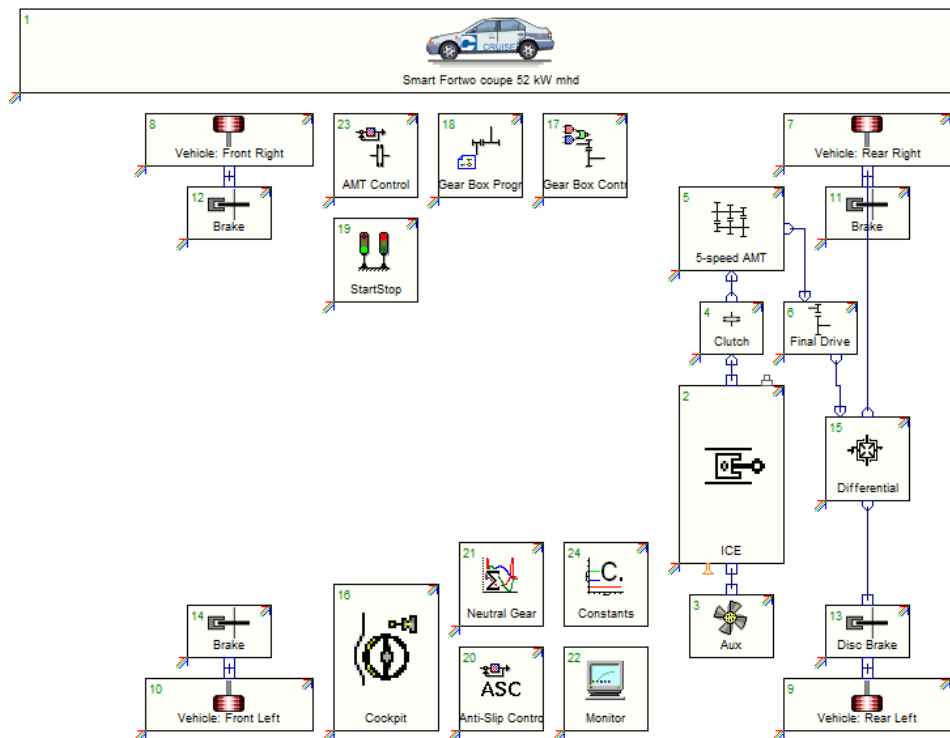


Figure 26: AVL CRUISE Model SMART Fortwo Coupe 52kW mhd

1.3.3.2.2. Simulation Input Data

Some of the main characteristic input data of the vehicle model is listed in Figure 27.


Vehicle 2		Combustion Engine	
OEM	SMART	Type	Gasoline, NA
Model	Fortwo coupe 52kW mhd	Displacement	1.0 L
Model Year	2010	Max. Power	52 / 5800 kW @ rpm
Class	A	Max. Torque	92 / 2800 Nm @ rpm
Powertrain	RWD	Transmission	
		Type	AMT
		No. of Gears	5
		Tire	
		Size	175/55 R15
		E-Machine	
		Max. Power	- kW
		Max. Torque	- Nm
		Battery	
		Capacity	- kWh

Figure 27: Simulation Input Data SMART Fortwo Coupe 52kW mhd

1.3.3.2.3. CRUISE Model Validation Results

The AVL CRUISE simulation model is validated against the published NEDC cycle fuel consumption.

The deviation between published and simulated vehicle fuel consumption is within the expected margin of error considering the accuracy and availability of the input data.

Detailed validation results are shown in Figure 28.


Vehicle 2 Smart Fortwo coupe		
NEDC hot Fuel Consumption		
simulated	3.9	l/100km
NEDC cold Fuel Consumption		
published	4.2	l/100km
simulated	4.3	l/100km
Deviation	3%	

Figure 28: Validation Result SMART Fortwo Coupe 52kW mhd

1.3.3.3. Vehicle 3 – Audi A1 etron

The Audi A1 etron is a front wheel driven (FWD) Range Extender (REX) vehicle on an Audi A1 platform. The range extender in this vehicle is a rotary engine. For range extender vehicles a lot of different operating strategies are possible (see Figure 29).

This vehicle is a demonstration vehicle of AVL for a very compact configuration of a range extender, the rotary engine being very small in size.

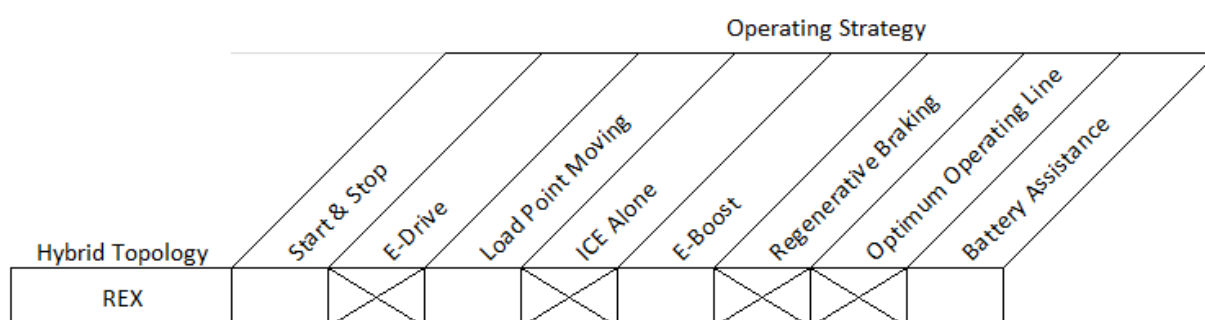


Figure 29: Hybrid Topology – Audi A1 etron

1.3.3.3.1. AVL CRUISE Model Layout

The vehicle layout in CRUISE is shown in Figure 30. The series layout of the drivetrain is clearly visible, starting from the ICE which drives the generator. The generator charges the battery which again supplies the electric energy to the electric motor which drives the wheels through a single transmission step. Typically the ICE is not running and the entire vehicle is driven only by electric energy similar like a purely electric vehicle. Only if the battery charge

falls below a defined threshold, the combustion engine is started and charges the battery through the generator.

The control of the range extender is done through various characteristic map and an externally linked control using c-code. The c-code is linked by a dynamic link library (DLL = pre-compiled code). In order to be able to change parameters of the control without touching the c-code itself (avoiding new compilation of the code for each change) the parameters and characteristics are defined as separate components in the CRUISE model.

For the Audi A1 etron most of the data of the control is available at AVL, however the full complexity of the real control cannot be modelled since not all of the necessary control information is available inside the CRUISE model.

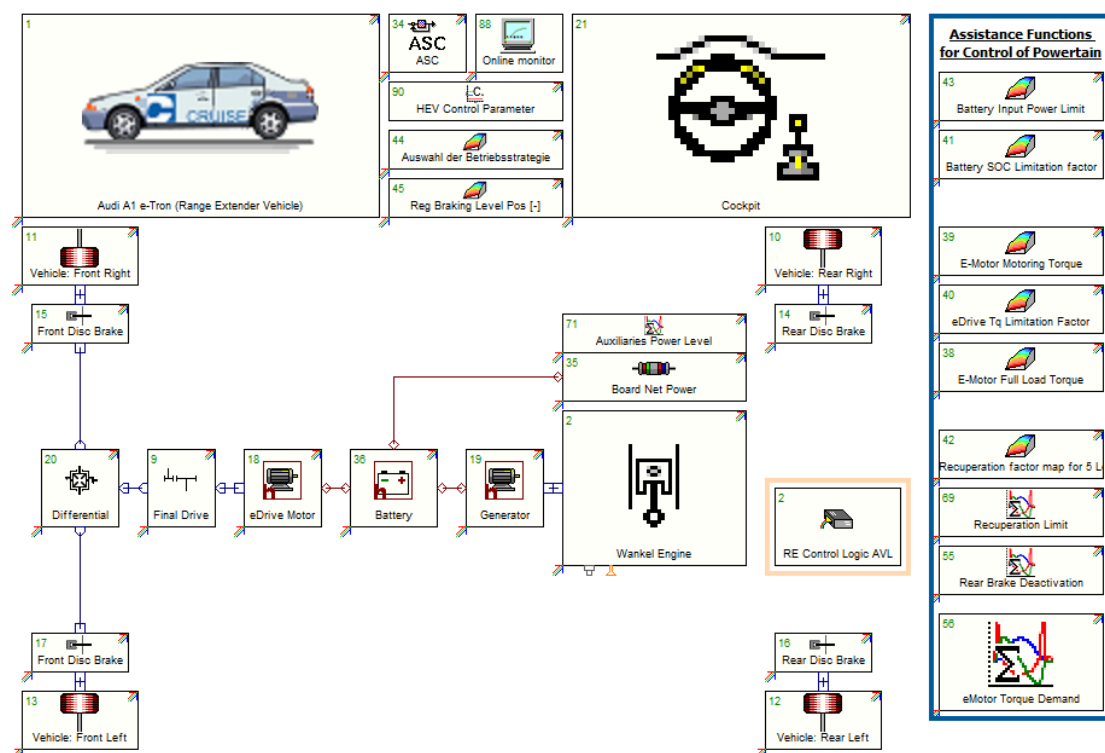


Figure 30: AVL CRUISE Model Audi A1 etron

1.3.3.3.2. Simulation Input Data

Some of the main characteristic input data of the vehicle model is listed in Figure 31.


Vehicle 3		Combustion Engine		
OEM	Audi	Type	Wankel	
Model	A1 etron	Displacement	0.3	L
Model Year	2012	Max. Power	-	kW @ rpm
Class	B	Max. Torque	-	Nm @ rpm
Powertrain	REX, FWD	Transmission		
		Type	-	
		No. of Gears	-	
		Tire		
		Size	215/40 R17	
		E-Machine		
		Max. Power	125	kW
		Max. Torque	300	Nm
		Battery		
		Capacity	12.8	kWh

Figure 31: Simulation Input Data Audi A1 etron

1.3.3.3.3. CRUISE Model Validation Results

The AVL CRUISE simulation model is validated against measured data from AVL test track.

The deviation between published and simulated vehicle fuel consumption is within the expected margin of error considering the accuracy and availability of the input data.

Detailed validation results for the e-machine are shown in Figure 32.

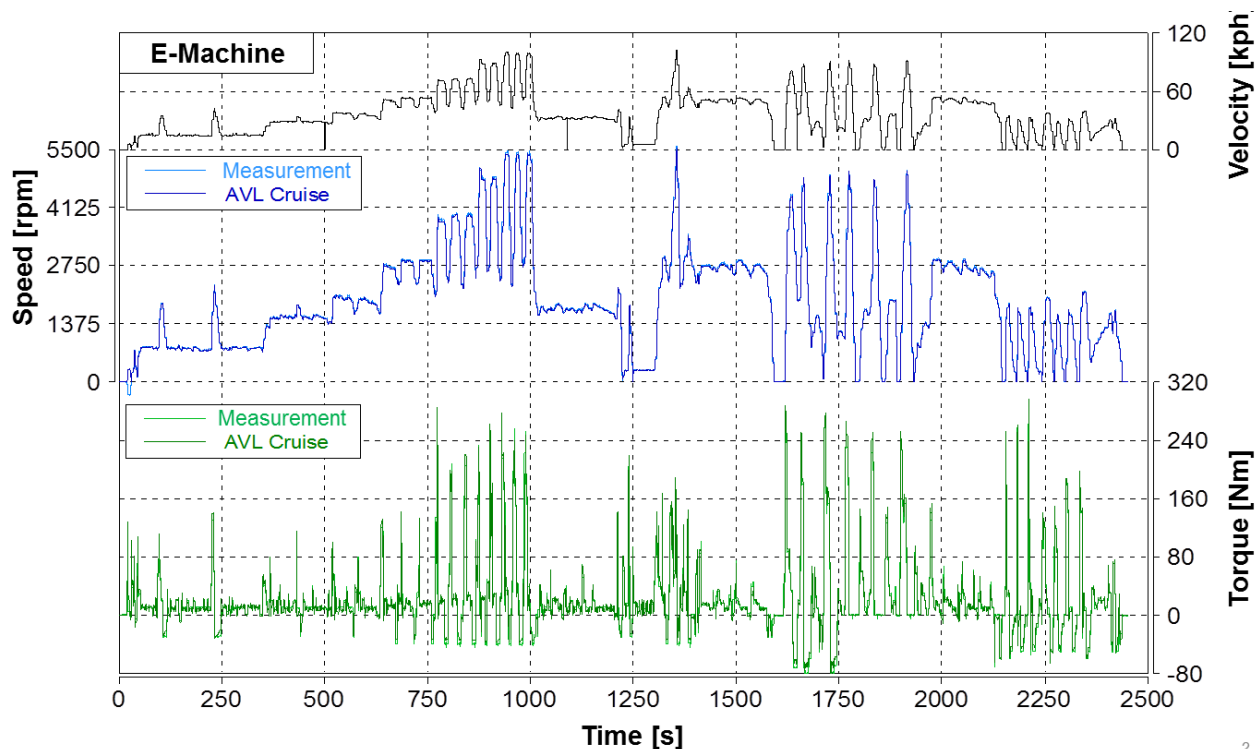


Figure 32: Simulation model validation results Audi A1 etron

The comparison shows a very good correlation between simulation and measurement.

1.3.3.4. Vehicle 4 – Audi A3 1.4 TFSI

The Audi A3 1.4 TFSI is a front wheel driven (FWD) conventional vehicle with start stop system. Only a limited number of different operating strategies are possible for this vehicle (see Figure 33).

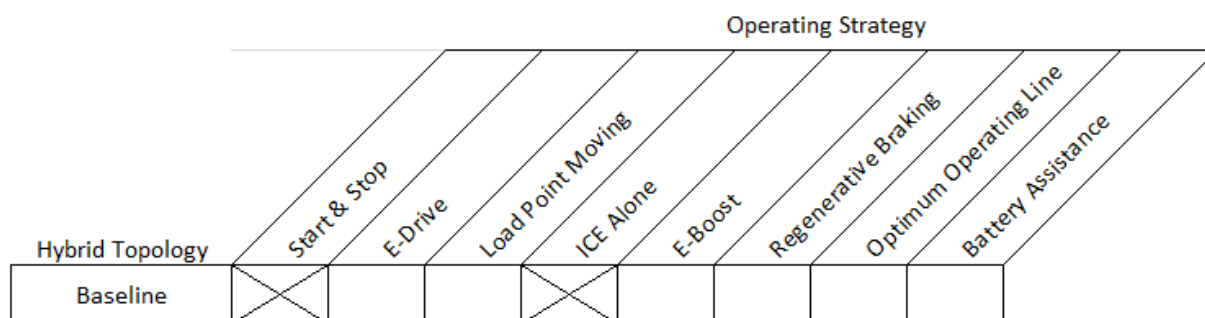


Figure 33: Hybrid Topology – Audi A3 1.4 TFSI

1.3.3.4.1. AVL CRUISE Model Layout

The vehicle layout in CRUISE is shown in Figure 34. It consists of the main parts of the drivetrain (ICE, clutch, gear box, final drive, brakes, front wheels), additional vehicle parts such as the vehicle itself and the rear wheels with their brakes and control systems. Auxiliaries such as the alternator are considered by a mechanical consumer.

Since the Audi A3 is equipped with an automated manual transmission (AMT), the controls include shifting controls for the AMT and the start-stop control. For most of these controls separate control elements exist within CRUISE which are used for this purpose.

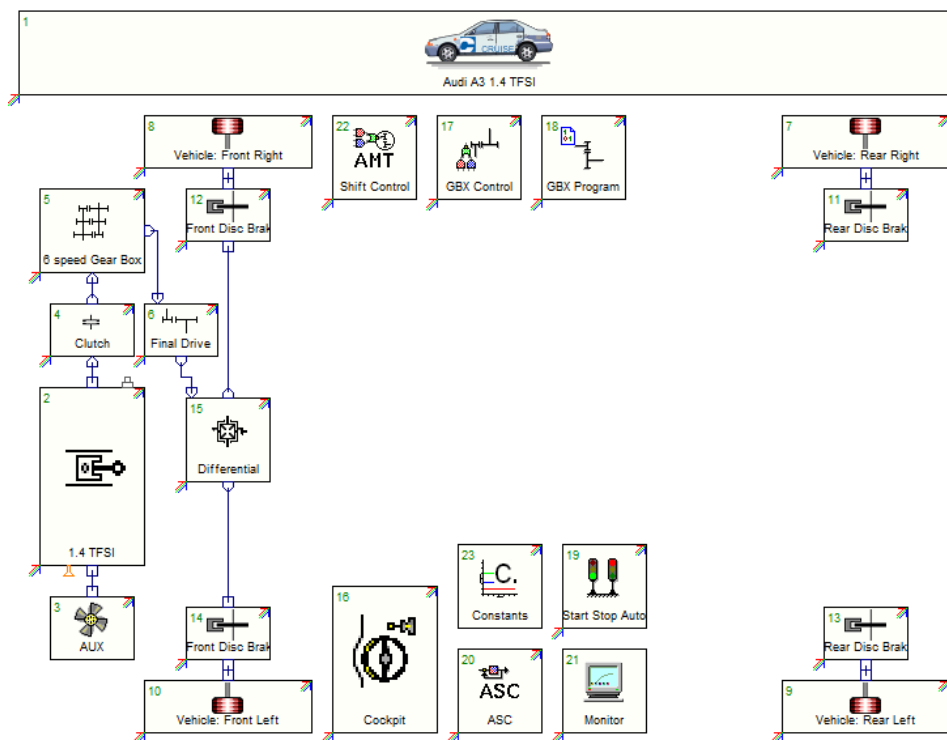


Figure 34: AVL CRUISE Model Audi A3 1.4 TFSI

1.3.3.4.2. Simulation Input Data

Some of the main characteristic input data of the vehicle model is listed in Figure 35.


Vehicle 4		Combustion Engine	
OEM	Audi	Type	Gasoline
Model	A3 1.4 TFSI	Displacement	1.4 L
Model Year	2012	Max. Power	92 / 5000 kW @ rpm
Class	C	Max. Torque	200 / 1400 Nm @ rpm
Powertrain	FWD	Transmission	
		Type	MT
		No. of Gears	6
		Tire	
		Size	205/55 R16
		E-Machine	
		Max. Power	- kW
		Max. Torque	- Nm
		Battery	
		Capacity	- kWh

Figure 35: Simulation Input Data Audi A3 1.4 TFSI

1.3.3.4.3. CRUISE Model Validation Results

The AVL CRUISE simulation model is validated against the published NEDC cycle fuel consumption.

The deviation between published and simulated vehicle fuel consumption is within the expected error margin considering the accuracy and availability of the input data.

Detailed validation results are shown in Figure 36.


Vehicle 4 Audi A3 1.4 TFSI		
NEDC hot Fuel Consumption		
simulated	4.7	l/100km
NEDC cold Fuel Consumption		
published	5.2	l/100km
simulated	5.2	l/100km
Deviation	0%	

Figure 36: Validation Result Audi A3 1.4 TFSI

1.3.3.5. Vehicle 5 – BMW 116i

The BMW 116i is a rear wheel driven (RWD) conventional vehicle with start stop system. Only a limited number of different operating strategies are possible for this vehicle (see Figure 37: Hybrid Topology – BMW 116i

).

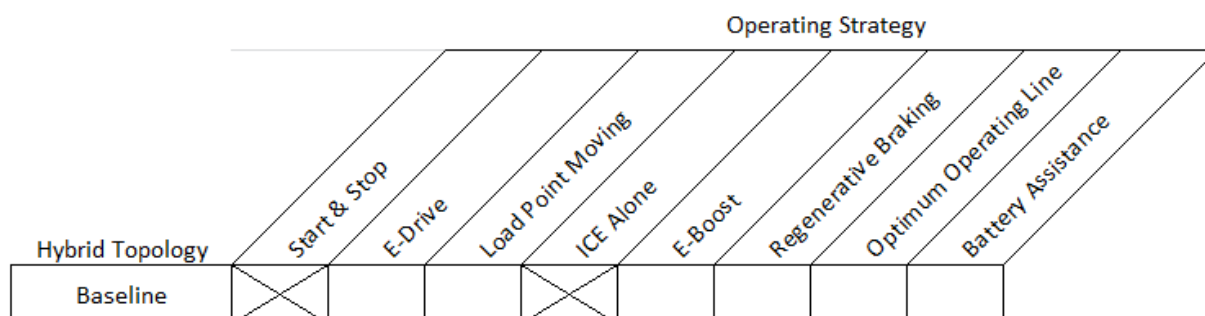


Figure 37: Hybrid Topology – BMW 116i

1.3.3.5.1. AVL CRUISE Model Layout

The vehicle layout in CRUISE is shown in Figure 38. It consists of the main parts of the drivetrain (ICE, clutch, gear box, final drive, brakes, rear wheels), additional vehicle parts such as the vehicle itself and the front wheels with their brakes and control systems. Auxiliaries such as the alternator are considered by a mechanical consumer.

The BMW 116i is equipped with a conventional manual gear box. Still the model features shifting controls since they allow a better definition of the shifting procedure compared to the driver model in CRUISE. The start-stop control is considered by a separate component in the CRUISE model.

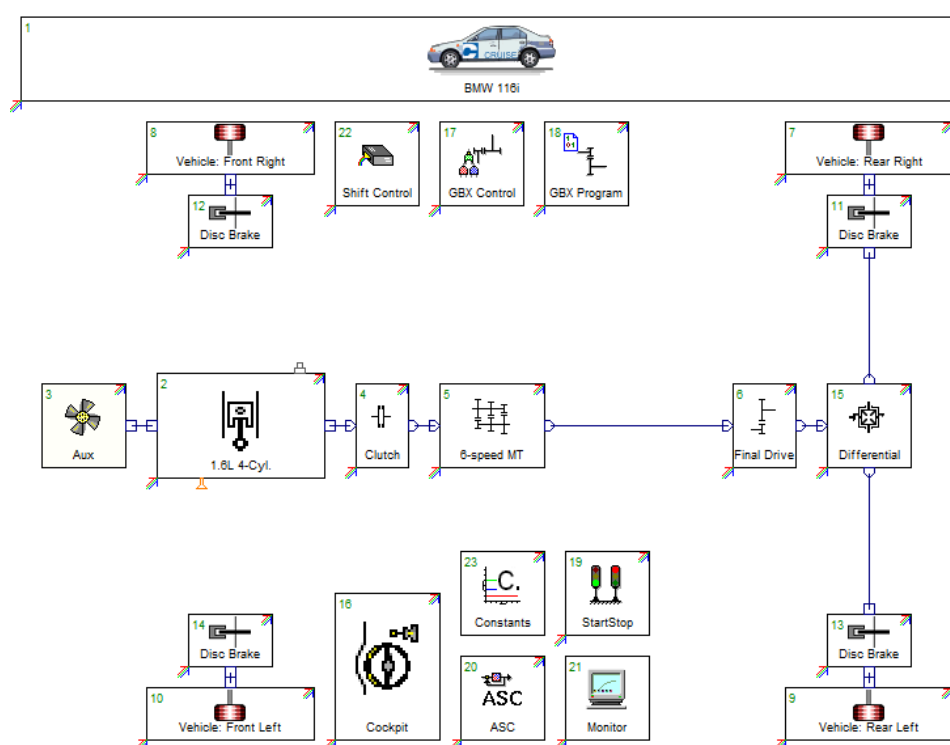


Figure 38: AVL CRUISE Model BMW 116i

1.3.3.5.2. Simulation Input Data

Some of the main characteristic input data of the vehicle model is listed in Figure 39.


Vehicle 5		Combustion Engine	
OEM	BMW	Type	Gasoline
Model	116i	Displacement	1.6 L
Model Year	2011	Max. Power	100 / 4400 kW @ rpm
Class	C	Max. Torque	220 / Nm @ rpm
Powertrain	RWD	1350	
		Type	MT
		No. of Gears	6
		Tire	
		Size	195/55 R16
		E-Machine	
		Max. Power	- kW
		Max. Torque	- Nm
		Battery	
		Capacity	- kWh

Figure 39: Simulation Input Data BMW 116i

1.3.3.5.3. CRUISE Model Validation Results

The AVL CRUISE simulation model is validated against the published NEDC cycle fuel consumption.

The deviation between published and simulated vehicle fuel consumption is within the expected margin of error considering the accuracy and availability of the input data.

Detailed validation results are shown in Figure 40.


Vehicle 5		BMW 116i
NEDC hot Fuel Consumption		
simulated	5.1	l/100km
NEDC cold Fuel Consumption		
published	5.5	l/100km
simulated	5.7	l/100km
Deviation	3%	

Figure 40: Validation Result BMW 116i

1.3.3.6. Vehicle 6 – Honda Civic Hybrid

The Honda Civic Hybrid is a front wheel driven (FWD) hybrid vehicle. The hybrid is a parallel topology with torque converter and CVT. Parallel topology means that ICE and electric motor act on the same drivetrain and are coupled to each other. In case of the Honda Civic Hybrid the electric motor is directly coupled to the ICE without any clutch in between. This means that ICE and electric motor always run with the same speed. Nearly all different operating strategies are possible for this vehicle (see Figure 41).

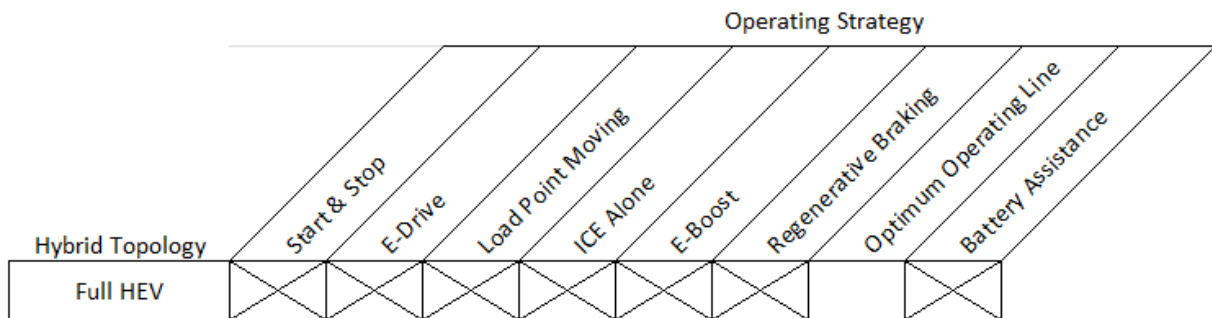


Figure 41: Hybrid Topology – Honda Civic Hybrid

1.3.3.6.1. AVL CRUISE Model Layout

The vehicle layout in CRUISE is shown in Figure 42. It consists of the main parts of the drivetrain (ICE, electric motor, torque converter, CVT, final drive, brakes, front wheels), additional vehicle parts such as the vehicle itself and the rear wheels with their brakes and control systems. Auxiliaries such as the alternator are considered by a mechanical consumer.

The electric network includes beside the electric motor also the battery and electrical consumers. The control is defined in Matlab Simulink and coupled to the CRUISE model. Additional data for the control such as characteristic maps and other functions are directly included in the CRUISE model. The control only controls the activation of electric motor and ICE and the loads for both engines. The transmission is controlled by a separate CVT control which defines the transmission ratio for the CVT.

Since no data of the control exist at AVL all data for the control were defined based on AVL internal experience.

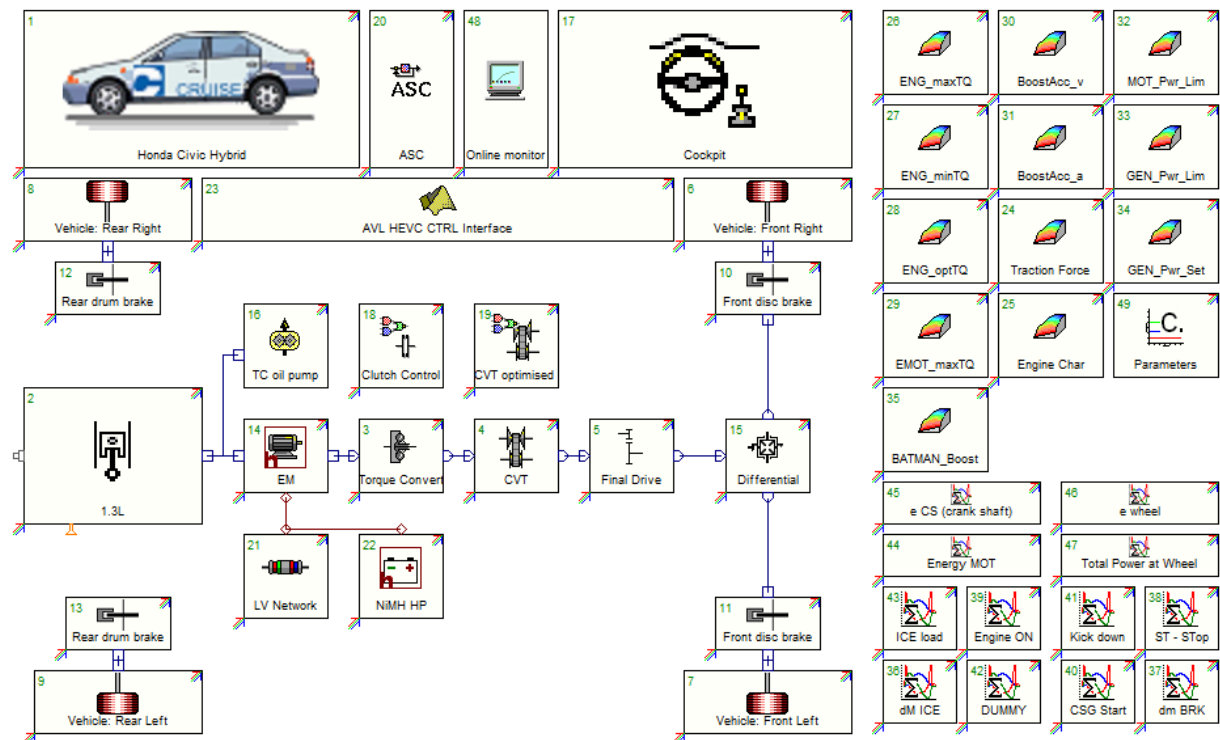


Figure 42: AVL CRUISE Model Honda Civic Hybrid including HCU control logic

1.3.3.6.2. Simulation Input Data

Some of the main characteristic input data of the vehicle model is listed in Figure 43.


Vehicle 6		Combustion Engine	
OEM	Honda	Type	Gasoline
Model	Civic Hybrid	Displacement	1.3 L
Model Year	2008	Max. Power	82 / 6000 kW @ rpm
Class	C	Max. Torque	167 / 2500 Nm @ rpm
Powertrain	Full Hybrid, FWD	Transmission	
		Type	CVT
		No. of Gears	-
		Tire	
		Size	195/65 R15
		E-Machine	
		Max. Power	15 kW
		Max. Torque	Nm
		Battery	
		Capacity	0.9 kWh

Figure 43: Simulation Input Data Honda Civic Hybrid

1.3.3.6.3. CRUISE Model Validation Results

The AVL CRUISE simulation model is validated against the published NEDC cycle fuel consumption.

The deviation between published and simulated vehicle fuel consumption is within the expected error margin considering the accuracy and availability of the input data.

Detailed validation results are shown in Figure 44.


Vehicle 6 Honda Civic Hybrid		
NEDC hot Fuel Consumption		
simulated	4.3	l/100km
NEDC cold Fuel Consumption		
published	4.6	l/100km
simulated	4.8	l/100km
Deviation	4%	

Figure 44: Validation Result Honda Civic Hybrid

1.3.3.7. Vehicle 7– Toyota Prius III

The Toyota Prius III is a front wheel driven (FWD) full hybrid vehicle with e-CVT. E-CVT means that there is no conventional CVT installed in the vehicle, but a planetary gear set is placed between ICE, electric motor, and wheels. At the wheel side an additional electric motor is installed. By controlling the speed of both electric motors different transmission ratios can be achieved. Nearly all different operating strategies are possible for this vehicle (see Figure 45).

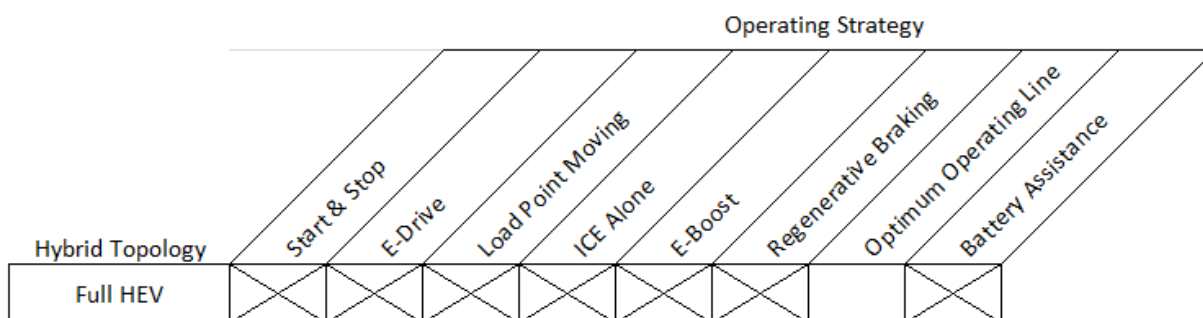


Figure 45: Hybrid Topology – Toyota Prius III

1.3.3.7.1. AVL CRUISE Model Layout

The vehicle layout in CRUISE is shown in Figure 46. The components as described before (2 electric motors, 1 ICE) are placed around the planetary gear box. The output finally drives through the final drive the front wheels. The electric system consists beside the 2 electric machines of the battery and an additional electric consumer.

The control of the hybrid system (activation of ICE and both electric machines) is defined in Matlab Simulink and is coupled to the CRUISE model. Additional data for the control such as characteristic maps, parameters, and other functions are directly included in the CRUISE model. The control controls the activation of both electric motors and the ICE, in this way also controlling the transmission ratio between ICE and final drive.

Since no data of the control exist at AVL all data for the control were defined based on AVL internal experience.

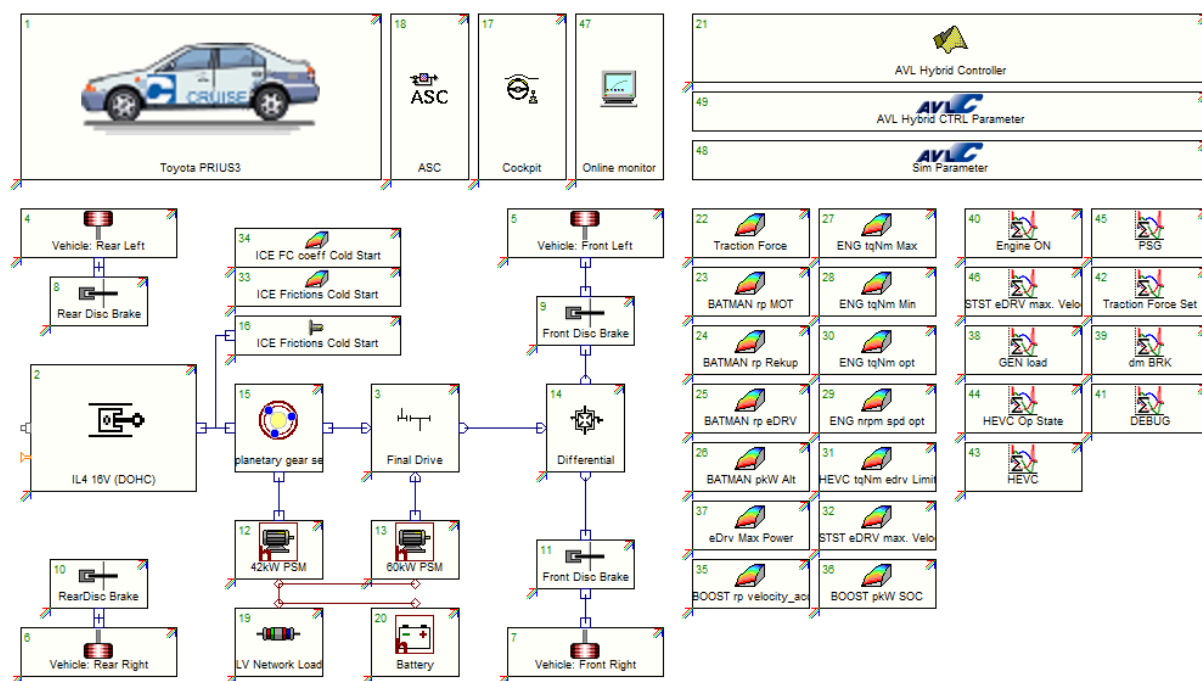


Figure 46: AVL CRUISE Model including Hybrid Control Logic of Toyota Prius III

1.3.3.7.2. Simulation Input Data

Some of the main characteristic input data of the vehicle model is listed in Figure 47.


Vehicle 7		Combustion Engine	
OEM	Toyota	Type	Gasoline
Model	Prius III	Displacement	1.8 L
Model Year		Max. Power	73 / 5200 kW @ rpm
Class	C	Max. Torque	142 / 4000 Nm @ rpm
Powertrain	Full hybrid, FWD	Transmission	
		Type	-
		No. of Gears	-
		Tire	
		Size	195/65 R15
		E-Machine	
		Max. Power	60 kW
		Max. Torque	545 Nm
		Battery	
		Capacity	1.3 kWh

Figure 47: Simulation Input Data Toyota Prius III

1.3.3.7.3. CRUISE Model Validation Results

The AVL CRUISE simulation model is validated against the published NEDC cycle fuel consumption.

The deviation between published and simulated vehicle fuel consumption is within the expected error margin considering the accuracy and availability of the input data.

Detailed validation results are shown in Figure 48.


Vehicle 7 Toyota Prius 3		
ECE cold Fuel Consumption		
published	3.9	l/100km
simulated	3.8	l/100km
EUDC hot Fuel Consumption		
published	3.7	l/100km
simulated	3.6	l/100km
NEDC cold Fuel Consumption		
published	3.9	l/100km
simulated	3.7	l/100km
Deviation	5%	

Figure 48: Validation Results Toyota Prius III

1.3.3.8. Vehicle 8 – Volvo C30 T5

The Volvo C30 T5 is a front wheel driven (FWD) conventional vehicle with automatic gear box. Only a limited number of different operating strategies are possible for this vehicle (see Figure 49).

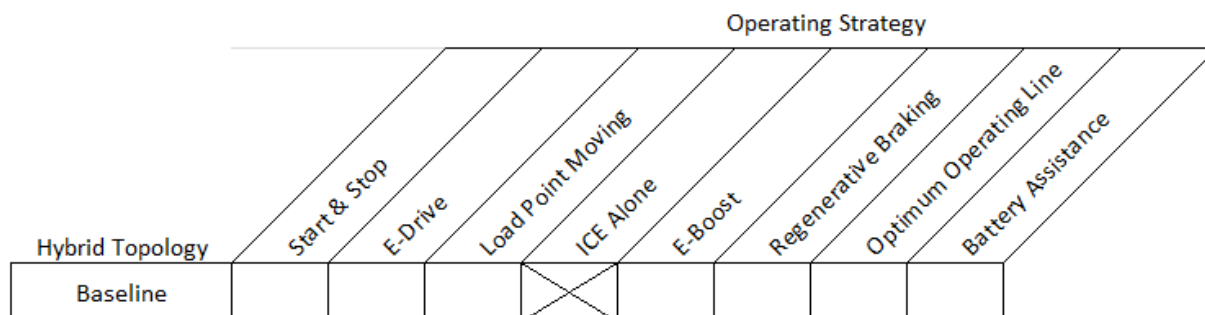


Figure 49: Hybrid Topology – Volvo C30 T5

1.3.3.8.1. AVL CRUISE Model Layout

The vehicle layout in CRUISE is shown in Figure 50. It consists of the main parts of the drivetrain (ICE, torque converter, gear box, final drive, brakes, front wheels), additional vehicle parts such as the vehicle itself and the rear wheels with their brakes and control systems. Auxiliaries such as the alternator are considered by a mechanical consumer.

The Volvo C30 is equipped with a conventional automatic transmission. The control for the gear shifting also include a special control which switches the gear box into idle during standstill, in this way avoiding losses during stop phases as the ICE does not have to drive the torque converter.

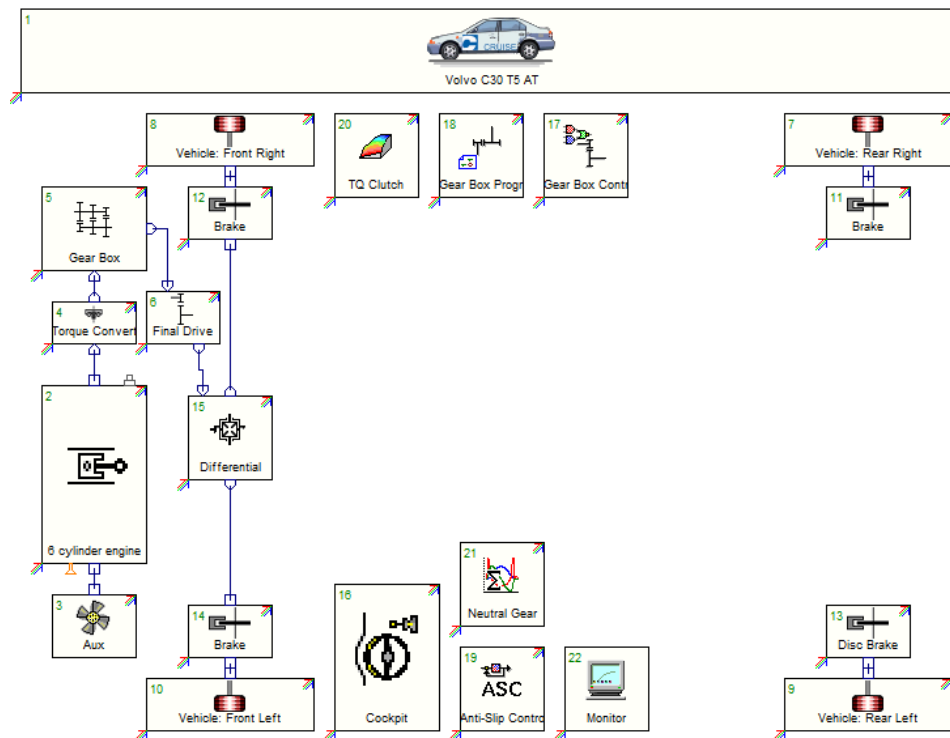


Figure 50: AVL CRUISE Model Volvo C30 T5

1.3.3.8.2. Simulation Input Data

Some of the main characteristic input data of the vehicle model is listed in Figure 51.


Vehicle 8		Combustion Engine	
OEM	Volvo	Type	Gasoline
Model	C30 T5	Displacement	2.5 L
Model Year	2012	Max. Power	169 / 5000 kW @ rpm
Class	C	Max. Torque	320 / 1500 Nm @ rpm
Powertrain	FWD	Transmission	
		Type	AT
		No. of Gears	5
		Tire	
		Size	205/55 R15
		E-Machine	
		Max. Power	- kW
		Max. Torque	- Nm
		Battery	
		Capacity	- kWh

Figure 51: Simulation Input Data Volvo C30 T5

1.3.3.8.3. CRUISE Model Validation Results

The AVL CRUISE simulation model is validated against the published NEDC cycle fuel consumption.

The deviation between published and simulated vehicle fuel consumption is within the expected error margin considering the accuracy and availability of the input data.

Detailed validation results are shown in Figure 52.


Vehicle 8 Volvo C30 T5		
NEDC hot Fuel Consumption		
simulated	8.0	l/100km
NEDC cold Fuel Consumption		
published	9.0	l/100km
simulated	8.8	l/100km
Deviation	2%	

Figure 52: Validation Result Volvo C30 T5

1.3.3.9. Vehicle 9 – VW Golf 1.4L TSI

The VW Golf 1.4L TSI is a front wheel driven (FWD) micro hybrid vehicle. Only a limited number of different operating strategies are possible for this vehicle (see Figure 53).

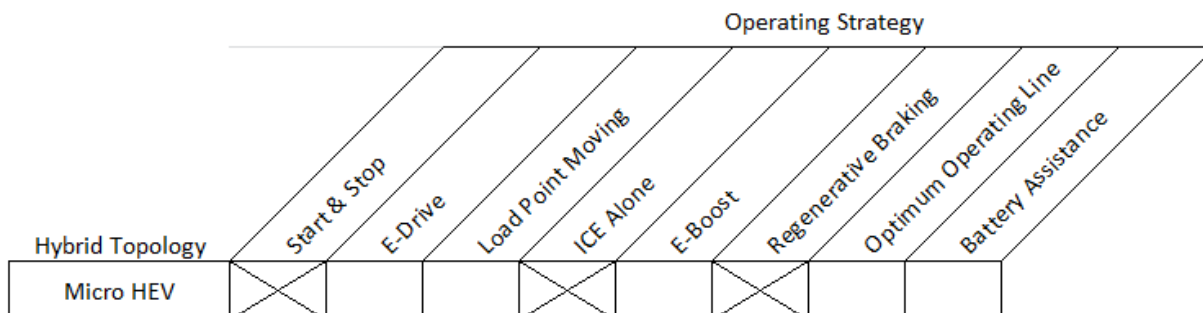


Figure 53: Hybrid Topology – VW Golf 1.4L TSI

1.3.3.9.1. AVL CRUISE Model Layout

The vehicle layout in CRUISE is shown in Figure 54. It consists of the main parts of the drivetrain (ICE, clutch, gear box, final drive, brakes, front wheels), additional vehicle parts such as the vehicle itself and the rear wheels with their brakes and control systems. Auxiliaries such as the alternator are considered by a mechanical consumer.

Since the VW Golf 1.4L TSI is equipped with an automated manual transmission (AMT), the controls include shifting controls for the AMT as well as the start-stop control. For most of these controls separate control elements exist within CRUISE which are used for this purpose.

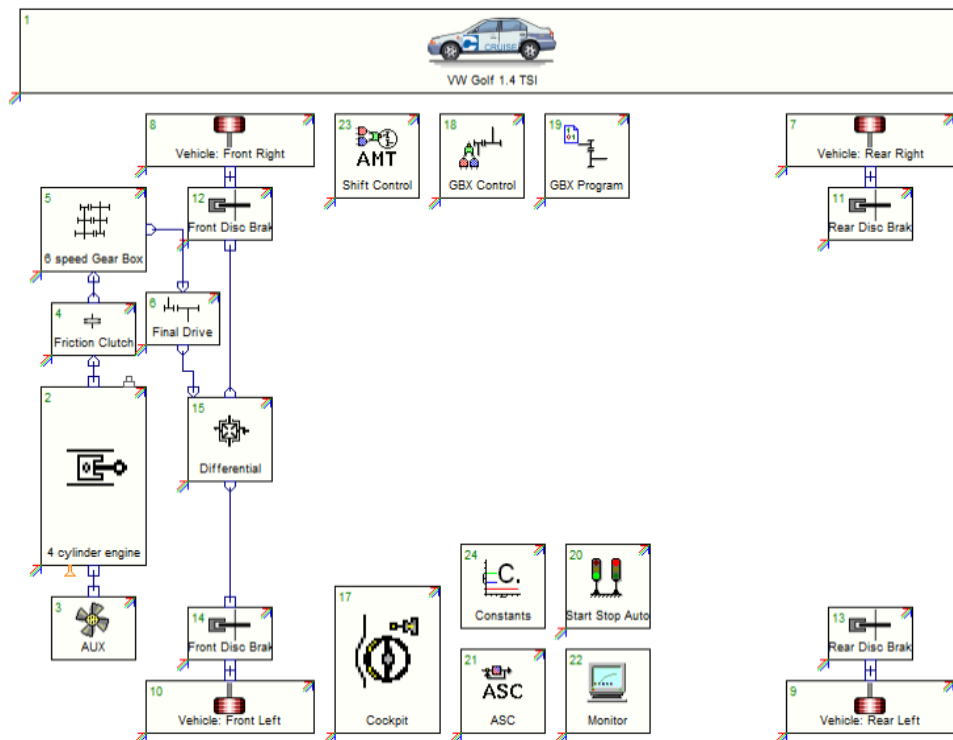


Figure 54: AVL CRUISE Model VW Golf 1.4L TSI

1.3.3.9.2. Simulation Input Data

Some of the main characteristic input data of the vehicle model is listed in Figure 55.


Vehicle 9		Combustion Engine	
OEM	VW	Type	Gasoline
Model	Golf 1.4 TSI	Displacement	1.4 L
Model Year	2012	Max. Power	103 / 4500 kW @ rpm
Class	C	Max. Torque	250 7 1500 Nm @ rpm
Powertrain	FWD	Transmission	
		Type	MT
		No. of Gears	6
		Tire	
		Size	495/65 R15
		E-Machine	
		Max. Power	- kW
		Max. Torque	- Nm
		Battery	
		Capacity	- kWh

Figure 55: Simulation Input Data VW Golf 1.4L TSI

1.3.3.9.3. CRUISE Model Validation Results

The AVL CRUISE simulation model is validated against the published NEDC cycle fuel consumption.

The deviation between published and simulated vehicle fuel consumption is within the expected error margin considering the accuracy and availability of the input data.

Detailed validation results are shown in Figure 56.


Vehicle 9 VW Golf 1.4 TSI		
NEDC hot Fuel Consumption		
simulated	4.8	l/100km
NEDC cold Fuel Consumption		
published	5.3	l/100km
simulated	5.3	l/100km
Deviation	1%	

Figure 56: Validation Result VW Golf 1.4L TSI

1.3.3.10. Vehicle 10 – Volvo S60 D5

The Volvo S60 D5 is an all wheel driven (AWD) conventional vehicle with start stop system and Diesel engine. Only a limited number of different operating strategies are possible for this vehicle (see Figure 57).

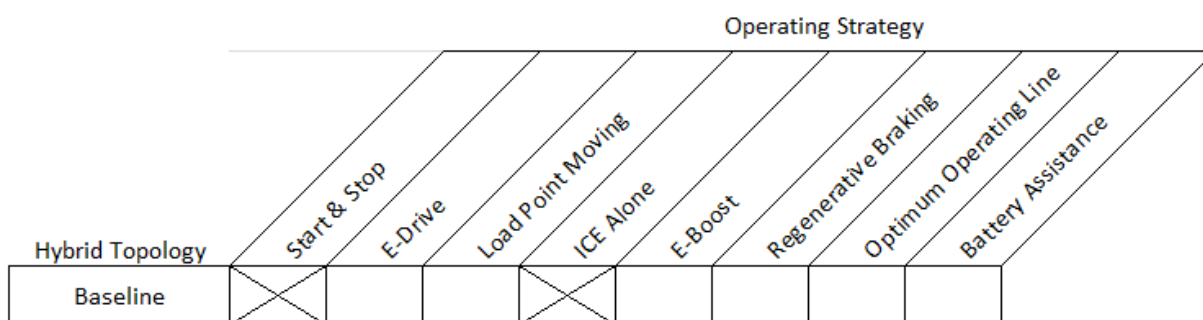


Figure 57: Hybrid Topology – Volvo S60 D5

1.3.3.10.1. AVL CRUISE Model Layout

The vehicle layout in CRUISE is shown in Figure 58. It consists of the main parts of the drivetrain (ICE, clutch, gear box, final drive, brakes, wheels), and additional vehicle parts such as the vehicle itself and control systems. As the considered model is an all wheel drive, the ICE drives front and rear wheels through a central differential. Auxiliaries such as the alternator are considered by a mechanical consumer.

The Volvo S60 D5 is equipped with an automated manual transmission (AMT). The controls include shifting controls for the AMT as well as the start-stop control. For most of

these controls separate control elements exist within CRUISE which are used for this purpose.

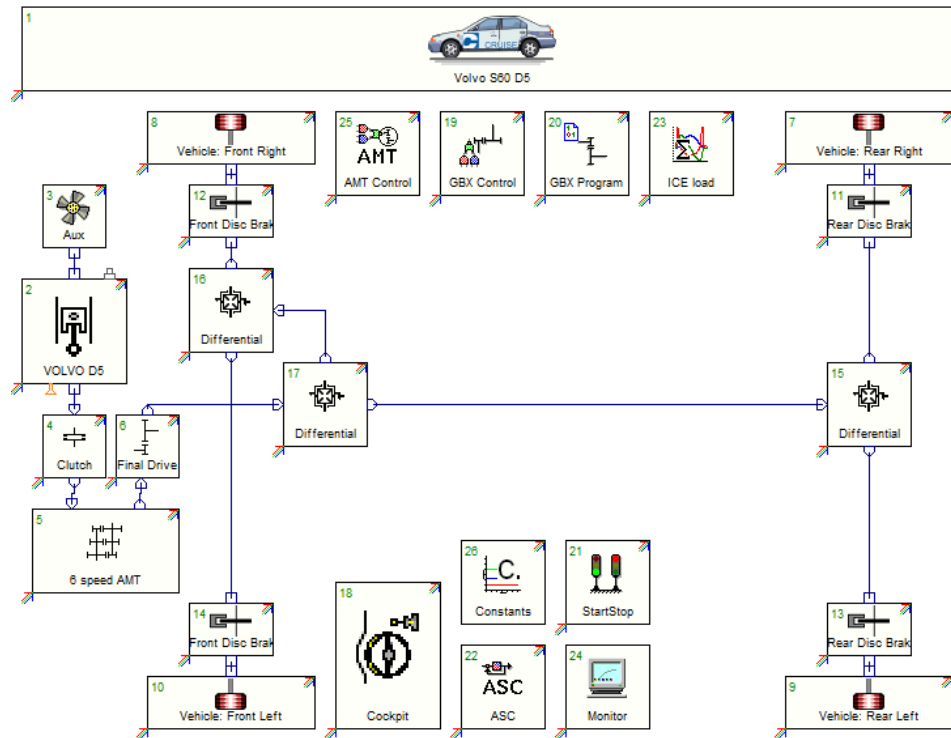


Figure 58: AVL CRUISE Model Volvo S60 D5

1.3.3.10.2. Simulation Input Data

Some of the main characteristic input data of the vehicle model is listed in Figure 59.


Vehicle 10		Combustion Engine	
OEM	Volvo	Type	Diesel
Model	S60 D5	Displacement	2.4 L
Model Year	2010	Max. Power	151 / 4000 kW @ rpm
Class	D	Max. Torque	420 / 1500 Nm @ rpm
Powertrain	AWD	Transmission	
		Type	AMT
		No. of Gears	6
		Tire	
		Size	215/55 R16
		E-Machine	
		Max. Power	- kW
		Max. Torque	- Nm
		Battery	
		Capacity	- kWh

Figure 59: Simulation Input Data Volvo S60 D5

1.3.3.10.3. CRUISE Model Validation Results

The AVL CRUISE simulation model is validated against the published NEDC cycle fuel consumption.

The deviation between published and simulated vehicle fuel consumption is within the expected error margin considering the accuracy and availability of the input data.

Detailed validation results are shown in Figure 60.


Vehicle 10 Volvo S60 D5		
NEDC hot Fuel Consumption		
simulated	5.6	l/100km
NEDC cold Fuel Consumption		
published	5.9	l/100km
simulated	6.2	l/100km
Deviation	5%	

Figure 60: Model Validation Volvo S60 D5

1.3.3.11. Vehicle 11 – Audi A6 3.0L TFSI quattro

The Audi A6 3.0L TFSI quattro is an all wheel driven (AWD) conventional vehicle with start stop system. Only a limited number of different operating strategies are possible for this vehicle (see Figure 61).

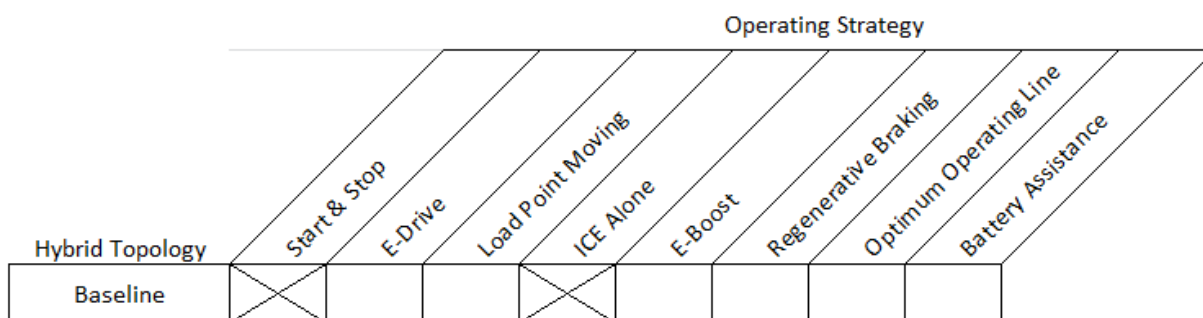


Figure 61: Hybrid Topology – Audi A6 3.0L TFSI quattro

1.3.3.11.1. AVL CRUISE Model Layout

The vehicle layout in CRUISE is shown in Figure 62. It consists of the main parts of the drivetrain (ICE, clutch, gear box, final drive, brakes, wheels), and additional vehicle parts such as the vehicle itself and control systems. As the considered model is an all wheel drive, the ICE drives front and rear wheels through a central differential. Auxiliaries such as the alternator are considered by a mechanical consumer.

The Audi A6 3.0L TFSI quattro is equipped with a Double Clutch Transmission (DCT). The controls include shifting controls for the DCT as well as the start-stop control. For most of

these controls separate control elements exist within CRUISE which are used for this purpose.

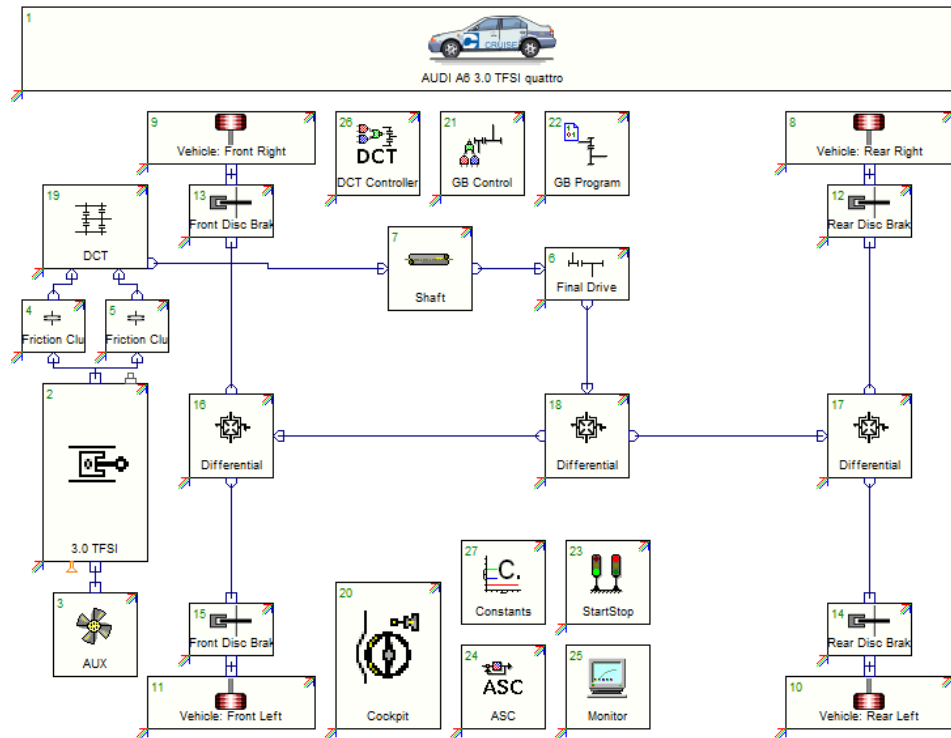


Figure 62: AVL CRUISE Model Audi A6 3.0L TFSI quattro

1.3.3.11.2. Simulation Input Data

Some of the main characteristic input data of the vehicle model is listed in Figure 63.


Vehicle 11		Combustion Engine	
OEM	Audi	Type	Gasoline
Model	A6 3.0L TFSI quattro	Displacement	3.0 L
Model Year	2011	Max. Power	220 / 5250 kW @ rpm
Class	E	Max. Torque	440 / 2900 Nm @ rpm
Powertrain	AWD		
		Type	DCT
		No. of Gears	7
		Tire	
		Size	225/55 R17
		E-Machine	
		Max. Power	- kW
		Max. Torque	- Nm
		Battery	
		Capacity	- kWh

Figure 63: Simulation Input Data Audi A6 3.0L TFSI quattro

1.3.3.11.3. CRUISE Model Validation Results

The AVL CRUISE simulation model is validated against the published NEDC cycle fuel consumption.

The deviation between published and simulated vehicle fuel consumption is within the expected error margin considering the accuracy and availability of the input data.

Detailed validation results are shown in Figure 64.


Vehicle 11 Audi A6 3.0 TFSI		
NEDC hot Fuel Consumption		
simulated	7.1	l/100km
NEDC cold Fuel Consumption		
published	8.2	l/100km
simulated	7.9	l/100km
Deviation	4%	

Figure 64: Validation Result Audi A6 3.0L TFSI quattro

1.3.3.12. Vehicle 12 – Fisker Karma

The Fisker Karma is a rear wheel driven (RWD) range extender vehicle (REX). The range extender in this vehicle is a conventional gasoline engine. For range extender vehicles a lot of different operating strategies are possible (see Figure 65).

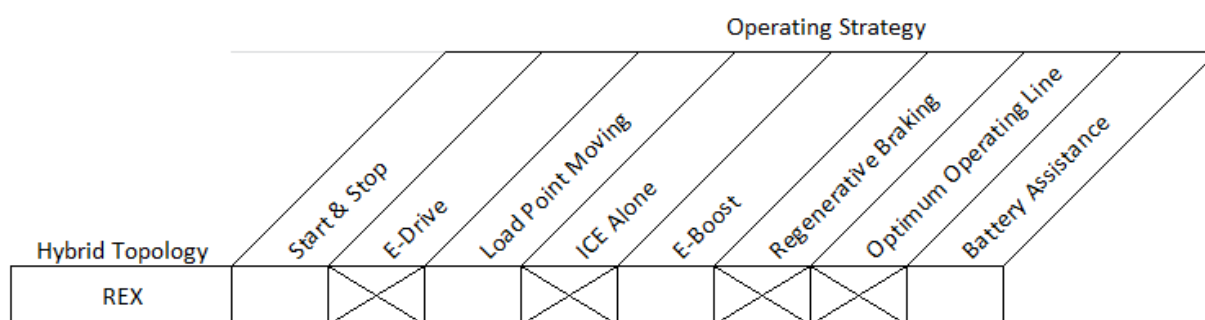


Figure 65: Hybrid Topology – Fisker Karma

1.3.3.12.1. AVL CRUISE Model Layout

The vehicle layout in CRUISE is shown in Figure 66. The main drivetrain consists of two electric motors driving through the final drive the rear wheels. The electric system additionally considers the battery, electrical consumers (e.g. for power steering), and the generator, which is driven by the ICE (range extender).

The control for the range extender is defined through c-code and coupled as dynamic link library (DLL) into the model. This DLL defines the basic functionality of the range extender. It can be controlled by parameters and characteristic maps which are directly introduced in the

CRUISE model (Figure 67), avoiding a new compilation if only a single parameter should be changed.

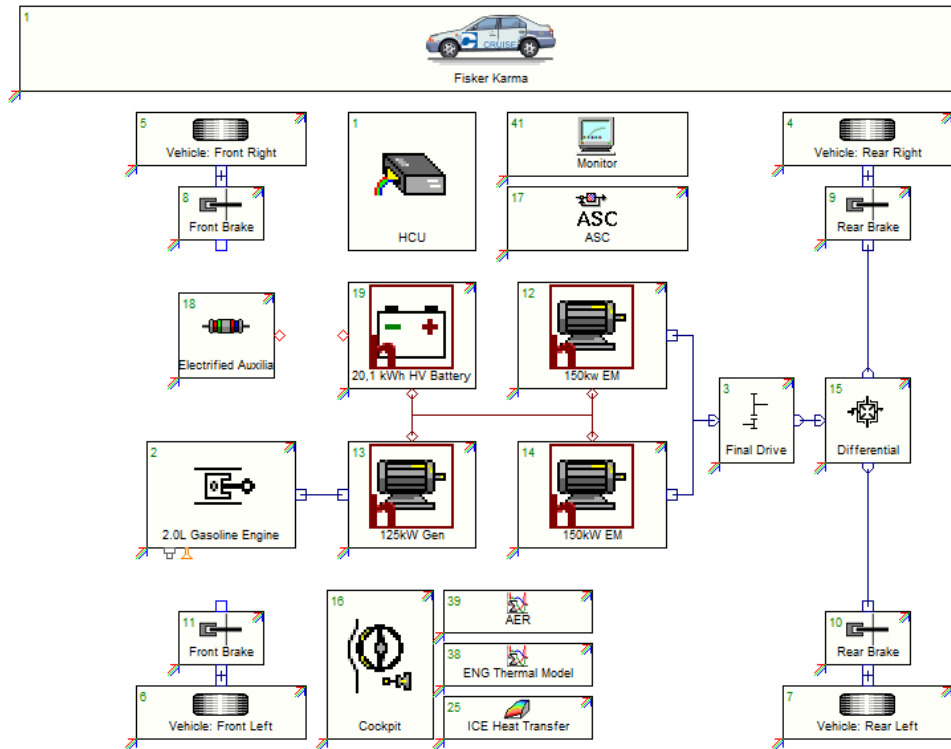


Figure 66: AVL CRUISE Model Fisker Karma

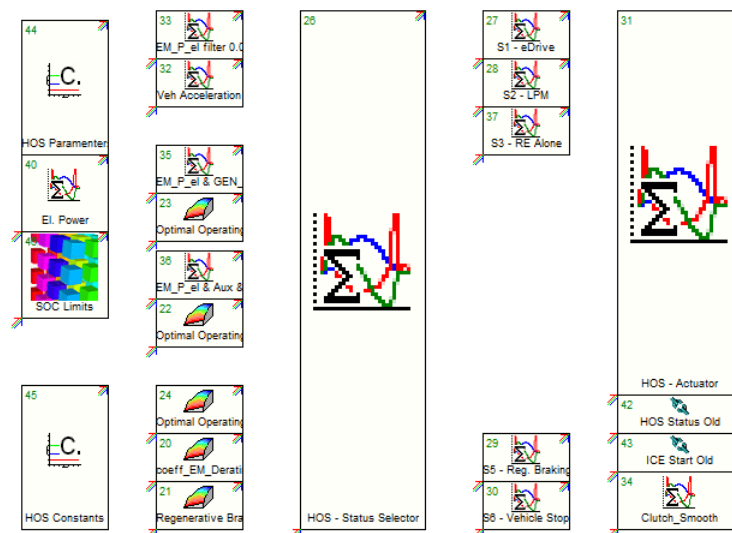


Figure 67: AVL CRUISE HCU Model Fisker Karma

1.3.3.12.2. Simulation Input Data

Some of the main characteristic input data of the vehicle model is listed in Figure 68.


Vehicle 12		Combustion Engine	
OEM	Fisker	Type	Gasoline
Model	Karma	Displacement	2.0 L
Model Year	2011	Max. Power	156 / 4900 kW @ rpm
Class	E	Max. Torque	Nm @ rpm
Powertrain	EV, RWD	Transmission	
		Type	-
		No. of Gears	-
		Tire	
		Size	385/35 R22
		E-Machine	
		Max. Power	300 kW
		Max. Torque	1300 Nm
		Battery	
		Capacity	20.1 kWh

Figure 68: Simulation Input Data Fisker Karma

1.3.3.12.3. CRUISE Model Validation Results

The AVL CRUISE simulation model is validated against the published NEDC cycle fuel consumption.

The deviation between published and simulated vehicle fuel consumption is within the expected error margin considering the accuracy and availability of the input data.

Detailed validation results are shown in Figure 69.


Vehicle 12 Fisker Karma		
NEDC hot Fuel Consumption		
simulated	4.0	l/100km
NEDC cold Fuel Consumption		
published	2.2	l/100km
simulated	2.4	l/100km
Deviation	7%	

Figure 69: Validation Results Vehicle Fisker Karma

1.3.3.13. Vehicle 13 – Mercedes Benz S400 Hybrid

The Mercedes Benz S400 Hybrid is a rear wheel driven (RWD) mild hybrid vehicle. Mild hybrid means that the system is not designed for pure electric driving, but only for supporting the ICE. Only a limited number of different operating strategies are possible for this vehicle (see Figure 70).

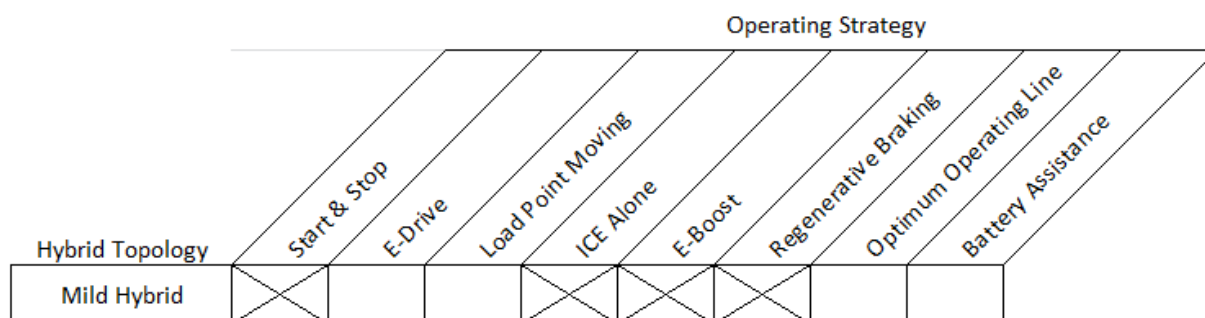


Figure 70: Hybrid Topology – Mercedes Benz S400 Hybrid

1.3.3.13.1. AVL CRUISE Model Layout

The vehicle layout in CRUISE is shown in Figure 71. It consists of the main parts of the drivetrain for a mild hybrid (ICE, electric motor, torque converter, gear box, final drive, brakes, wheels), and additional vehicle parts such as the vehicle itself and control systems. As the electric motor can also act as alternator, no separate mechanical consumer is considered in the model.

The ICE and the electric motor are directly coupled. This means both engines run at the same speed. The electric motor gets its electric power from a battery, which additionally drives an electric consumer which considered additional electric power requirements such as heating or power steering.

The main control for the mild hybrid is considered by an externally linked c-code (through a DLL). Setting of parameters for the c-code is done through additional functions and characteristic maps as shown in Figure 72.

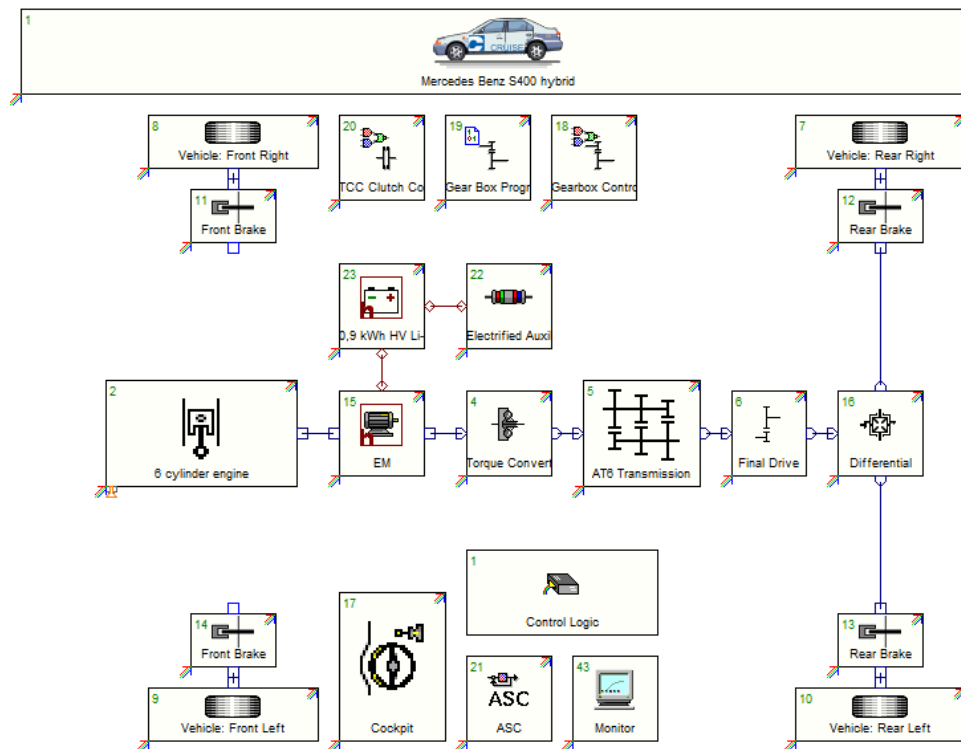


Figure 71: AVL CRUISE Model Mercedes Benz S400 Hybrid

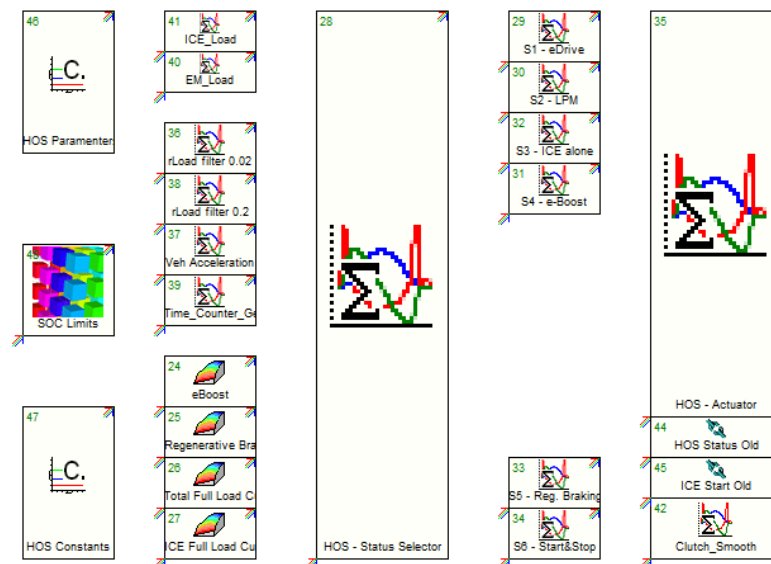


Figure 72: Hybrid Control Logic implemented in AVL CRUSIE

1.3.3.13.2. Simulation Input Data

Some of the main characteristic input data of the vehicle model is listed in Figure 73.


Vehicle 13		Combustion Engine	
OEM	Mercedes Benz	Type	Gasoline
Model	S400 Hybrid	Displacement	3.5 L
Model Year	2009	Max. Power	205 / 6000 kW @ rpm
Class	F	Max. Torque	350 / 2400 Nm @ rpm
Powertrain	Mild Hybrid, RWD	Transmission	
		Type	AT
		No. of Gears	7
		Tire	
		Size	235/55 R17
		E-Machine	
		Max. Power	15 kW
		Max. Torque	160 Nm
		Battery	
		Capacity	0.9 kWh

Figure 73: Simulation Input Data Mercedes Benz S400 Hybrid

1.3.3.13.3. CRUISE Model Validation Results

The AVL CRUISE simulation model is validated against the published NEDC cycle fuel consumption.

The deviation between published and simulated vehicle fuel consumption is within the expected error margin considering the accuracy and availability of the input data.

Detailed validation results are shown in Figure 74.


Vehicle 13 Mercedes Benz S400		
NEDC hot Fuel Consumption		
simulated	7.3	l/100km
NEDC cold Fuel Consumption		
published	7.9	l/100km
simulated	8.0	l/100km
Deviation	1%	

Figure 74: Validation Results Mercedes Benz S400 Hybrid

1.3.3.14. Vehicle 14 – BMW X1 2.0d sDrive

The BMW X1 2.0d sDrive is a rear wheel driven (RWD) micro hybrid vehicle with smart charging. Smart charging means that recharging the battery is controlled, so that the alternator only works when the engine is at low load. When the engine is at high load (e.g. during acceleration) the alternator is turned off, so that the load on the engine is lower and the

fuel consumption gets smaller. Only a limited number of different operating strategies are possible for this vehicle (see Figure 75).

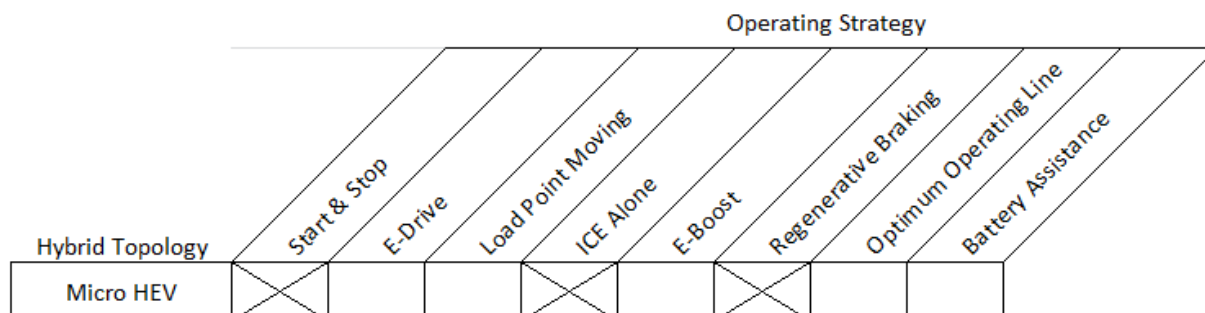


Figure 75: Hybrid Topology – BMW X1 2.0d sDrive

1.3.3.14.1. AVL CRUISE Model Layout

The vehicle layout in CRUISE is shown in Figure 76. It consists of the main parts of the drivetrain (ICE, clutch, gear box, final drive, brakes, wheels), and additional vehicle parts such as the vehicle itself and control systems. Due to the smart charging there are no mechanical consumers installed at the engine as all auxiliaries are electrically driven. The control of the smart charging is considered as so effective that it will have no effect on fuel consumption and emissions in the investigated driving cycles.

The BMW X1 is equipped with a conventional manual gear box. Still the model features shifting controls since they allow a better definition of the shifting procedure compared to the driver model in CRUISE. The start-stop control is considered by a separate component in the CRUISE model.

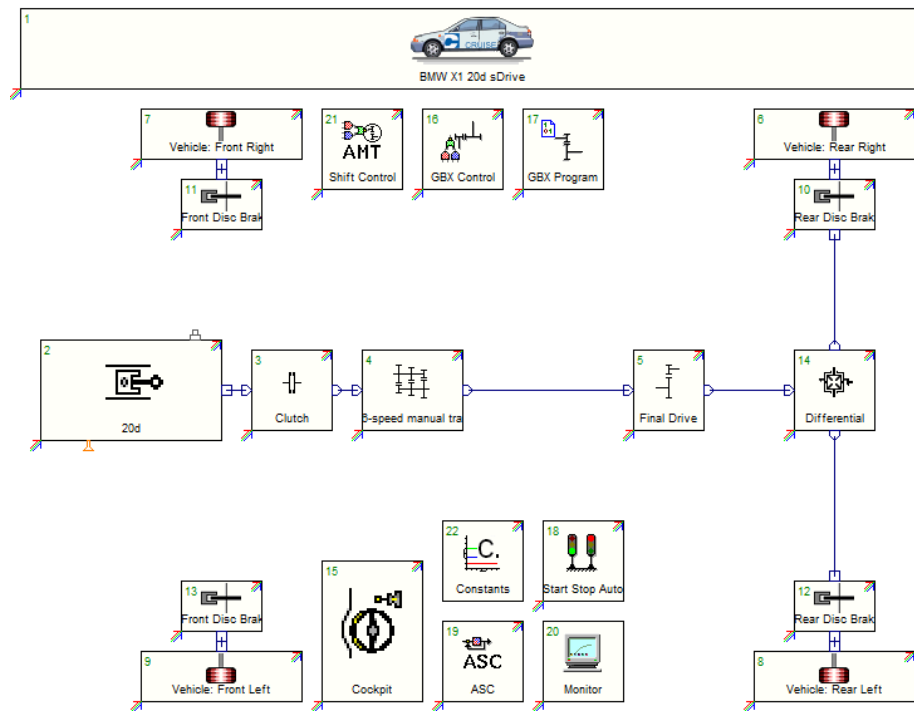


Figure 76: AVL CRUISE Model BMW X1 2.0d sDrive

1.3.3.14.2. Simulation Input Data

Some of the main characteristic input data of the vehicle model is listed in Figure 77.


Vehicle 14		Combustion Engine	
OEM	BMW	Type	Diesel
Model	X1 2.0d sDrive	Displacement	2.0 L
Model Year	2009	Max. Power	130 / 4000 kW @ rpm
Class	J	Max. Torque	350 / 1750 Nm @ rpm
Powertrain	RWD	Transmission	
		Type	MT
		No. of Gears	6
		Tire	
		Size	225/50 R17
		E-Machine	
		Max. Power	- kW
		Max. Torque	- Nm
		Battery	
		Capacity	- kWh

Figure 77: Simulation Input Data BMW X1 2.0d sDrive

1.3.3.14.3. CRUISE Model Validation Results

The AVL CRUISE simulation model is validated against the published NEDC cycle fuel consumption.

The deviation between published and simulated vehicle fuel consumption is within the expected error margin considering the accuracy and availability of the input data.

Detailed validation results are shown in Figure 78.


Vehicle 14 BMW X1 2.0d sDrive		
NEDC hot Fuel Consumption		
simulated	4.9	l/100km
NEDC cold Fuel Consumption		
published	5.3	l/100km
simulated	5.4	l/100km
Deviation	2%	

Figure 78: Validation Results BMW X1 2.0d sDrive

1.3.3.15. Vehicle 15 – Nissan Pathfinder 3.5L CVT

The Nissan Pathfinder 3.5L CVT is an all wheel driven (AWD) conventional vehicle with CVT transmission. Only a limited number of different operating strategies are possible for this vehicle (see Figure 79).

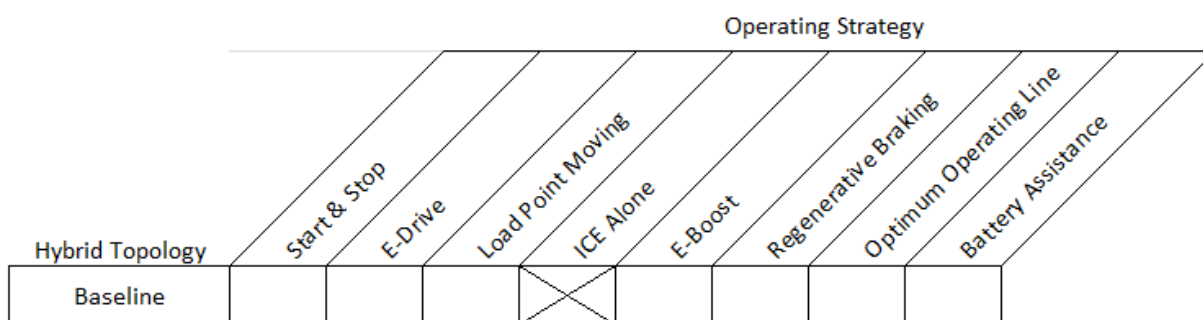


Figure 79: Hybrid Topology – Nissan Pathfinder 3.5L CVT

The vehicle model is validated against FTP cycle measurement data and shows a very good correlation between simulation and measurement

1.3.3.15.1. AVL CRUISE Model Layout

The vehicle layout in CRUISE is shown in Figure 80. It consists of the main parts of the drivetrain (ICE, torque converter, CVT, final drive, brakes, wheels), and additional vehicle parts such as the vehicle itself and control systems. Since the vehicle is an all wheel drive, the engine drives front and rear wheels through a central differential. Auxiliaries such as the alternator are considered by a mechanical consumer.

The Nissan Pathfinder is equipped with a continuously variable transmission (CVT). The model considers the controls for the CVT as well as for the lock up clutch (acting in parallel to the torque converter to reduce losses while there are no gears shifted).

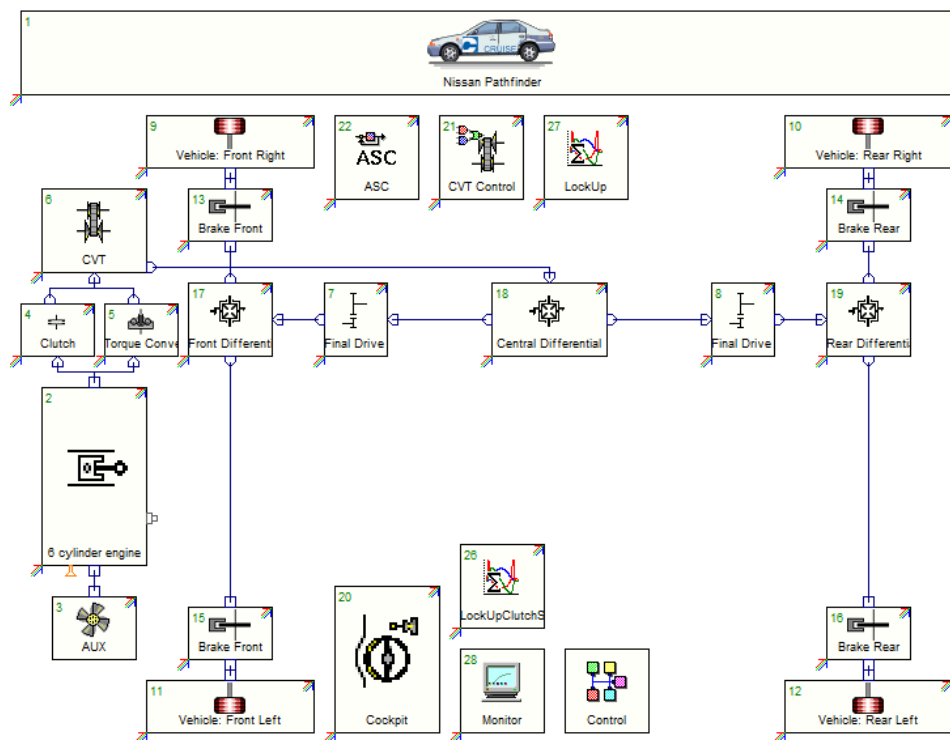


Figure 80: AVL CRUISE Model Nissan Pathfinder 3.5L CVT

1.3.3.15.2. Simulation Input Data

Some of the main characteristic input data of the vehicle model is listed in Figure 81.


Vehicle 15		Combustion Engine	
OEM	Nissan	Type	Gasoline, NA
Model	Pathfinder	Displacement	3.5 L
Model Year	2012	Max. Power	170 / 6000 kW @ rpm
Class	J	Max. Torque	300 / 4400 Nm @ rpm
Powertrain	AWD	Transmission	
		Type	CVT
		No. of Gears	-
		Tire	
		Size	235/55 R20
		E-Machine	
		Max. Power	- kW @ rpm
		Max. Torque	- Nm / rpm
		Battery	
		Capacity	- kWh

Figure 81: Simulation Input Data Nissan Pathfinder 3.5L CVT

1.3.3.15.3. CRUISE Model Validation Results

The CRUISE model of the Nissan Pathfinder vehicle has been validated against measured data of the FTP cycle, not only as total values in the FTP but also in time domain, since such data was available at AVL.

The deviation between measurement and simulation data is less than 3% (Figure 82).


Vehicle 15 Nissan Pathfinder		
FTP75 BagA		
measured	22.8	g/mile
simulated	23.2	g/mile
FTP75 BagB		
measured	23.7	g/mile
simulated	24.3	g/mile
FTP75 BagC		
measured	26.9	g/mile
simulated	26.3	g/mile
Deviation	2%	

Figure 82: Validation Results Nissan Pathfinder 3.5L CVT

Figure 83 shows a comparison between simulated and measured signals for engine speed and temperature as well as the vehicle velocity.

FTP75 – BagB:

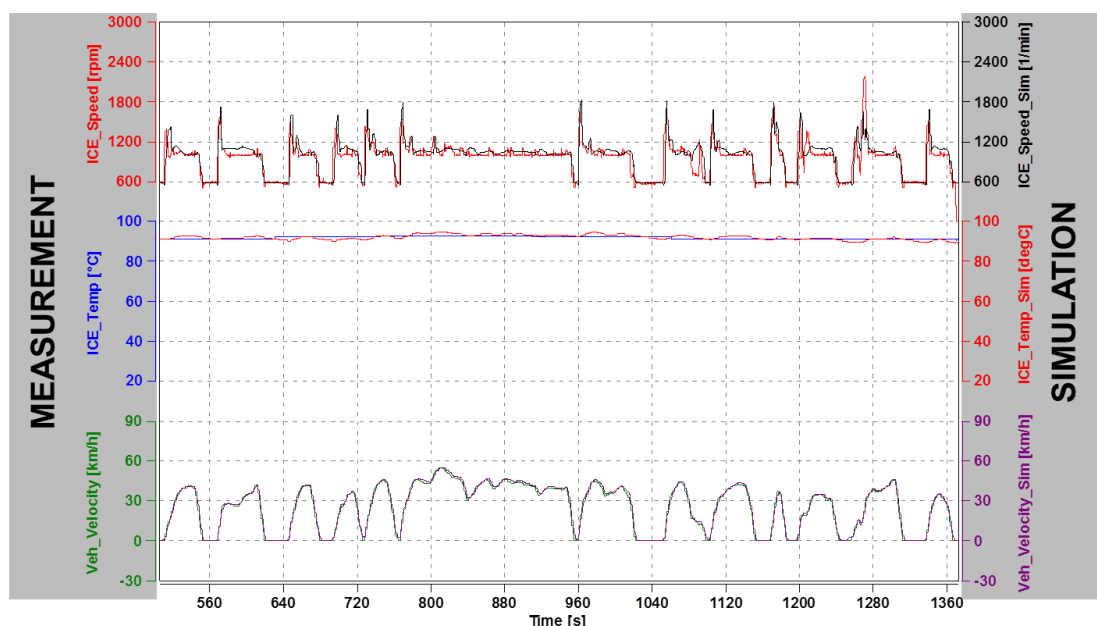


Figure 83: CRUISE Model validation results

1.3.3.16. Summary

Figure 84 gives an overview of the simulation results in comparison to published or measured data. The average error is 3% with a maximum reaching 7%. Although the difference in relative numbers seems sometimes high, this is often caused by the small overall consumption in total (e.g. Fisker Karma), where already a small absolute difference can lead to a high relative difference.

Another important aspect to be considered is the maturity of the input data. Typically data maturity from publications is not very high, since especially control strategies and fuel consumption or emission maps are often not provided and need either to be measured or estimated. Within the project these engine maps were estimated (with the exception of Audi A1 etron and Toyota Prius III where internal measurements at AVL were available).

Therefore the differences between published and simulated results are within the expected margin based on the data availability.

			Difference to Published Data/Measurements	
			Relative	Absolute
Mitsubishi i MiEV	A	EV	5%	7.5 km
SMART Fortwo coupe 52 kW mhd	A	Baseline	3%	0.1 l/100km
Audi A1 etron	B	REX	only time history comparison available	
Audi A3 1.4 TFSi	C	Baseline	0%	0 l/100km
BMW 116i	C	Baseline	3%	0.2 l/100km
Honda Civic Hybrid	C	Full HEV	4%	0.2 l/100km
Toyota Prius III	C	Full HEV	5%	0.13 l/100km
Volvo C30 T5	C	Baseline	2%	0.2 l/100km
VW Golf 1.4L TSI	C	Micro HEV	1%	0 l/100km
Volvo S60 D5	D	Baseline	5%	0.3 l/100km
AUDI A6 3.0 TFSi quattro	E	Baseline	4%	0.3 l/100km
Fisker Karma	E	REX	7%	0.2 l/100km
Mercedes Benz S 400 HYBRID	F	Mild Hybrid	1%	0.1 l/100km
BMW X1 20d sDrive	J	Micro HEV	2%	0.1 l/100km
Nissan Pathfinder 3.0L CVT	J	Baseline	2%	0.53 g/mile

Figure 84: Summary of simulation results

2 Macro Emission Models

2.1. GENERAL CONSIDERATIONS

The Macro emission model to be used in ICT-Emissions will have to be linked with a traffic macro model in order to be able to estimate the impacts of ICT measures on a general fleet level. There have been two macro emission models considered from the beginning of the project that are widely used in Europe: the COPERT (www.emisia.com/copert) and the HBEFA (www.hbefa.net) models. The development of both is coordinated by the ERMES group (www.ermes-group.eu), an ad-hoc research coordination work in the area of emission models in Europe. The two models are generally consistent in their approach and in the underlying data that feed the development of their emission factors. The main difference lies in their expression of emission factors: while COPERT estimates emissions on the basis of the average speed approach, HBEFA provides distinct emission factors for a number of default traffic situations (>250 unique cases) [4]. The latter has the potential to provide more precise emission factors once the actual driving pattern is recognized and correctly assigned to one of the default driving situation. However, macro traffic models only provide average speed estimates for each link and not a driving pattern. Hence, linking traffic models to HBEFA is not straight forward and needs additional considerations.

We were therefore interested in exploring whether COPERT, with its average speed approach, can satisfactorily be connected at a link-level with traffic macro models. The average speed is not the momentary speed of the vehicle, but the mean speed over a complete driving sequence. The emission factors in COPERT were built by assigning, to the extent possible, representative driving conditions for each average speed bin. However, when applying the model to a link level, the actual driving pattern in the link may be very different than the driving patterns considered in developing COPERT emission factors for the same speed. In such a case, the emission factor value estimated from COPERT might not be representative of the actual condition.

The current chapter examines the applicability of COPERT emission factors at a link level. The approach followed was to select two of the traffic sites monitored in ICT-Emissions (Madrid and Turin) and test whether the driving profiles simulated at different congestion levels are consistent with the COPERT approach. Emissions for the particular traffic sites have been modelled at a macro level with COPERT (average speed) and at micro-level with CRUISE (second by second speed profile). Also, individual traffic conditions, where measured data exist in the ERMES A300DB database, were also used in the comparison. The general trends of the COPERT expressions were then compared with measured and micro-simulation results and conclusions on the applicability of the average speed approach have been reached. The following sections describe in detail the approach followed in this validation exercise.

2.2. VALIDATION OF THE MACRO EMISSION APPROACH

2.2.1. GENERAL SCHEME FOLLOWED

The basic idea was to compare the fuel consumption calculated by COPERT using the average speed approach with simulated information on the exact driving profile that the

average speed corresponds to using the AVL CRUISE micro-simulator and with measured fuel consumption values collected from experiments on chassis dynamometer ('A300DB' or 'ARTEMIS' database). This concept is graphically summarized in the flowchart of Figure 85. The calculated and simulated data from various traffic conditions retrieved from Turin and Madrid were used as input, as well as measured data from measured driving cycles that approximated the monitored driving conditions. The approach was repeated for two passenger car categories, gasoline <1.4 l and diesel <2.0 l.

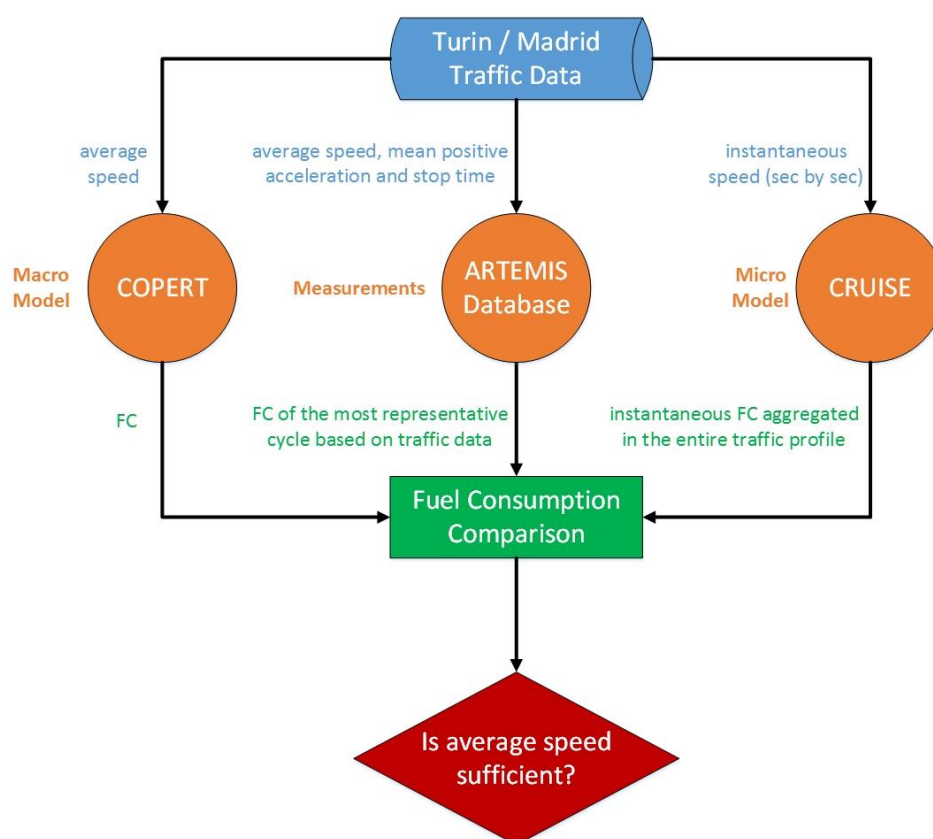


Figure 85: Flowchart of fuel consumption comparison.

For each traffic condition the fuel consumption was estimated with three different methods:

1. The average speed of each traffic condition was inserted in COPERT and the average fuel consumption was calculated for the two vehicle categories.
2. Using the average speed, mean positive acceleration and stop time of each traffic condition as a reference, the closest driving cycle from the ARTEMIS database was located, together with the corresponding measured fuel consumption.

3. The instantaneous speed profile of each traffic condition was inserted in the CRUISE vehicle models (one gasoline and one diesel) and the instantaneous fuel consumption was calculated, which then was integrated for the entire driving profile.

The purpose of comparing the fuel consumption calculated with COPERT and CRUISE was to find if the average speed – alone – is adequate for simulating various traffic conditions and ICT measures. If yes, the macro emissions model could be used “as is” to calculate fuel consumption. In the opposite case, other parameters should be also taken into account (e.g. saturation level).

2.2.2. TRAFFIC CONDITIONS USED FOR THE VALIDATION

For both Turin and Madrid data the average speed, mean positive acceleration and stop time of all traffic situations were calculated from the corresponding second by second speed data (Table 9 and Table 10).

The traffic data from Turin were actual measured driving situations with probe vehicles under urban driving conditions, while the Madrid data were simulated for one section of the (west) M30 urban ring highway using PTV VISUM software. This section is shown in Figure 86.

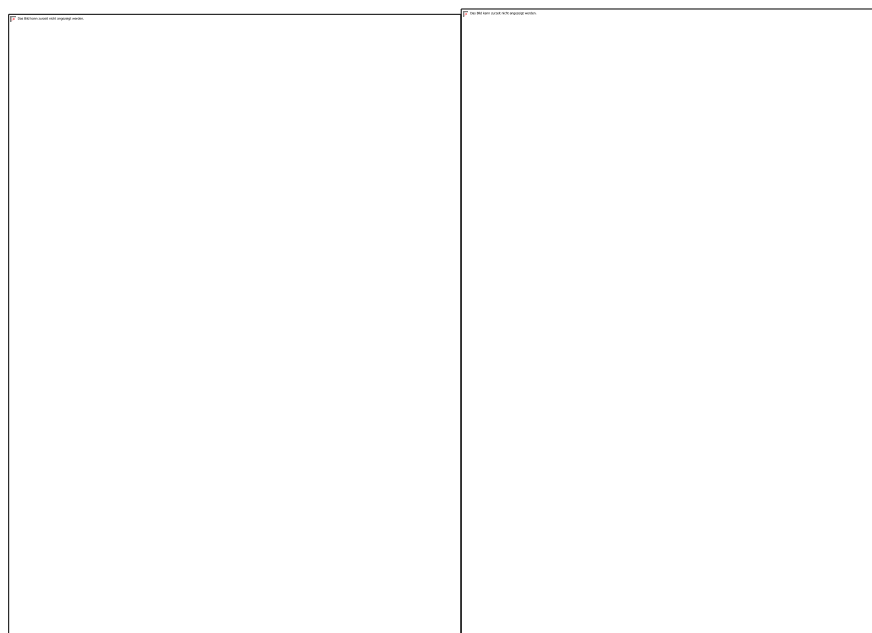


Figure 86: Schematic representation and map of the M30 Madrid section simulated with PTV VISUM.

Table 9: Calculated traffic characteristics from Turin measurements.

Traffic Condition	Speed [km/h]	Mean Positive Acceleration [m/s ²]	Stop Time [%]
Urban Saturated - UTC ON	19.6	0.69	45.1
Urban Saturated - UTC OFF	17.4	0.77	48.7
Urban Normal - UTC ON	24.8	0.54	39.9
Urban Normal - UTC OFF	21.5	0.67	39.0
Urban Free	32.8	0.46	30.0

Table 10: Calculated traffic characteristics from Madrid M30 highway simulation.

Saturation Level [%]	Average Speed [km/h]	Mean Positive Acceleration [m/s ²]	Stop Time [s]
10	90.2	0.19	0.00
20	90.1	0.23	0.00
30	90.1	0.17	0.00
40	90.1	0.25	0.00
50	90.1	0.23	0.00
60	90.2	0.20	0.00
70	90.1	0.18	0.00
80	81.9	0.77	0.00
90	23.1	1.51	12.2
100	21.4	1.49	10.0

The speed profiles for two cases are shown in the following charts as examples. In Figure 87 the impact of UTC measure on speed profile of a saturated traffic condition in Turin is depicted, while Figure 88 shows the effect of different saturation levels on speed in Madrid. In this latter case, the speed is almost constant when the saturation is small and the trip lasts for only few seconds because of the high speed. However, when the saturation level increases, the mean speed drops with much more dynamic variations, while the trip lasts much longer because of the low speed.

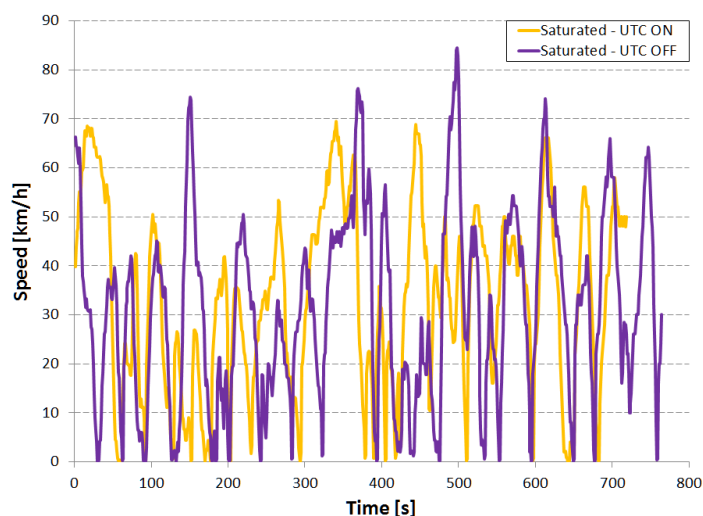


Figure 87: Effect of UTC implementation on average speed profiles during a saturated traffic condition (Turin).

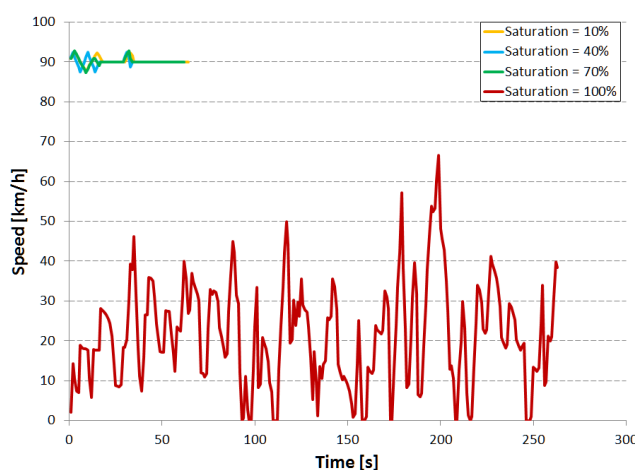


Figure 88: Speed profiles for different saturation levels on a section of the M30 urban highway (Madrid).

2.2.3. COPERT CALCULATIONS

The fuel consumption for the two vehicle types considered was calculated with COPERT 4 (V10.0) by inserting the average speed of each traffic situation in the software and selecting the emission values of the corresponding vehicle categories for both gasoline and diesel cases (Figure 89). The fuel consumption factors used were estimated by using the Gasoline 0.8-1.4 l Euro 3 and the Diesel 1.4 – 2.0 l Euro 3 classes in COPERT 4.

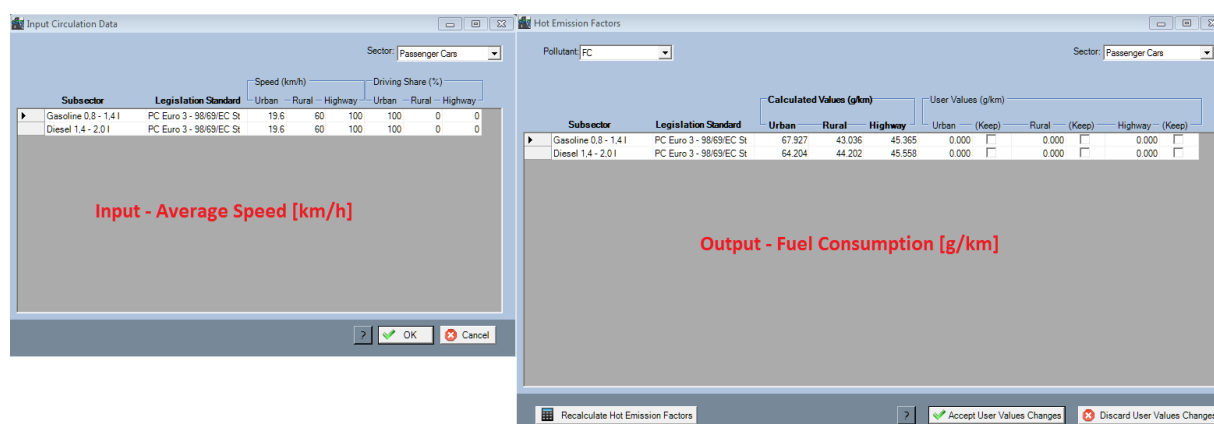


Figure 89: Inserting average speeds in COPERT and calculating fuel consumption.

2.2.4. COMPARISON WITH MEASURED VALUES

The ARTEMIS database contains more than 15000 fuel consumption measurements from various passenger cars in chassis dynamometer measurements over a range of driving cycles. The vehicles are categorized in the database based on the fuel used (gasoline, diesel), engine capacity (<1.4 l, 1.4 – 2.0 l and >2.0 l for gasoline, <2.0 and >2.0 l for diesel) and technology level (Euro 0, 1, 3 and 4). The vehicles were driven over several well-defined speed profiles (driving cycles) on chassis dynamometers and the fuel consumption was measured. This database is constantly enhanced and updated through the ERMES research group and tries to collect all available measurements in Europe that can feed emission models. Therefore, COPERT and HBEFA emission factors are based on this database. By selecting individual measured values from this database on driving cycles that approximate the various traffic conditions in Turin and Madrid one can explore what is the impact of these traffic conditions on the fuel consumption of individual vehicles in the database. Therefore, this delivers a third source of information (further to CRUISE and COPERT) on the impact of driving pattern on CO₂ emissions and fuel consumption.

All the available fuel consumption measurements in the ARTEMIS database for Euro 3 gasoline <1.4 l and Euro 3 diesel <2.0 l passenger cars were collected and some statistics were calculated for the driving cycles that these vehicles were measured on. These included average speed, mean positive acceleration, and stop time, to be compared against the corresponding values of the Turin and Madrid traffic conditions.

All the values collected from the ARTEMIS database for the particular vehicle types are shown in Figure 90 for the gasoline vehicle category and in Figure 91 for the diesel vehicle category. The speed on the horizontal axis corresponds to the average speed of the different driving cycles that the database contains. Each point in both graphs is a unique measurement of one of the vehicles in the database over the driving cycle with the specific average speed.

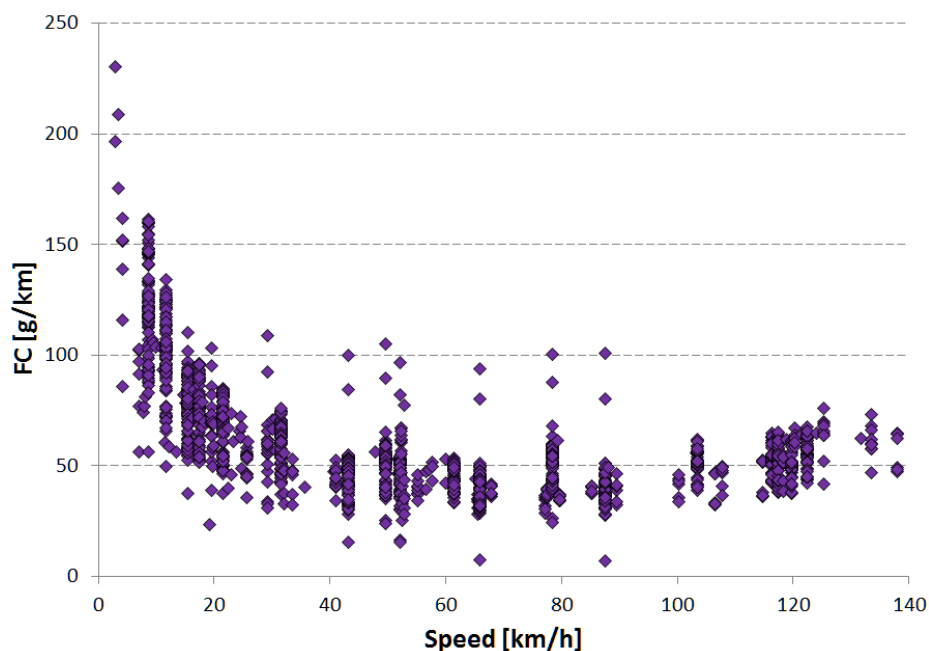


Figure 90: Available fuel consumption measurements in the ARTEMIS database for Euro 3 gasoline passenger cars < 1.4 l as a function of the average speed of the cycle.

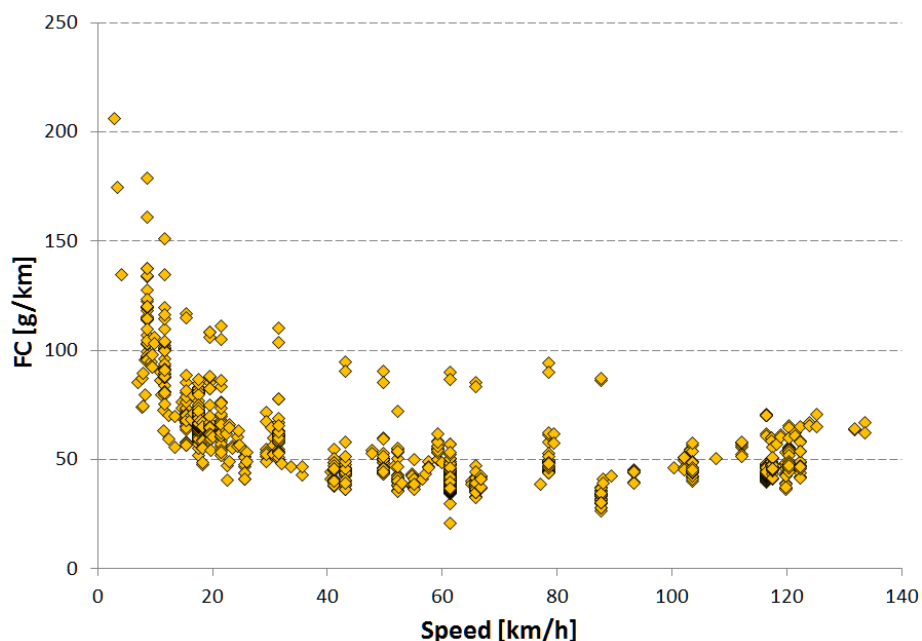


Figure 91: Available fuel consumption measurements in the ARTEMIS database for Euro 3 diesel passenger cars < 2.0 l as a function of the average speed of the cycle.

In order to select the appropriate measurements from this database, the average speed, mean positive acceleration and stop time calculated from Turin (Table 9) and Madrid traffic data (Table 10) were used as 'reference' values. Then, the corresponding characteristics of all driving cycles in the ARTEMIS database were compared with these values and the cycles that best approximated the reference values were selected. The procedure is shown in Figure 92 that presents the relative distance of the ARTEMIS driving cycles from the 'reference'

values in the case of Turin, saturated, UTC_OFF. The driving cycle characteristics are normalised over the reference values which are assigned the value of 100. In the example shown in Figure 92, the Artemis Urban cycle shows the best correspondence with the actual monitored driving situation, in particular in terms of average speed and mean positive acceleration. It only contains a much shorter duration of stop time. However, none of the available driving cycles contained as much stop time as the actual Turin recordings. Due to the small impact of idle duration on total fuel consumption, the selected driving cycle is considered to satisfactorily approximate the recorded driving condition. The same procedure was repeated for each of the Madrid and Turin cases and the average fuel consumption of the vehicles measured in each cycle was collected. Attention was given that the average fuel consumption was collected from the same vehicle sample measured in each of the selected cycles.

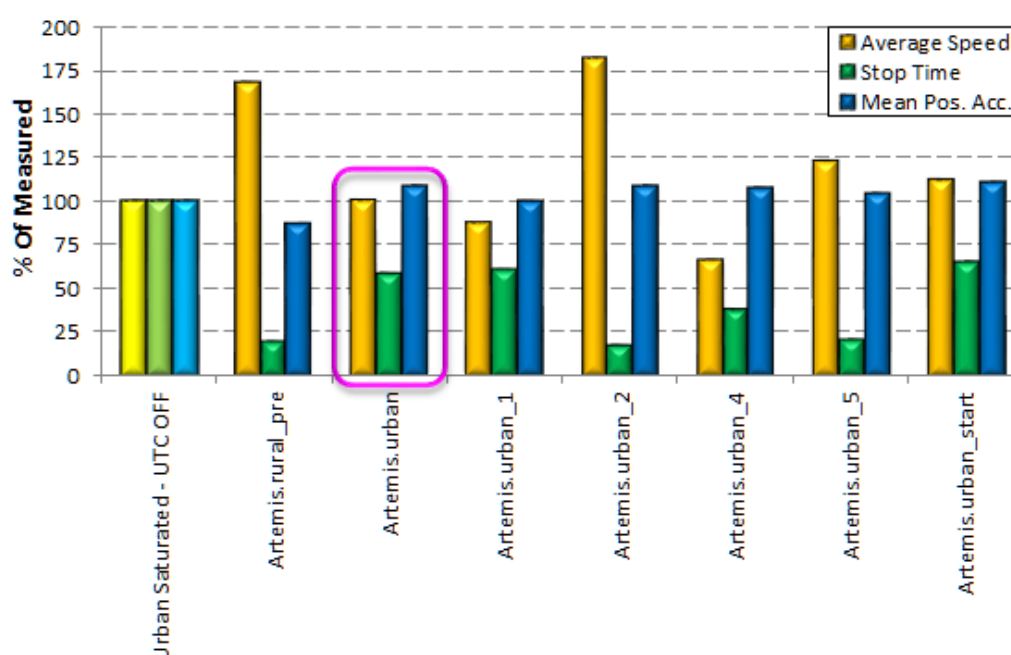


Figure 92: Relative comparison of the available driving cycles in the ARTEMIS database with one of the monitored conditions (example shown: urban saturated condition – UTC OFF)

2.2.5. MICRO SIMULATIONS

In order to simulate fuel consumption and emissions for the driving profiles in Turin and Madrid, we utilized two different AVL CRUISE vehicle models. For the diesel case, a generic vehicle model of a 1.9 l car was used, while for the gasoline case, a generic vehicle model of a 1.2 l car was used. Both vehicle models were pre-validated with available fuel consumption measurements, with a similar approach as the one described in section 1 of this report.

The speed profile of each traffic situation – from Turin and Madrid data – was input to the corresponding CRUISE vehicle model and the instantaneous fuel consumption was calculated. The average fuel consumption over the entire speed profile was then calculated by summing the instantaneous fuel consumption values and dividing by the distance driven.

2.3. RESULTS OF THE VALIDATION EXERCISE

2.3.1. TURIN TRAFFIC DATA – GASOLINE VEHICLE

Figure 93 shows the estimated fuel consumption calculated with the COPERT approach for the six different driving conditions in Turin. The results indicate what one would generally expect, i.e. that fuel consumption per unit of distance travelled increases as the saturation level increases. Moreover, for the same vehicle and traffic condition, activation of the leads to lower fuel consumption due to the higher average speed (UTC eases traffic). Therefore, the general trends that COPERT calculates are consistent with the general trends that one would expect for these conditions.

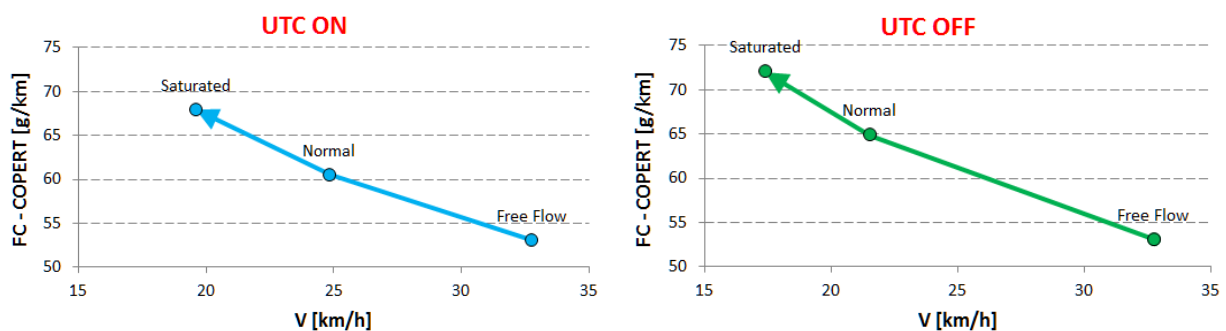


Figure 93: Calculated gasoline fuel consumption with COPERT for UTC on (left) and off (right).

Based on these trends, Figure 94 presents a comparison between traffic characteristics and fuel consumption of saturated and normal traffic condition. Regardless of the UTC measure, the saturated condition corresponds to a lower average speed, higher stop time and higher mean positive acceleration compared with the normal one. The calculated fuel consumption is higher during the saturated conditions by 11-12% compared to the normal case, regardless of whether the UTC is on or off.

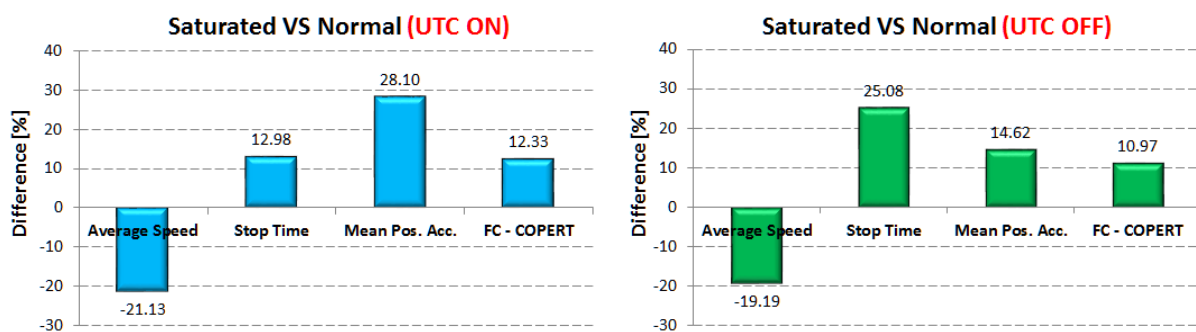


Figure 94: Comparison of driving characteristics and COPERT fuel consumption for saturated over normal conditions; UTC ON (left), UTC OFF (right).

The comparison of fuel consumption calculated with both COPERT and CRUISE, as well the measured fuel consumption over the selected driving cycles (ARTEMIS data), for all traffic conditions is shown in Figure 95. In general, the calculated fuel consumption from all traffic

conditions and with all methods are close to each other. However, the calculated fuel consumption from CRUISE seems to be closer to the COPERT results than to ARTEMIS.

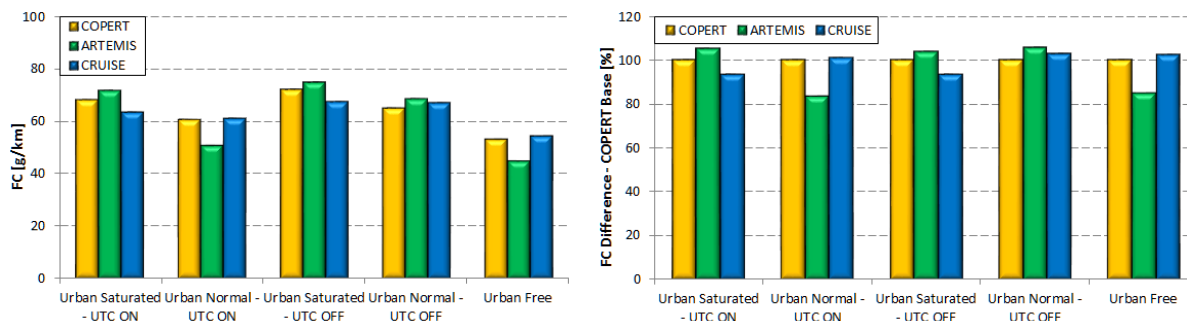


Figure 95: Absolute (left) and relative over COPERT (right) fuel consumption for all driving conditions.

Moving from free to saturated traffic condition all methods calculate an increase in fuel consumption (Figure 96). The trends of fuel consumption calculated with CRUISE and COPERT are similar regardless if UTC is on or off.

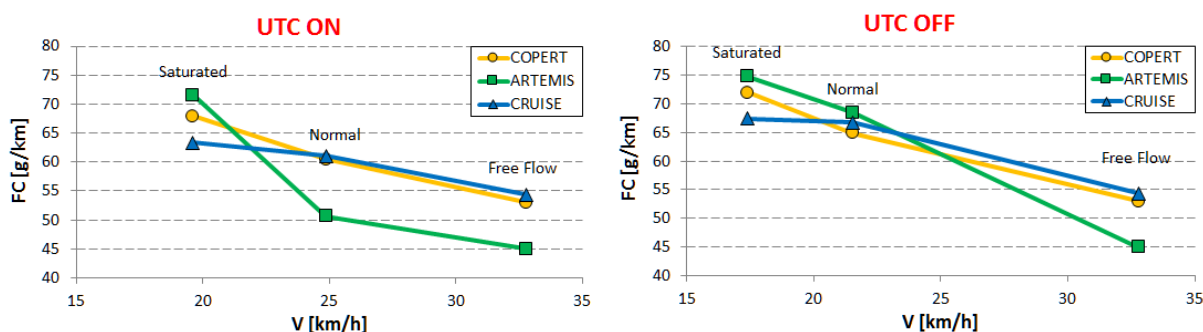


Figure 96: Effect of saturation level and UTC condition on fuel consumption estimated with all available methods.

A comparison of the relative fuel consumption calculated with all the available methods and with all traffic conditions is presented in Figure 97. In general, COPERT gives somewhat higher fuel consumption differences than CRUISE in all cases, regardless of the UTC measure. This is not surprising since CRUISE calculates similar fuel consumption levels in both normal and saturated condition. The selected driving cycles from ARTEMIS database exhibited much higher relative fuel consumption differences.

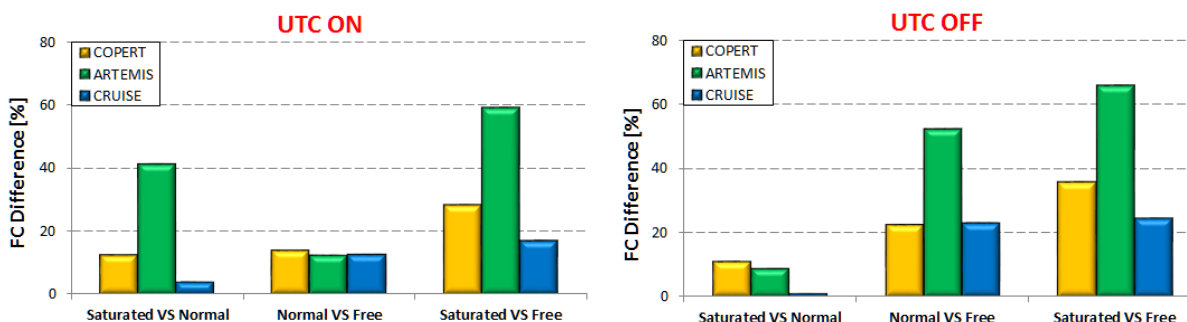


Figure 97: Relative impact of the calculation method on fuel consumption for different conditions.

2.3.2. TURIN TRAFFIC DATA – DIESEL VEHICLE

The comparison of fuel consumption calculated with both COPERT and CRUISE, as well the measured fuel consumption of the selected ARTEMIS cycle, for the various traffic conditions is shown in Figure 98 for the diesel vehicle. The results indicate that there is a good agreement between COPERT and CRUISE results except for free flow condition, where CRUISE calculates lower fuel consumption.

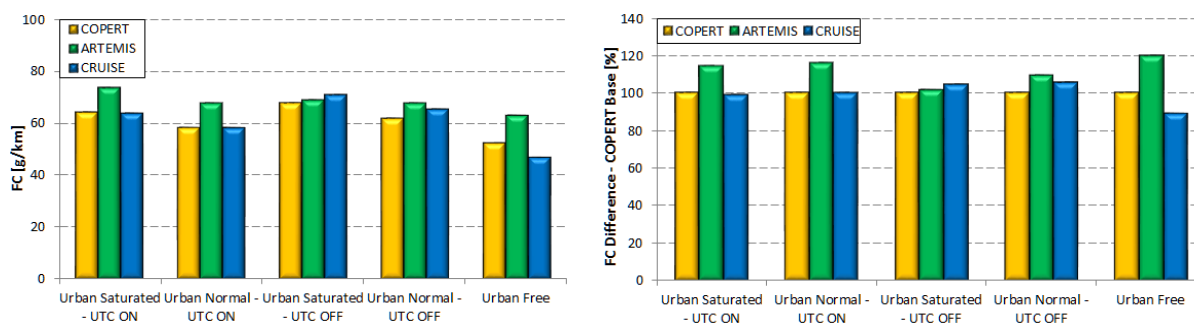


Figure 98: Absolute (left) and relative over COPERT (right) fuel consumption for all driving conditions.

The trends of fuel consumption calculated with CRUISE and COPERT are closer when UTC is active (Figure 99). The selected driving cycles from ARTEMIS database presented the highest fuel consumption in all traffic conditions, apart from saturated – UTC off.

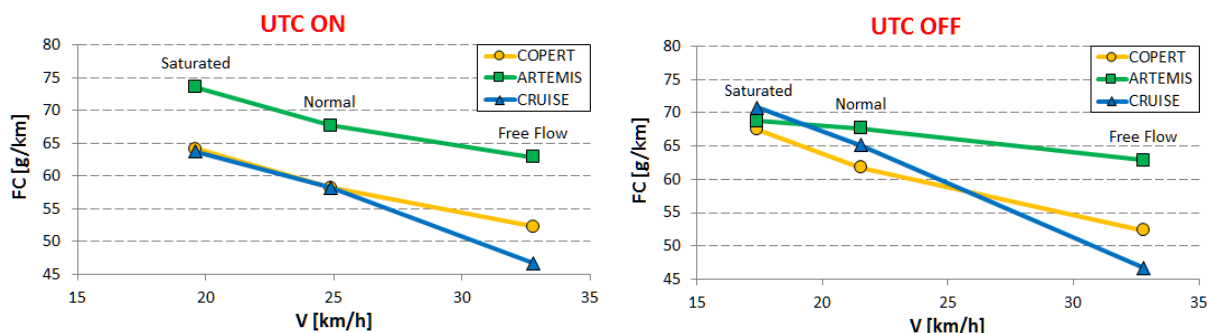


Figure 99: Effect of saturation level and UTC condition on fuel consumption estimated with all available methods.

In saturated vs. normal condition, COPERT and CRUISE give similar fuel consumption differences (Figure 100). However, CRUISE gives the highest differences on normal vs. free and on saturated vs. free, regardless of the UTC condition. On the other hand, the selected ARTEMIS cycles exhibited the lowest fuel consumption differences among the available methods.

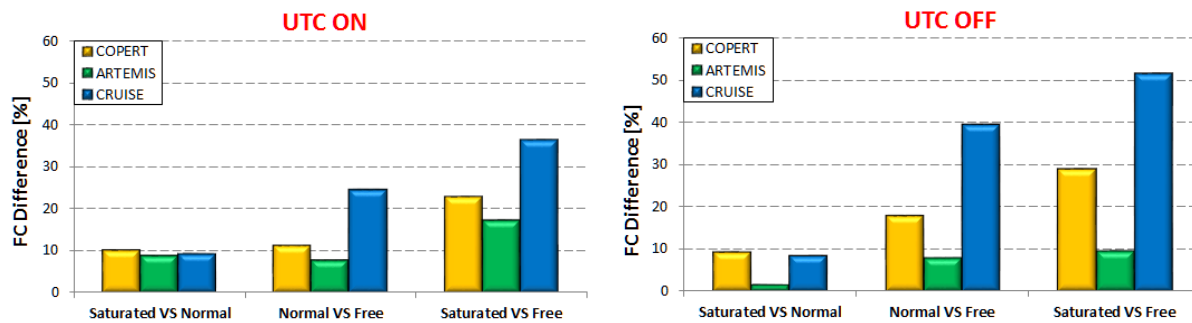


Figure 100: Relative impact of the calculation method on fuel consumption for different conditions.

2.3.3. MADRID TRAFFIC DATA – GASOLINE VEHICLE

The effect of different saturation levels on fuel consumption in the case of the Madrid urban highway is presented in Figure 101. The results indicate that up to 80% saturation level there is no significant change in average speed, so the macro emissions model calculates almost constant fuel consumption. However, at higher saturation levels there is a large increase in calculated fuel consumption.

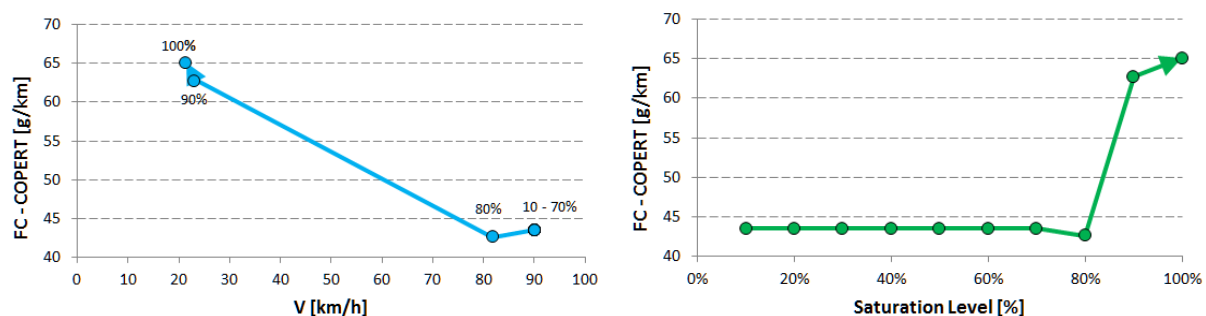


Figure 101: Fuel consumption estimated with COPERT for different saturation levels in the Madrid highway as a function of speed (left) and saturation level (right).

The results of Figure 101 are not surprising if the average traffic characteristics presented in Figure 102 are taken into account. When the saturation level starts to exceed 80% the instantaneous speed profile changes dramatically; there are a lot of accelerations and decelerations that cause an increase in stop time and mean positive acceleration, while the average speed decreases as a result of the congested driving conditions.

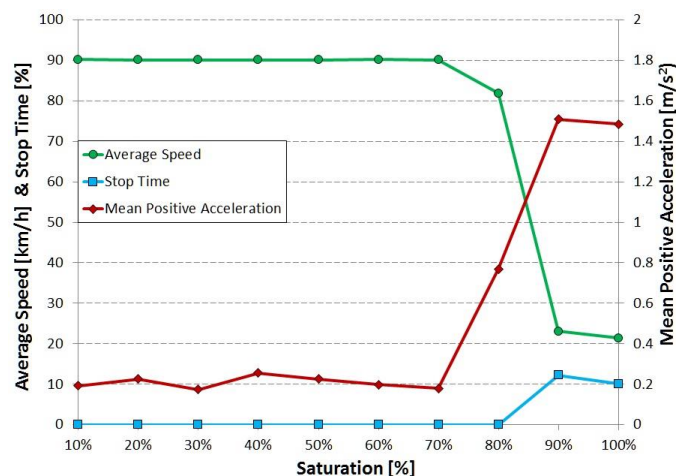


Figure 102: Impact of saturation level on the parameters of the driving.

The effect of saturation on fuel consumption is also reflected on the results from the selected driving cycles (ARTEMIS data) and CRUISE model (Figure 103). Up to 80% saturation there is consistency among the three methods. A large increase in fuel consumption takes place above this 80% saturation. It is evident that CRUISE calculates the highest fuel consumption in these saturation levels.

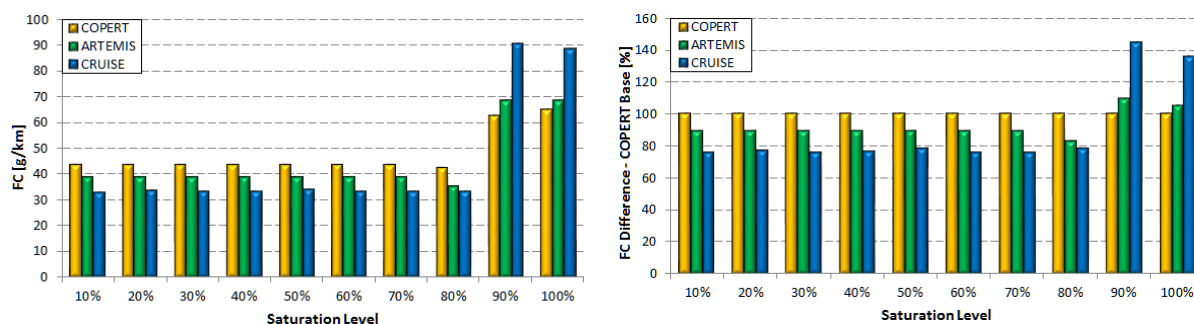


Figure 103: Absolute (left) and relative over COPERT (right) fuel consumption for all driving conditions.

Moving from saturation level 10 to 100% all methods calculate an increase in fuel consumption (Figure 104). After 80% saturation neither COPERT nor the selected ARTEMIS cycles can reproduce the effect of increased saturation on the M30 highway.

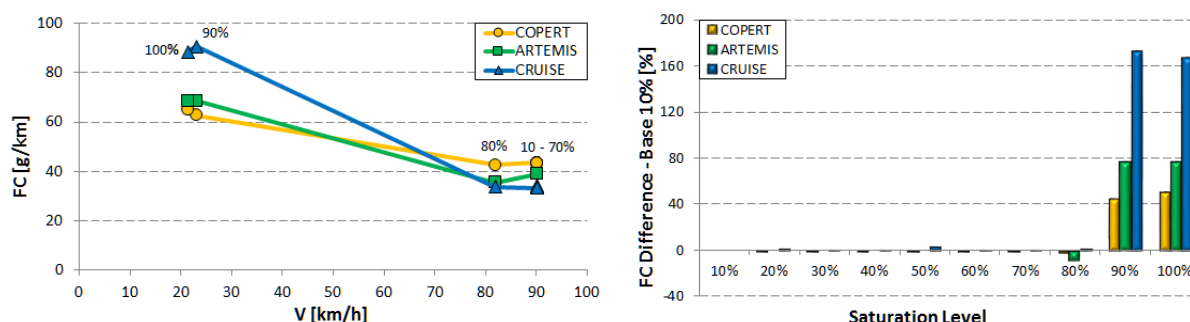


Figure 104: Effect of saturation level on fuel consumption calculated with all the available methods (left). Relative fuel consumption at 10% saturation as reference (right).

2.3.4. MADRID TRAFFIC DATA – DIESEL VEHICLE

Similar to gasoline case, the calculated fuel consumption for the diesel vehicle follows the same behaviour (Figure 105). Up to 80% saturation there is consistency among the three methods, while at higher saturation levels a large increase in fuel consumption occurs. When saturation exceeds 80% CRUISE model calculates almost the double fuel consumption compared to COPERT and the selected ARTEMIS cycle (100% difference), while in gasoline case this difference was around 40%.

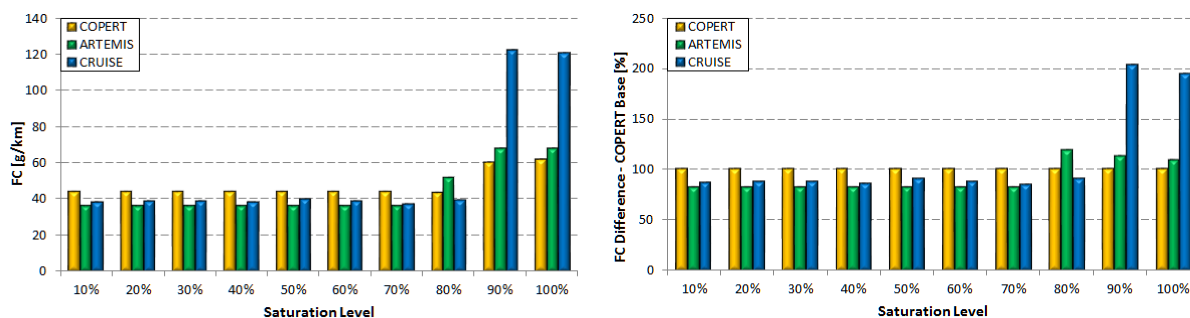


Figure 105: Absolute (left) and relative over COPERT (right) fuel consumption for all driving conditions.

Due to the increased fuel consumption that CRUISE calculates at high saturation levels, CRUISE trend differs substantially from the corresponding trends of COPERT and the selected driving cycle (Figure 106).

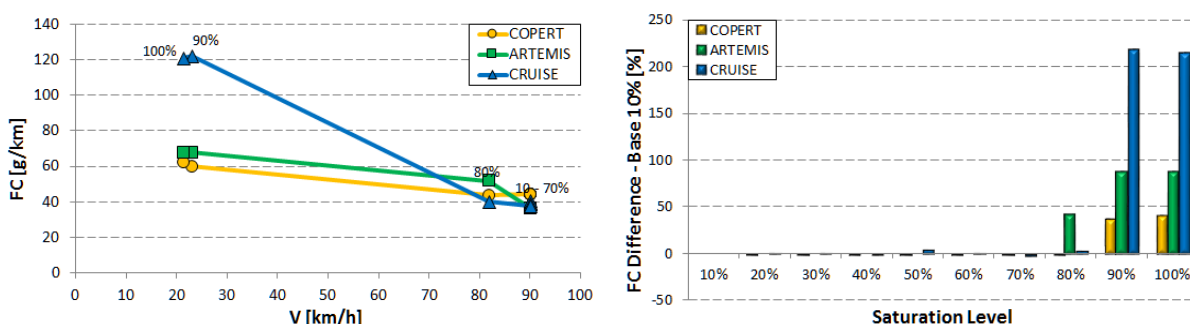


Figure 106: Effect of saturation level on fuel consumption calculated with all the available methods (left). Using fuel consumption at 10% saturation as reference (right).

2.3.5. EXTRA CASE STUDY – TURIN TRAFFIC DATA (DIESEL VEHICLE)

The results from Madrid traffic data – both for gasoline and diesel vehicle – indicated that after a certain saturation level – in the order of 80% – the average speed fails to adequately express changes in the driving pattern. However, since those calculations were performed using urban highway traffic data, another case study was conducted in order to investigate if such a deviation is present also in saturated urban traffic conditions.

An urban corridor in Turin, “Corso Lecce”, in its part between “Corso Regina” and “Via Lera”, was selected as a case study. This corridor consisted of 6 sections and 5 junctions and was simulated using AIMSUN. Only vehicle entering from the southmost entrance and exit from the north end of the corridor were considered in the simulations. Three different

simulations were performed corresponding to three hours of a typical weekday (5:00 – 6:00, 12:00 – 13:00 and 8:00 – 9:00), as well as to three traffic conditions (free, normal and saturated). A graphical representation of the simulated road in AIMSUN is shown in Figure 107.

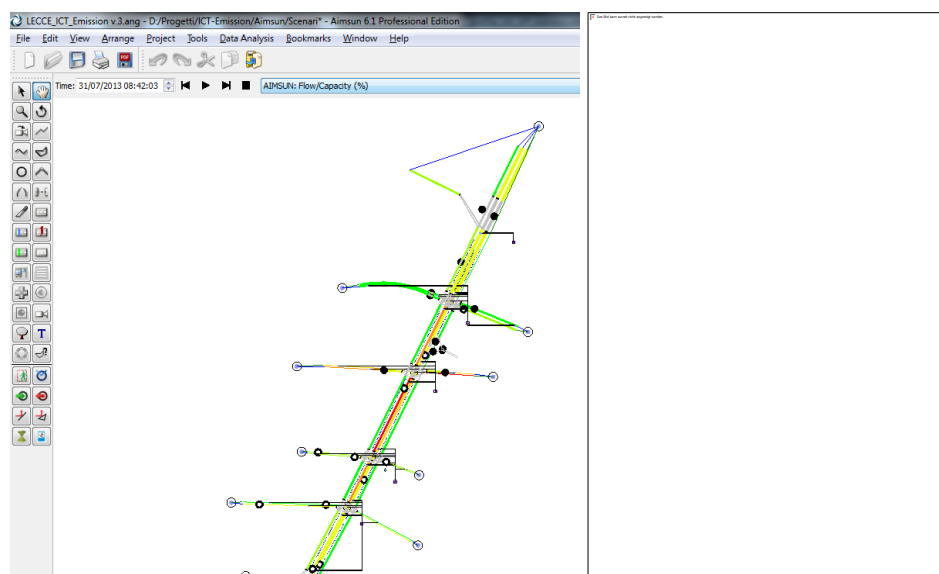


Figure 107: Schematic representation and map of an urban road in Turin simulated with AIMSUN.

The average statistics for each traffic condition are summarized in Table 11. Moving from free to saturated flow means that the increased vehicle flow – over the same road capacity – causes a reduction in average vehicle speed. As a consequence, there is a substantial increase in travel time, number of stops and stop time with increasing saturation.

Table 11: Average traffic characteristics from an urban road in Turin simulated with AIMSUN.

Traffic Condition	Free Flow	Normal Flow	Saturated Flow
Hour Of The Day	5:00 - 6:00	12:00 - 13:00	8:00 - 9:00
Average Speed [km/h]	39.0	27.7	23.2
Travel Time [sec]	152	214	256
Flow [veh/h]	15	453	780
Number Of Stops [-]	2.7	4.4	5.1
Stop Time [sec]	48	98	132

Since the time required to micro-simulate (with CRUISE) all the vehicles for each traffic condition would be enormous, it was decided to use some representative vehicles. Thus, using the simulated data from AIMSUN, 3 random vehicles were selected for every traffic condition, so, in total, 9 vehicles were examined. For all vehicles, and independently for each of the 6 sections of the simulated road, the average speed, mean saturation, as well as the fuel consumption from COPERT and CRUISE (BMW X1 model – 2.0 l, diesel, Euro 5) were calculated.

The same calculation was repeated for all vehicles, but by increasing the number of sections considered in order to examine the impact of road length on the results. Therefore, a composite of section one and two, was considered, then sections one, two and three, and moving along until finally the complete corridor, consisting of the six sections was simulated. The previous procedure was repeated, but taking this time an “average vehicle” for each traffic condition (3 vehicles). The necessary values of the “average vehicle” were produced by taking the average values of speed, saturation etc. of the selected 3 vehicles for each traffic condition. Finally, the calculated fuel consumption values retrieved from both COPERT and CRUISE were compared using absolute and relative differences.

The average speed and saturation levels for the 6 sections are presented in Figure 108. In general, the saturation for each road section varies from 0% up to almost 100%. The highest saturation – in saturated traffic flow conditions – occurs in section 3 (over 90%). In all sections the effect of saturation is accompanied by a reduction in the average speed of the vehicles. This effect is more evident in sections 4 and 5.

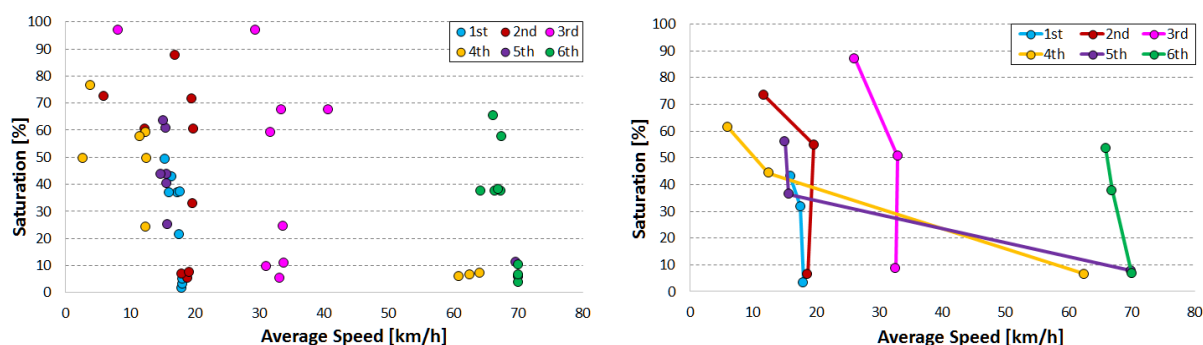


Figure 108: Average speed vs. saturation of the 6 sections of the simulated urban road in Turin based on selected 9 vehicles (left) and the 3 average vehicles (right).

In order to calculate the average fuel consumption with COPERT, 54 average vehicle speeds (9 vehicles x 6 road sections), along with 18 speeds for the average vehicles (3 vehicles x 6 road sections) were used. Using the fuel consumption factors of the Euro 5 Diesel <2.0 l category, the fuel consumption values were retrieved. Similarly in CRUISE, the instantaneous vehicle speeds were inserted in the BMW X1 model and the fuel consumption values were calculated for all driving profiles. Then, the average fuel consumption was calculated by summing the instantaneous fuel consumption over the entire driving profile. The consumptions calculated by both COPERT and CRUISE are shown in Figure 109.

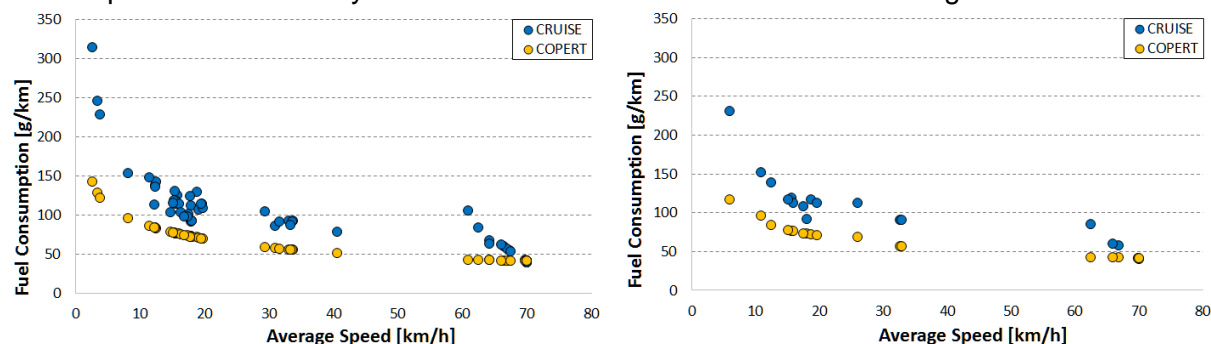


Figure 109: Fuel consumption calculated with both CRUISE and COPERT based on driving profiles of the selected 9 vehicles (left) and the 3 average vehicles (right).

Comparing the absolute values of fuel consumption (Figure 109), it is evident that COPERT calculates lower fuel consumption values than CRUISE over the entire speed range. However, this is not so important, as COPERT values are average for a complete class while CRUISE absolute values are specific to a single vehicle only. What is important in this comparison is to judge whether the relative differences as an outcome of the different saturation levels are consistently reported between COPERT and CRUISE. This is shown in Figure 110.

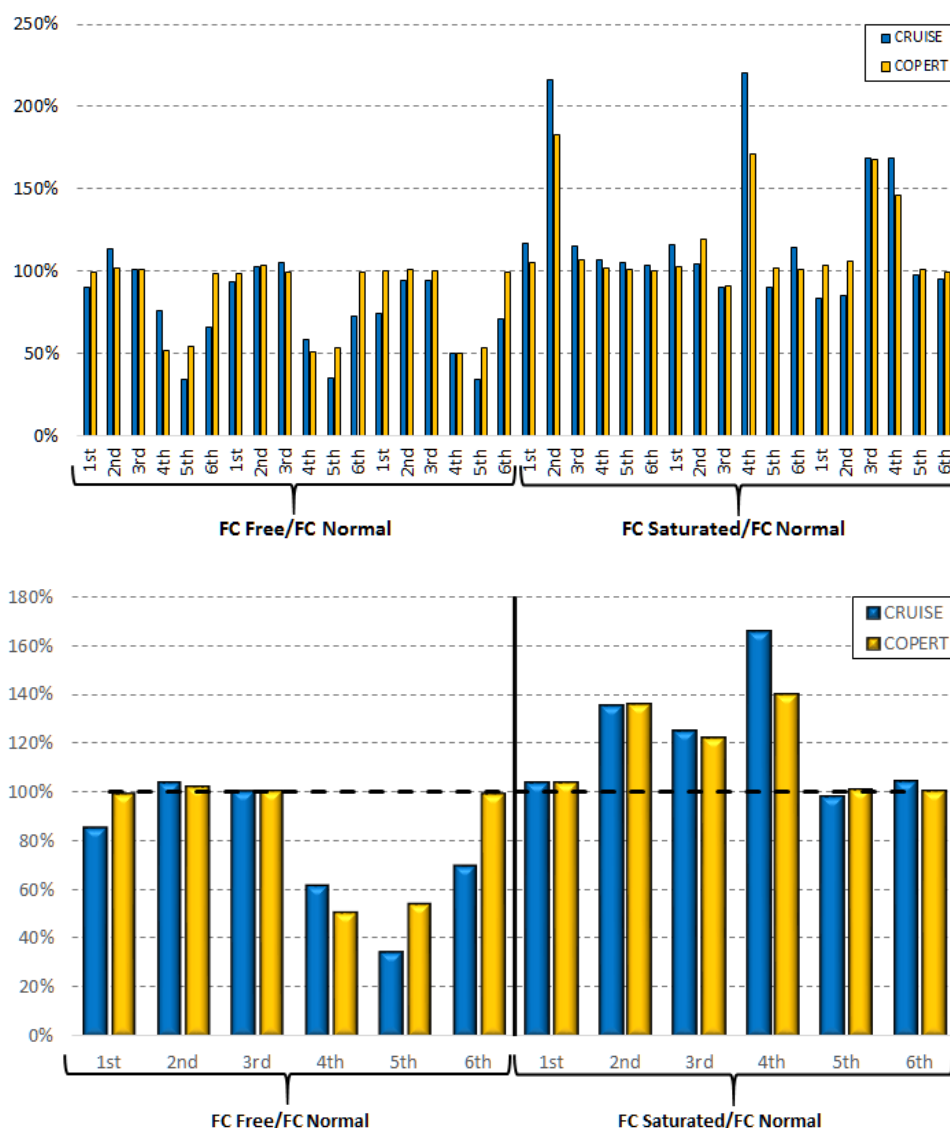


Figure 110: Relative fuel consumption differences calculated with both CRUISE and COPERT based on driving profiles of the selected 9 vehicles (up) and the 3 average vehicles (down). The calculated fuel consumption in normal traffic conditions was used as the 100% basis in both software tools.

Both charts in Figure 110 indicate that the relative fuel consumption differences calculated with both COPERT and CRUISE are comparable. In other words, COPERT seems to satisfactorily predict the impact of saturation even within an urban network. When single vehicles are concerned (Figure 110 top chart), the difference between CRUISE and COPERT

increases, than when averaged vehicles are considered. This is also expected, as macro scale modelling tries to simulate fleet level effects and no effects on single vehicles.

The impact of road length is examined in the following chart (Figure 111), where the saturation level and average vehicle speed are calculated over the 6 road sections, by increasing gradually the road length (1st section only, 1st and 2nd section, up until the entire road is completed – 1st to 6th section). In general as the road length increases the average vehicle speed increases too (the 1st to 6th section curve is on the leftmost side of the chart), while saturation level does not change substantially.

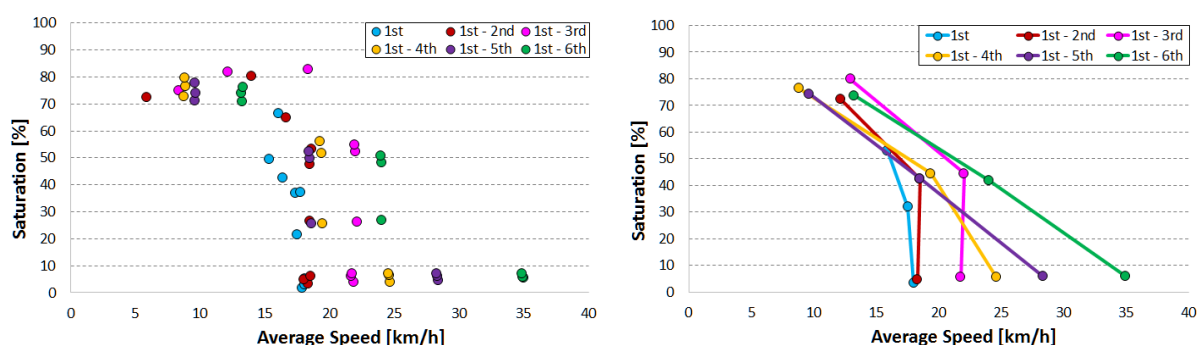


Figure 111: Average speed vs. saturation of the simulated urban road in Turin based on selected 9 vehicles (left) and the 3 average vehicles (right); impact of road length.

A longer road section seems to smooth out the differences between relative fuel consumption calculated with both COPERT and CRUISE. The charts in Figure 112 imply that as the road length increases there is a shift from micro towards the macro level in terms of driving profile and fuel consumption. A longer driving profile (i.e. 1st to 6th – corresponding to the entire simulated road) will have much more “average” characteristics than a shorter one (i.e. 1st section only). In this way, the average speed of a vehicle circulating in a large road would be more representative and closer to COPERT average speed, while in short roads the average vehicle speed is probably not representative of the driving profile.

In the bottom chart of Figure 112 the values of relative fuel consumption calculated with COPERT are always below the corresponding CRUISE values on the free over normal part of the chart. This indicates that the absolute fuel consumption values on free flow conditions are higher than the corresponding values calculated with CRUISE. In free flow conditions the vehicle activity is low, hence, by definition it is not a frequent condition, while its contribution to the total consumption is small. Moreover, if an urban network is in free flow conditions, there is little you can do to substantially improve fuel consumption. Moreover, such differences on the exact absolute levels should be seen in the light of the fact that the CRUISE simulations have been done on a single vehicle only. Other vehicles with different efficiency characteristics might result into a different performance. Hence, general trends need to be only revealed in this comparison.

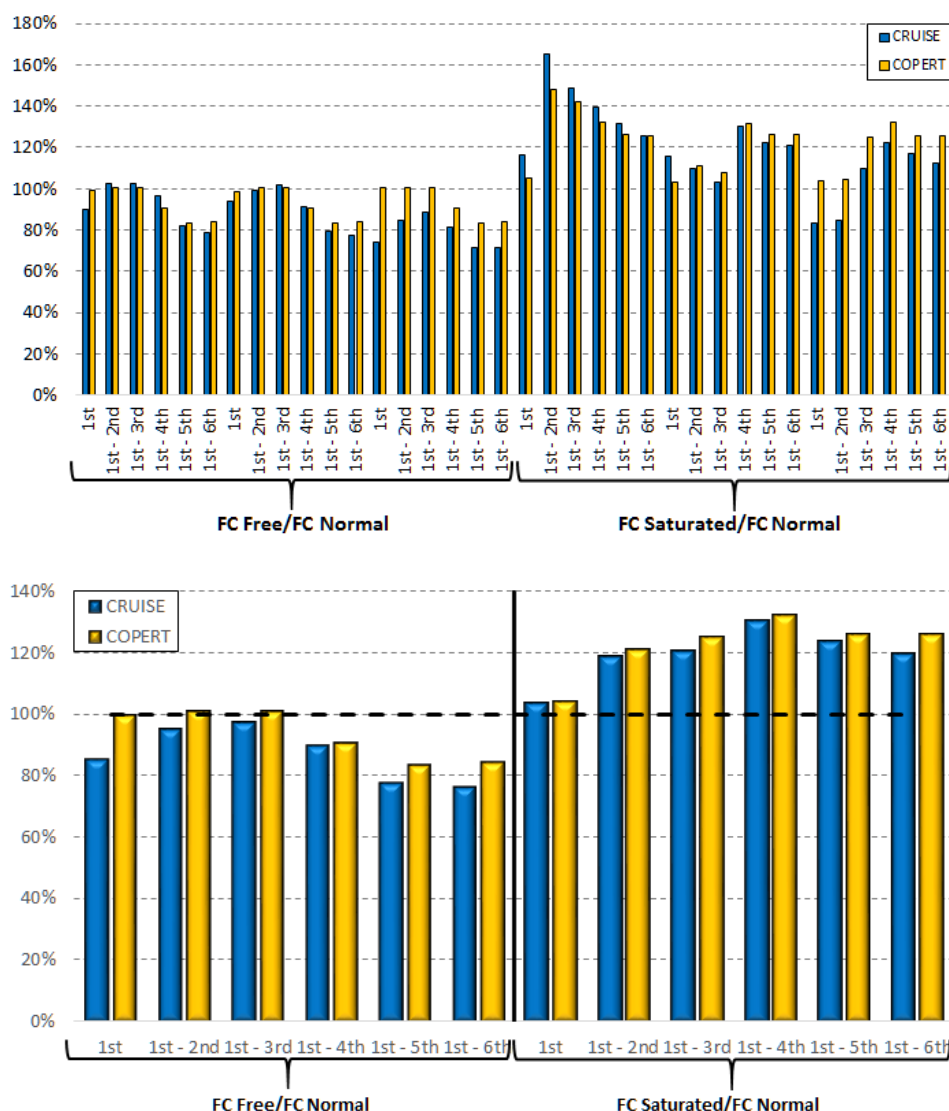


Figure 112: Relative fuel consumption differences calculated with both CRUISE and COPERT based on driving profiles of the selected 9 vehicles (up) and the 3 average vehicles (down). The calculated fuel consumption in normal traffic conditions were used as basis in both software; impact of road length

The combined effect of saturation and road length is shown in Figure 113. When the ratio $(FC_{CRUISE} / FC_{CRUISE_{normal}}) / (FC_{COPERT} / FC_{COPERT_{normal}})$ equals one, both COPERT and CRUISE calculate the same relative fuel consumption difference when either the distance or the level of saturation change. Consequently, in the areas where the ratio is equal to one – or close to one, it is considered “safe” to use COPERT for calculating fuel consumption.

Most of the chart is covered by cyan colour (ratio = 1), so, in most of the cases there is a good agreement between COPERT and CRUISE regarding relative fuel consumption differences. However, there are two areas in the chart that should be highlighted. Both areas are related with short road lengths (below 400 m); the first one is related with low saturation (below 20%), while the other one with high saturation levels (above 80%) – yellow and dark blue colour correspondingly in the chart. These two areas summarizing actually the shortcomings of the average speed approach. If COPERT is applied to a short road section only (below 400 m), then uncertainty increases. In several cases, as the one simulated in this

case study, COPERT will not be able to adequately reproduce fuel consumption changes, since the average speed over such a short road length does not represent the traffic situation adequately. The same applies in quite saturated conditions (saturation above 80%), as it was also shown in Madrid test case.

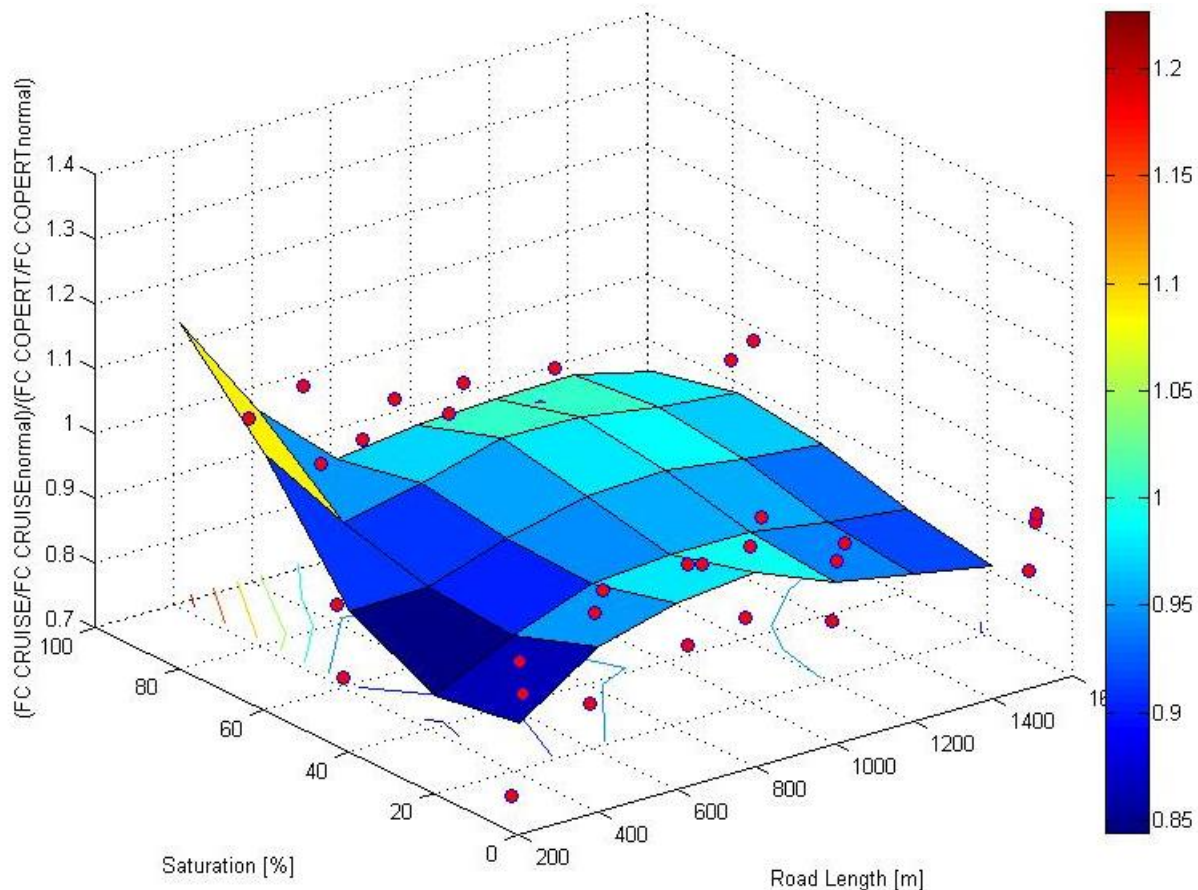


Figure 113: Impact of saturation and road length on ratio of relative fuel consumption calculated with both CRUISE and COPERT.

This last chart could be used as a guide regarding the application of various ICT-measures on macro level. It indicates the areas where the average speed approach is valid, while it highlights the areas where special care should be taken.

2.4. DISCUSSION

The results from case studies revealed the application range and the limitations of using the average vehicle speed as the only traffic parameter to estimate fuel consumption and emissions macro emissions models, such as COPERT. The analysis was conducted on the basis of measured and simulated data in an urban corridor and in simulated data on an urban highway. In most of the traffic situations studied, the emissions and consumption calculated using the average speed satisfactorily predicted both the trend and the magnitude of the change, compared to a baseline condition. There were of course individual differences between the fuel consumption derived by using the exact driving profile in CRUISE and the one calculated by COPERT on the basis of the average speed. However, these differences

are sporadic and rather random in nature and they do not seem to introduce any particular bias, so that the simulation could be considered invalid. The CRUISE simulations were conducted on single vehicles only, hence individual differences with COPERT may also depend on vehicle particularities, as the COPERT functions refer to a fleet of vehicles and not to single vehicles only. Using a different vehicle model or the same vehicle over a different driving pattern with the same average speed might produce a difference which is in the opposite direction than we currently observed. These findings further confirm the largely accepted practice that the average speed based emission factor is a satisfactory approach in estimating emissions at a macro level.

Our findings go one step further. In measured cases with an ICT measure on and off (in our case the implementation or not of UTC-driven traffic lights), average speed is still a good indicator of fuel consumption at a macro level. Again, the consumption calculated on the basis of average speed was very well predicted and, in most cases, even the magnitude of the difference was close to the one calculated with the exact driving profile. Some difference was observed between the free and the normal or congested conditions, with COPERT estimating higher consumption in free driving conditions than the actual one. This is to be expected: COPERT tries to cover these driving conditions that are mostly frequent and mostly contribute to total fuel consumption. The 'free' condition is consistent with low activity – hence by definition it is not a frequent condition, with a rather small contribution to total consumption and does not match the COPERT profiles. But in any case, the "free" condition is not of particular importance in ICT-Emissions. In case an urban network is free, there is little you can do to substantially improve fuel consumption.

There were two characteristic cases though where the macro emission model based on average speed failed to satisfactorily predict emissions. The first had to do with predicting emissions in very short links, i.e. those with a length of less than 400 m. In this case, average speed was not proven to be a very good determinant of emissions and consumption. This is to be expected since, by definition, very short links cannot be modelled at a macro level. For such short distances, the stylized driving pattern cannot be correctly represented by an average speed model. The results collected therefore show that COPERT maximum resolution is down to approximately 400 m. if shorter distances need to be modelled at a macro level, then it would be safer to aggregate short links to larger conglomerates. An activity within WP5 examines what is the sensitivity of macro modelling to different aggregation possibilities of short links.

The second characteristic case where average speed failed as a determinant of emissions and consumption was for congestion levels higher than approximately 80%. The results of the simulation in the Madrid highway showed that when saturation exceeded this threshold the mean speed dropped by more than 4 times (down to 20 km/h) and the mean positive acceleration became 8 times higher. Basically, driving becomes a constant stop and go event with little idling and harsh accelerations to keep up with the jerky traffic. This is different than urban driving with the same average speed. Hence, COPERT emission factors which are based on urban conditions for a speed of 20 km/h tend to underestimate the impact of saturation on CO₂ emissions and fuel consumption. For the Turin case, the impact of saturation was not as clear. This might also have been an effect of the selection of the particular urban corridor. Due to its layout, high congestion in this corridor appears only on a single segment (segment 3) which acts as a bottleneck for the subsequent segments. Hence, we could not observe saturation levels above 80% for the complete corridor in order to come up to reliable conclusions. However, at this stage we have to recommend that COPERT

macro should not be used in congested networks where saturation exceeds 80%. If this has to be conducted, then the following recommendations are given:

1. COPERT should be expected to underestimate emissions and consumption at high congestion levels. Hence, if a measure is introduced that decreases congestion, then the actual (positive) impact on emissions and consumption will be higher than what COPERT estimates.

2. If high congestion occurs only in specific short segments (<400 m) then it is safe to aggregate these with neighbouring segments. This would lead to an overall uncongested case and a speed which can be a reliable input to COPERT.

3. If congestion occurs on a relatively wide part of the network, then the recommendation would be that the results of the micro modelling are also included to correct macro-scale emissions for the particular congested network. Micro simulations will be conducted for both the congested and the uncongested simulations, hence, there will be a calculation of what is the impact of saturation in the micro scale. In this case, it is proposed to correct the macro calculation according to the following ratio:

$$MACRO_{CONG,CORR} = MICRO_{CONG} \times \frac{MACRO_{UNCONG}}{MICRO_{UNCONG}}$$

the selection of the micro values to be used in this ratio need to take into account the vehicle type (fuel, category, etc.).

3 Model validation by chassis dynamometer measurements

3.1. INTRODUCTION

The performance of the AVL CRUISE model and the particular vehicle models that were simulated with CRUISE were validated using fuel consumption measurements conducted in the chassis dynamometer facility of the Laboratory of Applied Thermodynamics. As it was not possible to validate all 30 vehicle bins, a selection was made to validate some of the most popular vehicle categories and include two gasoline and two diesel passenger cars of the Tier 2 category in segments C', D', and E'.

The measurement setup is shown in Figure 114.



Figure 114: LAT experimental setup.

3.2. VEHICLE VALIDATION

The diesel passenger cars selected for measurements were a Peugeot 308 e-HDi FAP, a BMW X1 sDrive20d Efficient Dynamics while the petrol vehicles were a Volkswagen Golf 1.4 TSI and a Toyota Avensis 1.6 VVT-i. These vehicles were measured over the New European Driving Cycle (NEDC), and to the Artemis driving cycles (Urban and Road). In addition, BMW X1 was measured over the Worldwide harmonized Light Duty Test Cycle (WLTC). The driving profiles can be seen in Figure 115.

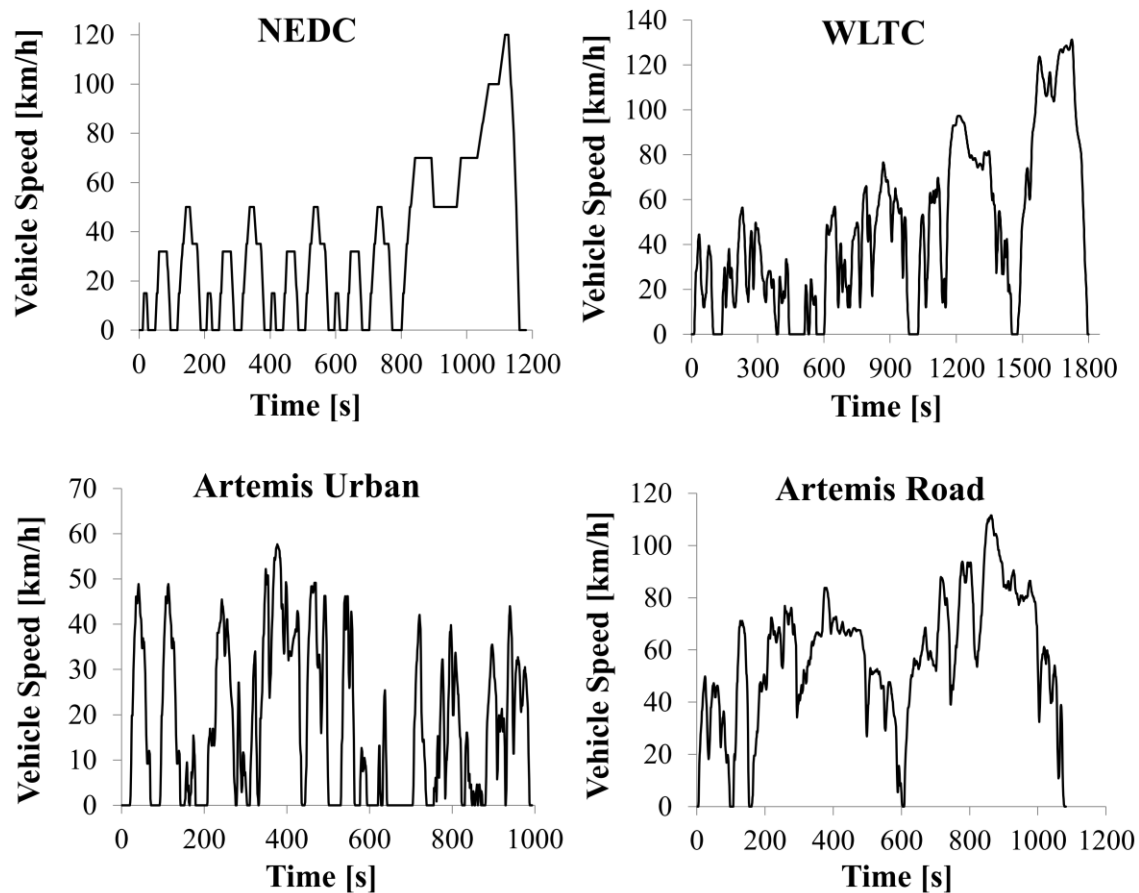


Figure 115: Experimental driving cycles.

The first and most important step is the approximation of fuel consumption engine map for each particular vehicle model. For this purpose the instantaneous fuel consumption from the carbon balance and BMEP is calculated using the second by second raw exhaust emissions measured on the chassis dynamometer. Following a synchronisation of the different sets of measured data, fuel consumption values are assigned to particular operating modes of the engine. Thus the engine map for each car can be created which is the most important factor for the accurate modelling of a vehicle. An overview of the process is shown in Figure 116.

For the technical characteristics necessary for setting up the model, data from car manufacturer web-pages, internet databases or model brochures are gathered and implemented in the model. Initial simulations are performed in order to compare the vehicle 0-100 km/h acceleration with the published one. Then the initial model is modified according to the fuel consumption results and revised simulations are run. Finally the model is validated with the chassis dyno measurement data. This is a procedure which may be repeated multiple times before then final model is created. An overview of the above is shown in Figure 117.

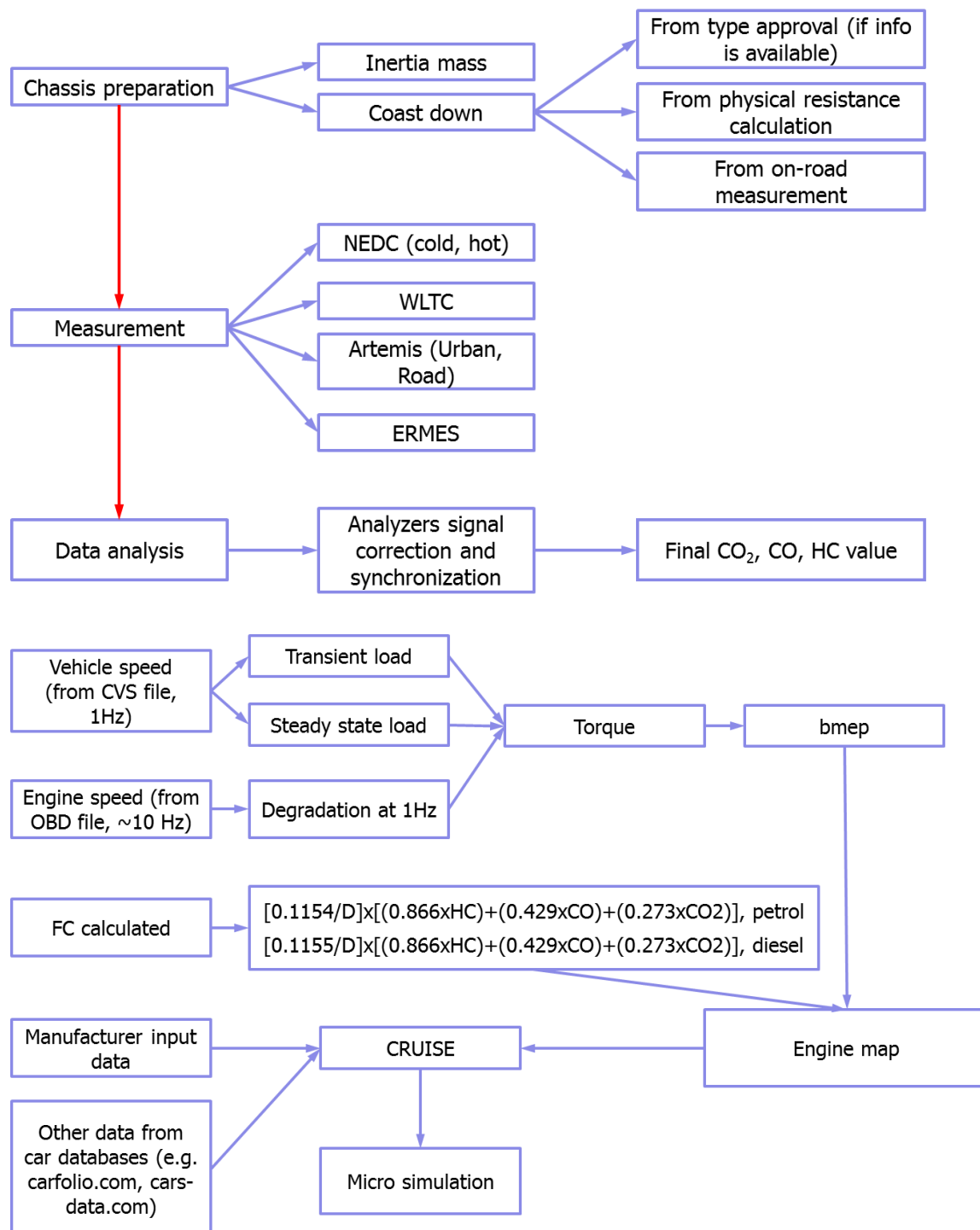


Figure 116: Overview of the process to create engine maps from chassis dyno tests

3.3. RESULTS OF VALIDATION

Overall simulated fuel consumption is compared with the experimental for all four measured vehicles in NEDC and Artemis Road. Also the second-by-second BMEP and engine speed comparison depict a good correlation of all models with real conditions.

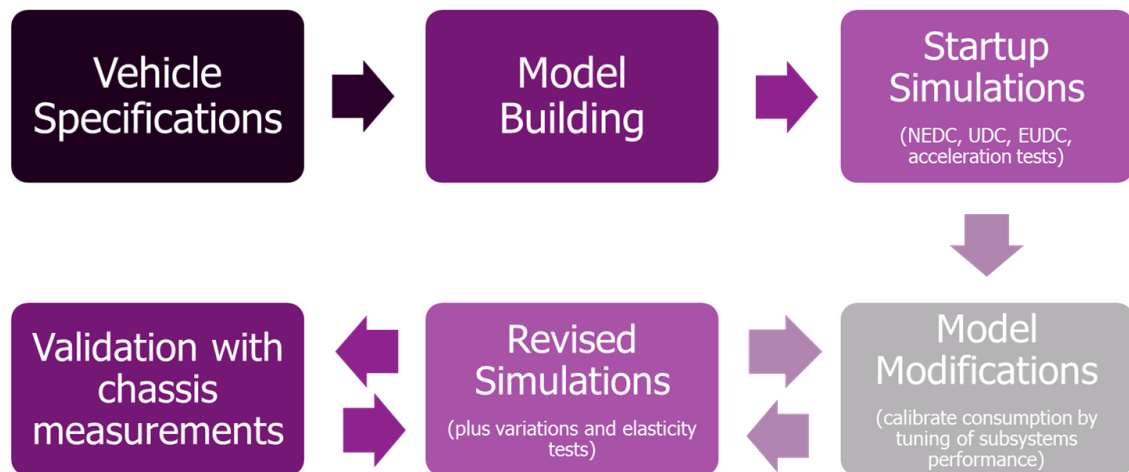


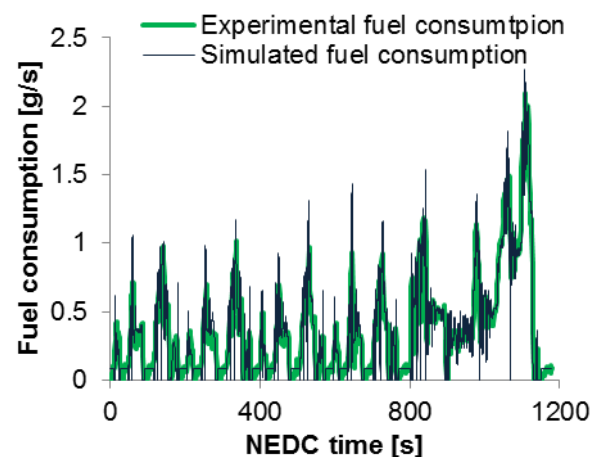
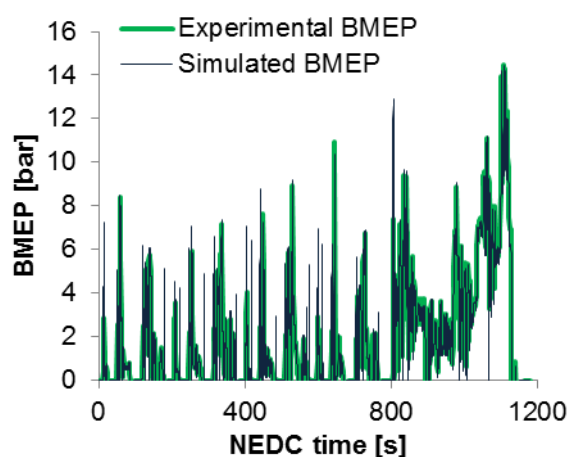
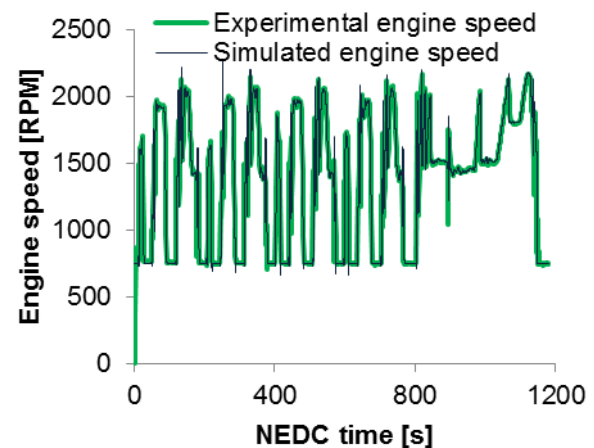
Figure 117: Simulation validation overview.

Sections 3.3.1 through 3.3.8 that follow present a summary of the validation of the engine speed, BMEP and fuel consumption for each of the four test vehicles under two different driving cycles; NEDC and Artemis Road. The overall fuel consumption accuracy obtained from the validations is within a 5% error for most of the simulations.

3.3.1. PEUGEOT 308 NEDC

This page shows how the model approaches the engine speed, bmep and fuel consumption of the vehicle. There is a very good match of the fuel consumption, which is in the order of 2% over the complete NEDC.

Peugeot 308 e-Hdi FAP	
Displacement [cm ³]	1560
Curb weight [kg]	1293
Max Engine Power [kW@RPM]	82@3600
Max Engine Torque [Nm@RPM]	270@1750
Gearbox	6 gear manual transmission
Tyre size	205/55 R16
Type approval CO ₂ [g/km]	109



Top left: Peugeot 308 characteristics.

Top right: Experimental and simulated engine speed during NEDC.

Bottom left: Experimental and simulated BMEP during NEDC.

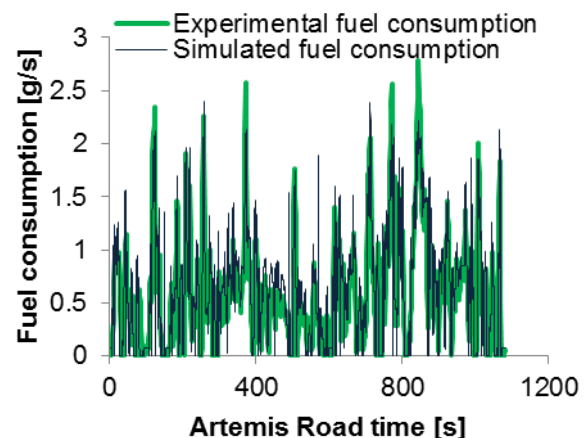
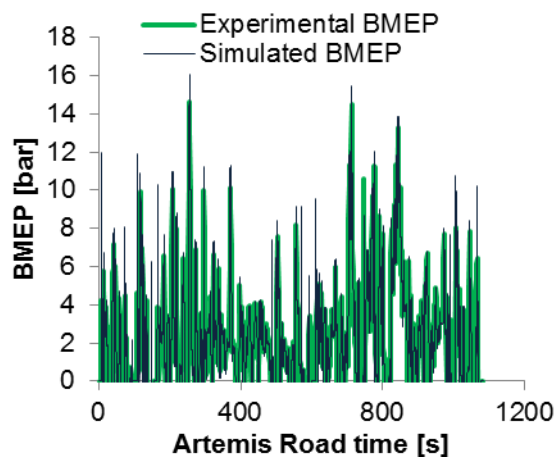
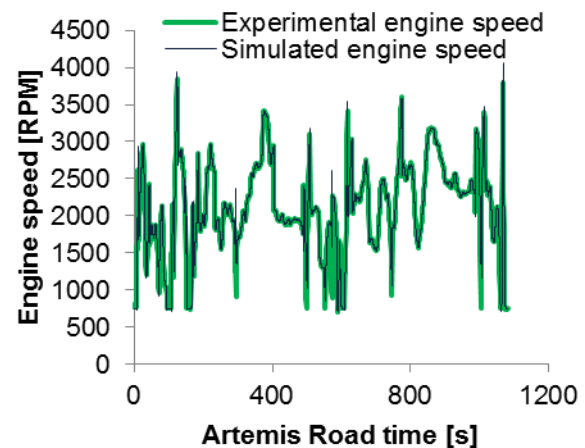
Bottom right: Experimental and simulated fuel consumption during NEDC.

Driving cycle	Fuel consumption [l/100 km]		Deviation [%]
	Experimental	Simulated	
UDC	5.5	5.8	5.5
EUDC	4.1	4.1	0.0
NEDC	4.6	4.7	2.2

3.3.2. PEUGEOT 308 ARTEMIS ROAD

The same criteria signals used over the NEDC are presented here over the Artemis Road driving cycle. There is again a very good match between measured and simulated signals. The fuel consumption is approached satisfactorily over the Artemis Urban (<3%) and less satisfactorily over the Artemis Road. The Artemis cycles are in general more aggressive and difficult to simulate. However, the overall quality of the simulation is satisfactory.

Peugeot 308 e-Hdi FAP	
Displacement [cc]	1560
Curb weight [kg]	1293
Max Engine Power [kW@RPM]	82@3600
Max Engine Torque [Nm@RPM]	270@1750
Gearbox	6 gear manual transmission
Tires	205/55 R16
CO ₂ emissions [g/km]	109



Top left: Peugeot 308 characteristics.

Top right: Experimental and simulated engine speed during Artemis Road.

Bottom left: Experimental and simulated BMEP during Artemis Road.

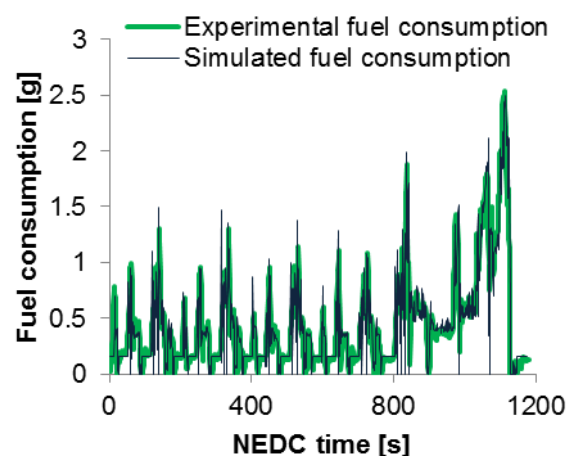
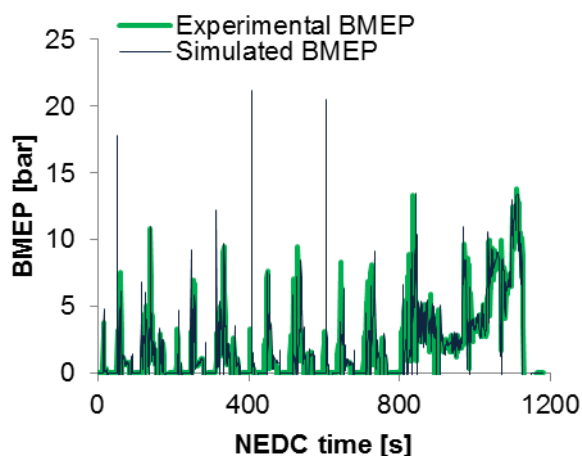
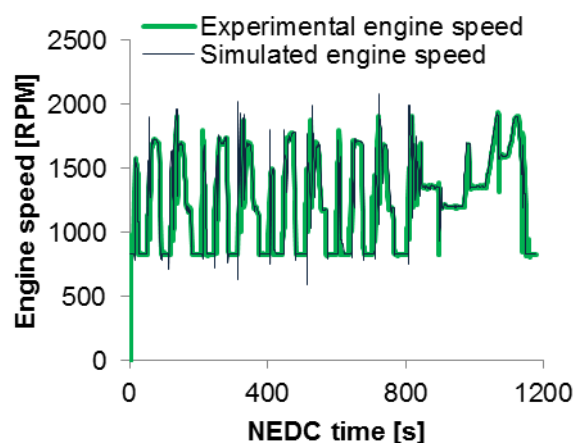
Bottom right: Experimental and simulated fuel consumption during Artemis Road.

Driving cycle	Fuel consumption [l/100 km]		Deviation [%]
	Experimental	Simulated	
Artemis Urban	6.9	6.7	-2.9
Artemis Road	4.5	4.9	8.9

3.3.3. BMW X1 NEDC

The BMW X1 is an advanced vehicles with micro-hybrid characteristics (energy recuperation during braking). The simulated vehicle over NEDC matches the measurement very well in all signals shown. The mean difference of fuel consumption over the NEDC is less than 2%.

BMW X1 sDrive20d Efficient Dynamics	
Displacement [cc]	1995
Curb weight [kg]	1465
Max Engine Power [kW@RPM]	120@4000
Max Engine Torque [Nm@RPM]	380@1750
Gearbox	6 gear manual transmission
Tires	225/50 R17
CO ₂ emissions [g/km]	119



Top left: BMW X1 characteristics.

Top right: Experimental and simulated engine speed during NEDC.

Bottom left: Experimental and simulated BMEP during NEDC.

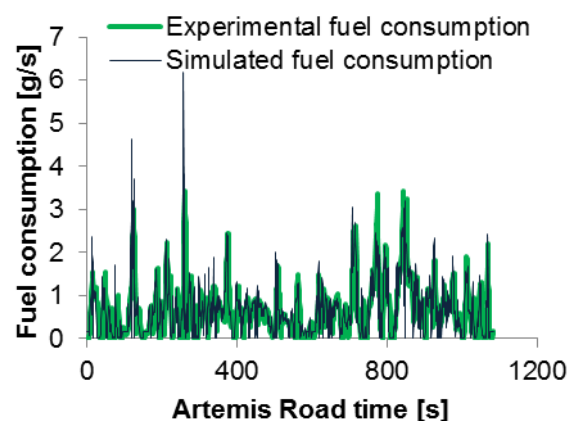
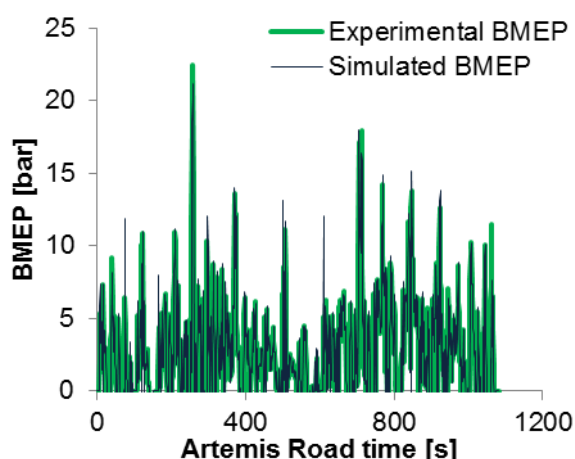
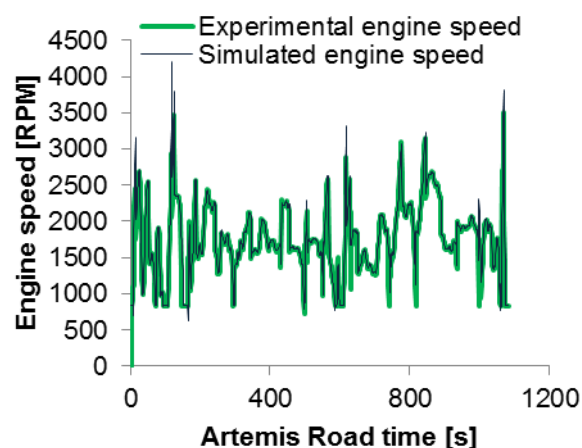
Bottom right: Experimental and simulated fuel consumption during NEDC.

Driving cycle	Fuel consumption [L/100 km]		Deviation [%]
	Experimental	Simulated	
UDC	7.3	7.1	-2.7
EUDC	4.9	4.9	0.0
NEDC	5.8	5.7	-1.7

3.3.4. BMW X1 ARTEMIS ROAD

The BMW X1 simulated model performs very well also over the ARTEMIS and the new type-approval WLTC cycles with mean fuel consumption differences less than 2% on average for the three cycles. All monitored individual simulated signals also very well matched the measured ones during the cycles.

BMW X1 sDrive20d Efficient Dynamics	
Displacement [cc]	1995
Curb weight [kg]	1465
Max Engine Power [kW@RPM]	120@4000
Max Engine Torque [Nm@RPM]	380@1750
Gearbox	6 gear manual transmission
Tires	225/50 R17
CO ₂ emissions [g/km]	119



Top left: BMW X1 characteristics.

Top right: Experimental and simulated engine speed during Artemis Road.

Bottom left: Experimental and simulated BMEP during Artemis Road.

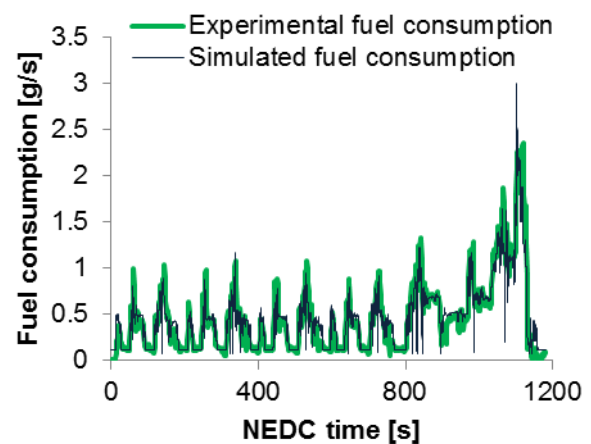
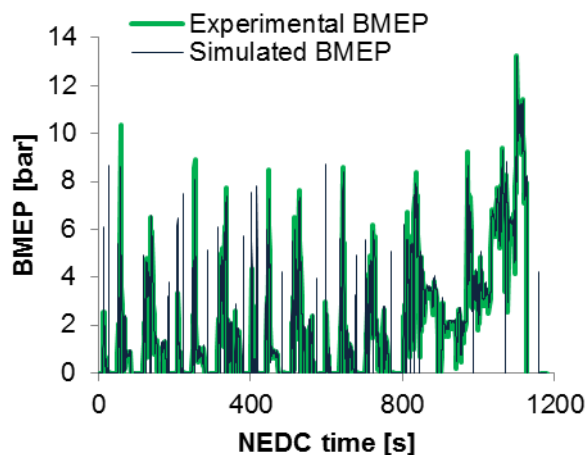
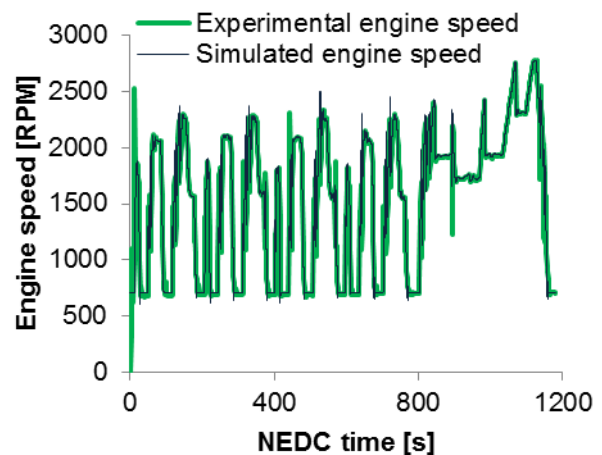
Bottom right: Experimental and simulated fuel consumption during Artemis Road.

Driving cycle	Fuel consumption [L/100 km]		Deviation [%]
	Experimental	Simulated	
Artemis Urban	9	8.8	-2.2
Artemis Road	5.2	5.1	-1.9
WLTC	5.7	5.7	0

3.3.5. VOLKSWAGEN GOLF NEDC

The VW Golf tested is a vehicle with a gasoline direct injection engine which is known as a technology that improves fuel efficiency. The overall fuel consumption difference between simulation and measurements was 0% over the NEDC for this vehicle but individual differences existed between the UDC and EUDC subparts of the cycle. Second by second modelling of individual signals was also satisfactory.

Volkswagen Golf 1.4 TSI 90 kW	
Displacement [cc]	1390
Curb weight [kg]	1465
Max Engine Power [kW@RPM]	90@5000
Max Engine Torque [Nm@RPM]	200@1500
Gearbox	6 gear manual transmission
Tires	205/55 R16
CO ₂ emissions [g/km]	144



Top left: Volkswagen Golf characteristics.

Top right: Experimental and simulated engine speed during NEDC.

Bottom left: Experimental and simulated BMEP during NEDC.

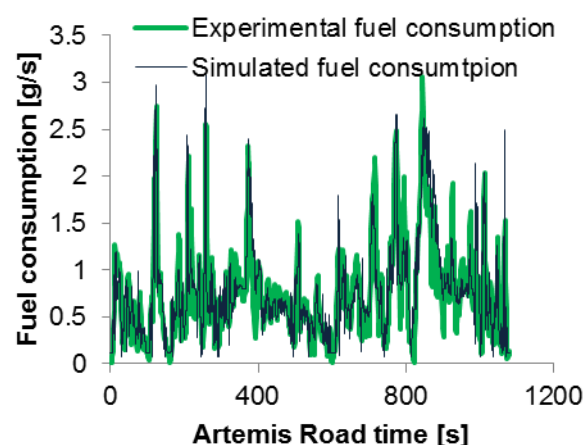
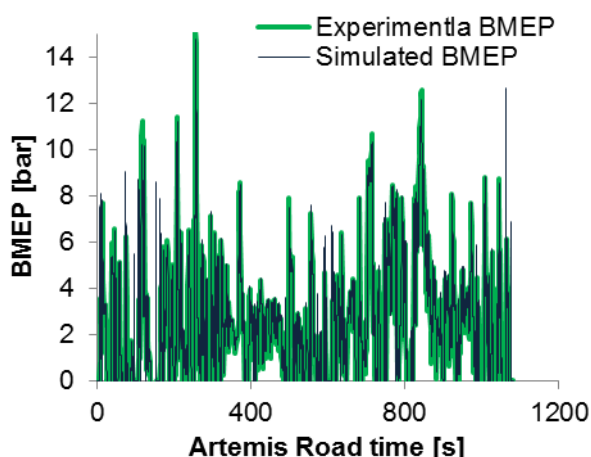
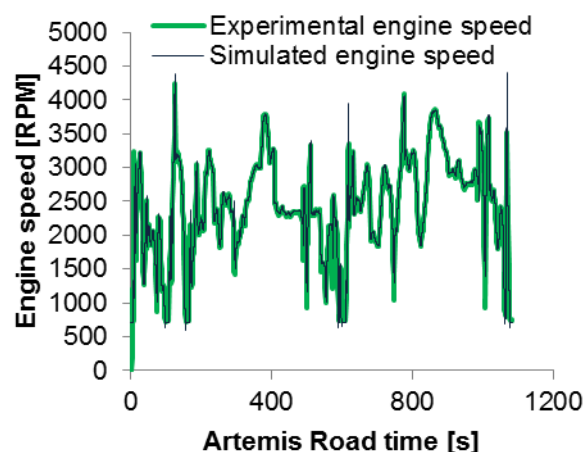
Bottom right: Experimental and simulated fuel consumption during NEDC.

Driving cycle	Fuel consumption [L/100 km]		Deviation [%]
	Experimental	Simulated	
UDC	8.3	8.7	4.8
EUDC	5.6	5.4	-3.6
NEDC	6.6	6.6	0

3.3.6. VOLKSWAGEN GOLF ARTEMIS ROAD

The satisfactory simulation of the VW Golf over the NEDC is also confirmed over the Artemis cycles with mean fuel consumption differences that did not exceed 3%. The consistency of the simulated values with the measured ones extends also in the second by second values over the driving cycle.

Volkswagen Golf 1.4 TSI 90 kW	
Displacement [cc]	1390
Curb weight [kg]	1465
Max Engine Power [kW@RPM]	90@5000
Max Engine Torque [Nm@RPM]	200@1500
Gearbox	6 gear manual transmission
Tires	205/55 R16
CO ₂ emissions [g/km]	144



Top left: Volkswagen Golf characteristics.

Top right: Experimental and simulated engine speed during Artemis Road.

Bottom left: Experimental and simulated BMEP during Artemis Road.

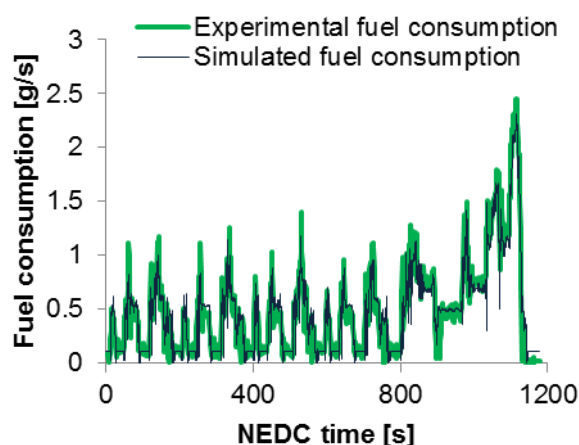
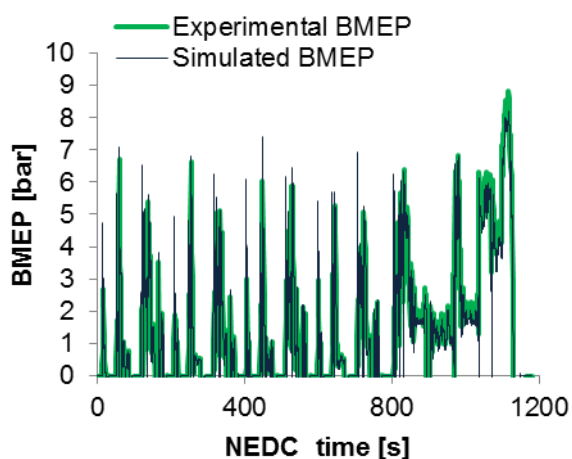
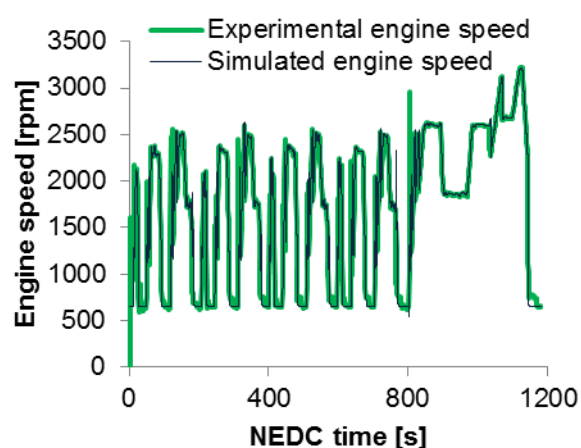
Bottom right: Experimental and simulated fuel consumption during Artemis Road.

Driving cycle	Fuel consumption [L/100 km]		Deviation [%]
	Experimental	Simulated	
Artemis Urban	10.3	10	-2.9
Artemis Road	6.3	6.4	1.6

3.3.7. TOYOTA AVENSIS NEDC

The Toyota Avensis tested is a typical gasoline passenger car. The model achieves a relatively good match of the simulated with the measured fuel consumption with individual deviations between the urban and the extra urban parts of the NEDC. Again, signals are very well matched during the driving cycle.

Toyota Avensis 1.6 VVT-i	
Displacement [cc]	1598
Curb weight [kg]	1340
Max Engine Power [kW@RPM]	97@6400
Max Engine Torque [Nm@RPM]	160@4400
Gearbox	6 gear manual transmission
Tires	215/55 R17
CO ₂ emissions [g/km]	152



Top left: Toyota Avensis characteristics.

Top right: Experimental and simulated engine speed during NEDC.

Bottom left: Experimental and simulated BMEP during NEDC.

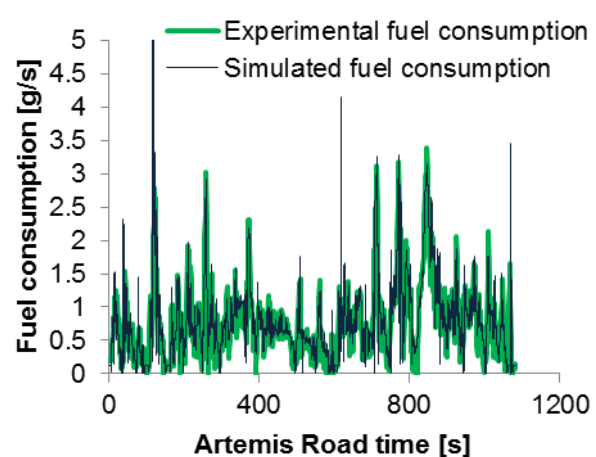
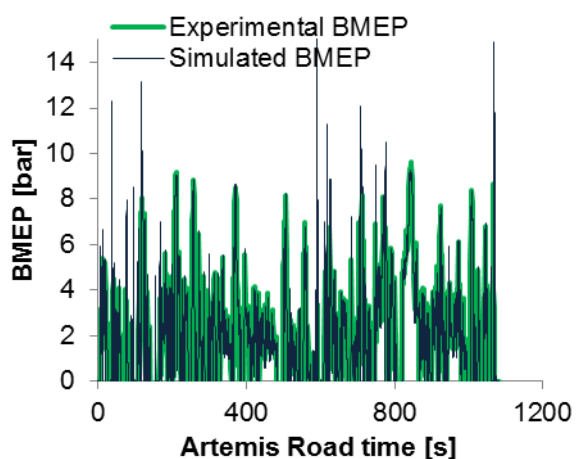
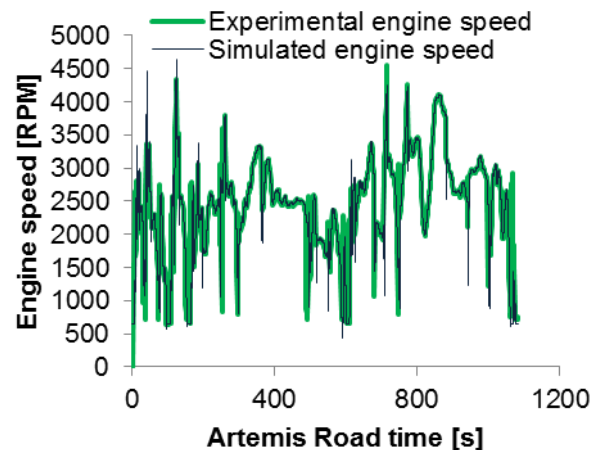
Bottom right: Experimental and simulated fuel consumption during NEDC.

Driving cycle	Fuel consumption [L/100 km]		Deviation [%]
	Experimental	Simulated	
UDC	8.8	8.9	1.1
EUDC	6.1	5.8	-4.9
NEDC	7.1	6.8	-4.2

3.3.8. TOYOTA AVENSIS ARTEMIS ROAD

The simulated fuel consumption for the Toyota Avensis over the Artemis driving cycles is somewhat higher than the measured one, by up to 5%. Still deviations do not seem to be systematic during the driving cycle.

Toyota Avensis 1.6 VVT-i	
Displacement [cc]	1598
Curb weight [kg]	1340
Max Engine Power [kW@RPM]	97@6400
Max Engine Torque [Nm@RPM]	160@4400
Gearbox	6 gear manual transmission
Tires	215/55 R17
CO ₂ emissions [g/km]	152



Top left: Toyota Avensis characteristics.

Top right: Experimental and simulated engine speed during Artemis Road.

Bottom left: Experimental and simulated BMEP during Artemis Road.

Bottom right: Experimental and simulated fuel consumption during Artemis Road.

Driving cycle	Fuel consumption [L/100 km]		Deviation [%]
	Experimental	Simulated	
Artemis Urban	10.8	11.1	2.8
Artemis Road	6.4	6.6	4.7

3.3.9. TOYOTA PRIUS III PLUGIN

The Toyota Prius III Plugin is a front wheel driven (FWD) full hybrid vehicle with e-CVT. The main difference to the Toyota Prius III as described in chapter 1.3.3.7 is that this model is equipped with Plugin functionality. This means that the battery can be charged by an external power supply, while for the conventional model the battery can be charged only internally by brake energy recuperation or by the ICE. Due to the external charging the vehicle is equipped with a larger battery and a stronger electric motor. This enables the vehicle for a longer distance of pure electric driving compared to the conventional model. Except of this the layout is the same as for the conventional Toyota Prius. Therefore the same operating strategies are possible (see Figure 118).

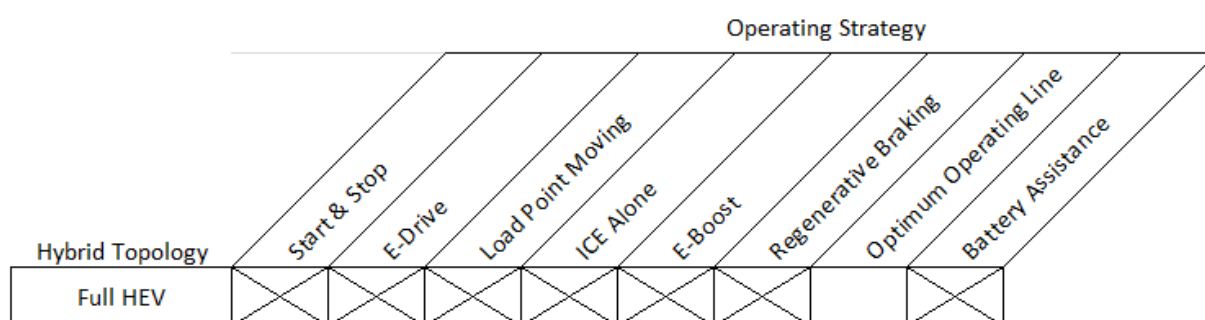


Figure 118: Hybrid Topology – Toyota Prius III Plugin

3.3.9.1. Measurements

A Toyota Plug-In Prius model 2010 vehicle was delivered by Toyota Motor Europe for testing at LAT. Different test cycles were performed on the vehicle at different battery state of charge levels. The measurement protocol that the vehicle has been tested on is shown in Figure 119

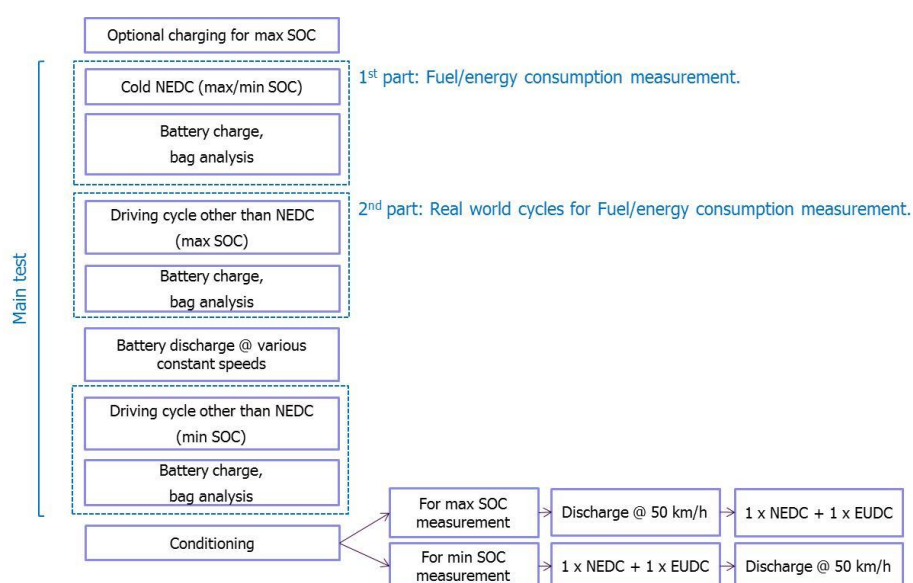


Figure 119: Schematic of the test protocol of the Toyota Prius III Plugin

Based on this measurement protocol, Figure 120 shows a measurement over 5 consecutive NEDC cycles. The green line shows the battery state of charge (SOC) and the purple line shows the CO₂ emissions of the vehicle. No emissions practically occur during the first two cycles as the vehicle is powered solely by electricity (with the exception of two instances of high speed driving). This phase is called the charge depleting mode. After this distance has been covered (vehicle electric distance), the vehicle shifts to the charge sustaining mode where its operation is similar to a normal full hybrid vehicle. Therefore, for plug-in hybrids, an additional component – this of the total distance driven – becomes relevant to the calculations.

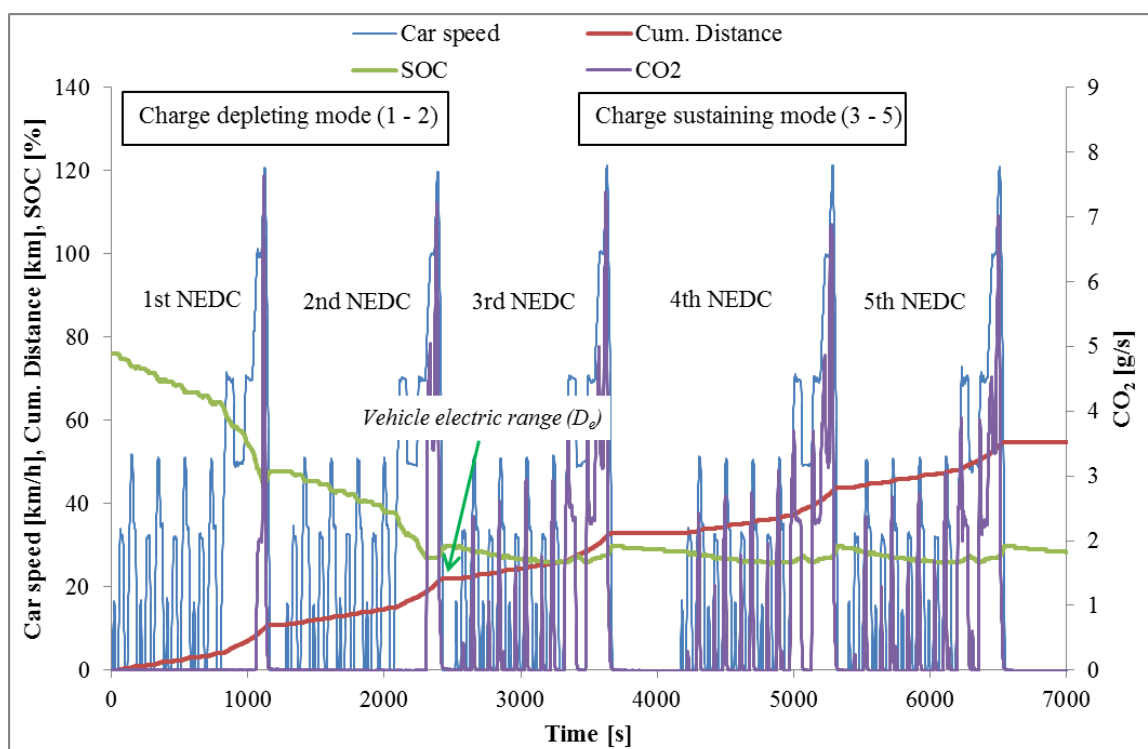


Figure 120: Schematic of the test protocol of the Toyota Prius III Plug-in

3.3.9.2. Simulation - AVL CRUISE Model Layout

The vehicle layout in CRUISE is shown in Figure 121. The model is based on the standard installation model of CRUISE which uses a simpler controller compared to the model of the standard Toyota Prius III as used for vehicle 7. The full model as shown in Figure 46 cannot be delivered outside of AVL due to confidentiality reasons. The layout of the main parts of the drivetrain (2 electric motors, 1 ICE) is the same as for the conventional Prius III model. However additional resistances as used in the conventional Prius III model (electrical resistance and mechanical resistance) are not considered for the plugin model.

The control of the hybrid system (activation of ICE and both electric machines) is defined in Matlab Simulink and is coupled to the CRUISE model. All characteristic maps, parameters, are directly included in the Matlab model. The control controls the activation of both electric motors and the ICE, in this way also controlling the transmission ratio between ICE and final

drive. The Matlab model is unmodified compared to the controller of the standard installation model.

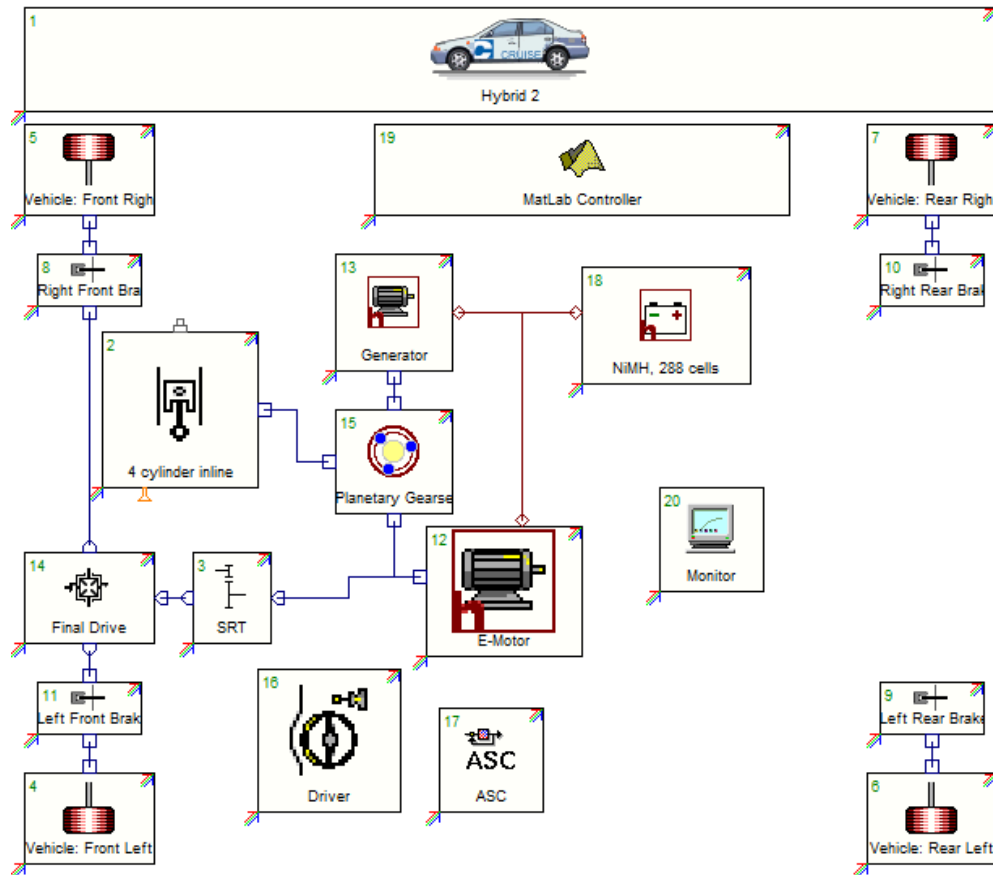


Figure 121: AVL CRUISE Model including Hybrid Control Logic of Toyota Prius III Plug-in

3.3.9.3. Simulation Input Data

Some of the main characteristic input data of the vehicle model is listed in Figure 122.

Engine	
Type	4 cylinder (in line), 4 stroke
Bore x Stroke	80.5 x 88.3 mm
Displacement	1.8 L
Max power output	73.1 kW @ 5200 rpm
Max torque output	142 Nm @ 4000 rpm
Inertia weight	1470 kg
Transmission	CVT
Electric motor	
Max power output	60 kW
Max torque output	207 Nm
Battery type	Lithium-ion
Battery capacity	5.2 Ah
Battery quantity	288 cells
Overall voltage	345.6 V

Figure 122: Simulation Input Data Toyota Prius III Plug-in

3.3.9.4. CRUISE Model Validation Results

Simulation-measurement comparison was carried out for different driving cycles (NEDC, WLTC, Artemis Urban, Artemis Road).

3.3.9.4.1. NEDC

Figure 123 shows the comparison for the fuel consumption in time domain for the NEDC cycle as well as the overall results.

It is visible that in some areas the simulation predicts that the ICE is running ($FC > 0$) while the measurements show that it is stopped ($FC=0$), e.g. in the area around 100s. In some other areas the situation is vice versa (between 200s and 600s). This shows that the control logic does not represent reality. However since there is no disclosure of Toyota about the real control logic, the reason for the difference remains unclear. The information available from the measurements about the electric system is too less to make a proper reverse engineering of the control logic. A reverse engineering of the control requires additional measurements about the electric flow between the components and signal information directly from the control unit and a significant number of measurements for different states of charge of the battery and different driving conditions, especially to determine the transition areas between the different operating strategies.

Despite the differences in the time traces the overall difference in fuel consumption is only 0.29 l/100km or 5.6%.

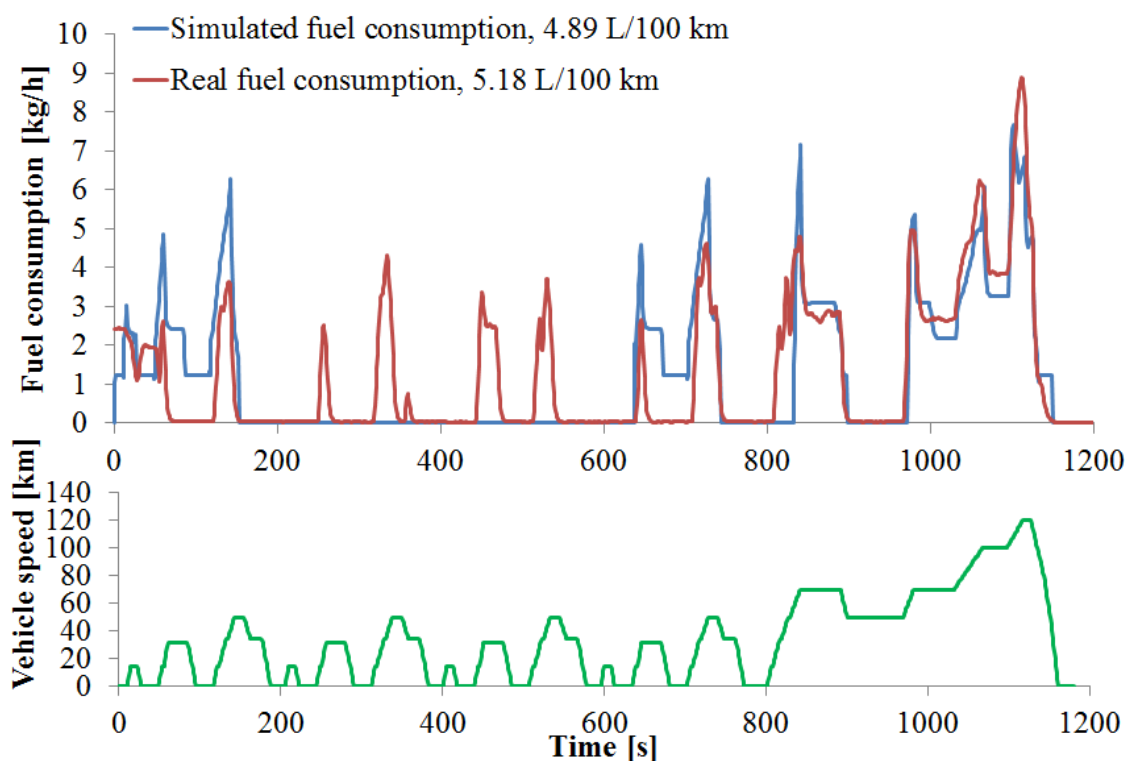


Figure 123: Simulation-Measurement Comparison Toyota Prius III Plugin - NEDC

3.3.9.4.2. WLTC

Figure 124 shows the comparison for the fuel consumption in time domain for the WLTC cycle as well as the overall results.

Similar differences as for the NEDC cycle can be observed in the areas 0-100s and 500-600s (engine running in simulation, while not running on the test bed). In general the agreement between simulation and measurement for the WLTC cycle is much better compared to the NEDC cycle. The difference in the overall fuel consumption is 0.02 l/100km or 0.4%.

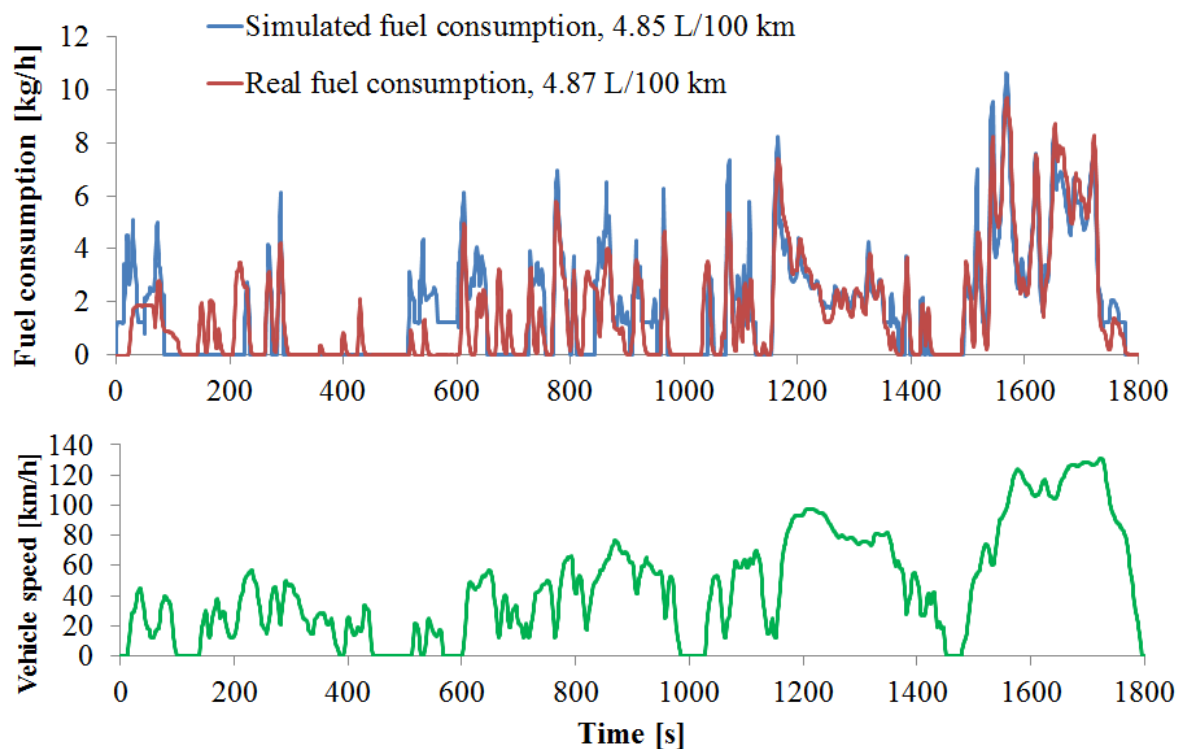


Figure 124: Simulation-Measurement Comparison Toyota Prius III Plugin - WLTC

3.3.9.4.3. Artemis Urban

Figure 125 shows the comparison for the fuel consumption in time domain for the Artemis Urban cycle as well as the overall results.

Main differences between simulation and measurement are visible in the time area 0-100s and 900-1000s. In these areas the fuel consumption in the simulation is mostly higher compared to the measurement indicating higher load on the engine. Some other areas (e.g. between 600s and 750s) show that the ICE is running during the measurements (indicated by $FC > 0$) while it remains stopped in the simulation (indicated by a $FC = 0$). The total fuel consumption in simulation is 0.42 l/100km or 6.1% smaller compared to the measurement.

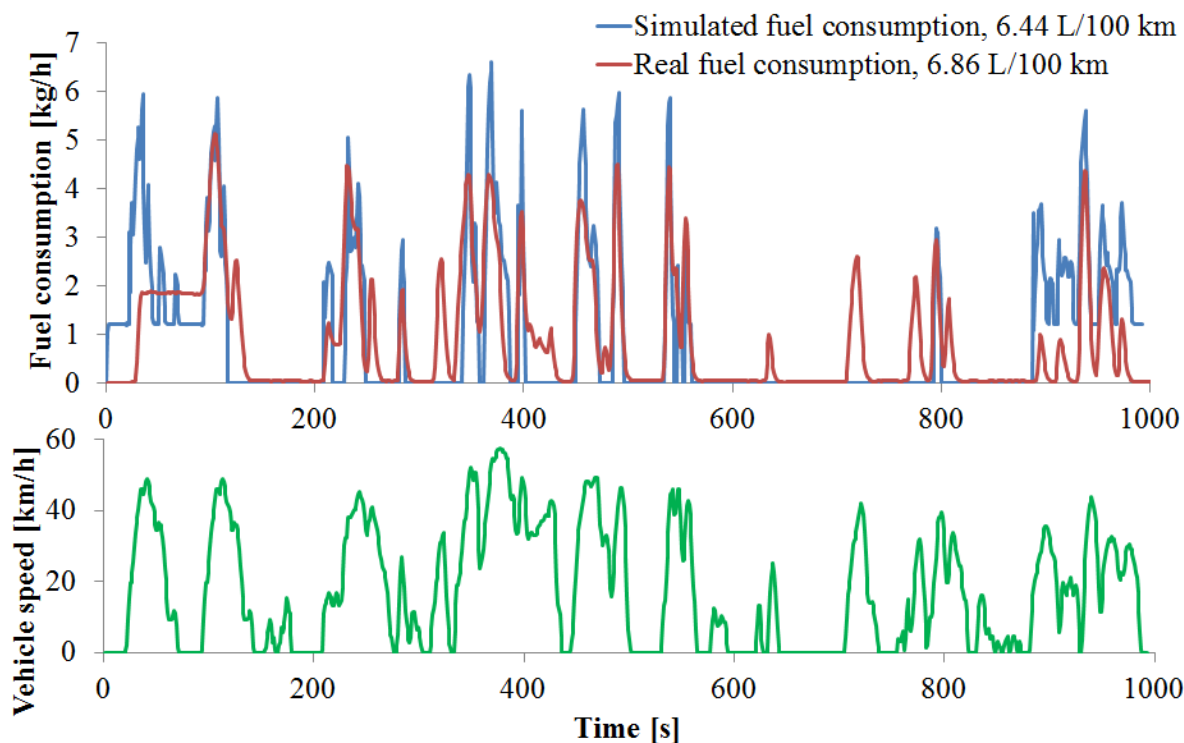


Figure 125: Simulation-Measurement Comparison Toyota Prius III Plugin – Artemis Urban

3.3.9.4.4. Artemis Road

Figure 126 shows the comparison for the fuel consumption in time domain for the Artemis Road cycle as well as the overall results.

In comparison to the Artemis Urban cycle the agreement between simulation and measurement is significantly better. Only in the initial phase (up to 100s) the simulation shows higher FC compared to the measurement. The total fuel consumption in simulation is 0.21 l/100km or 4.9% higher compared to the measurement.

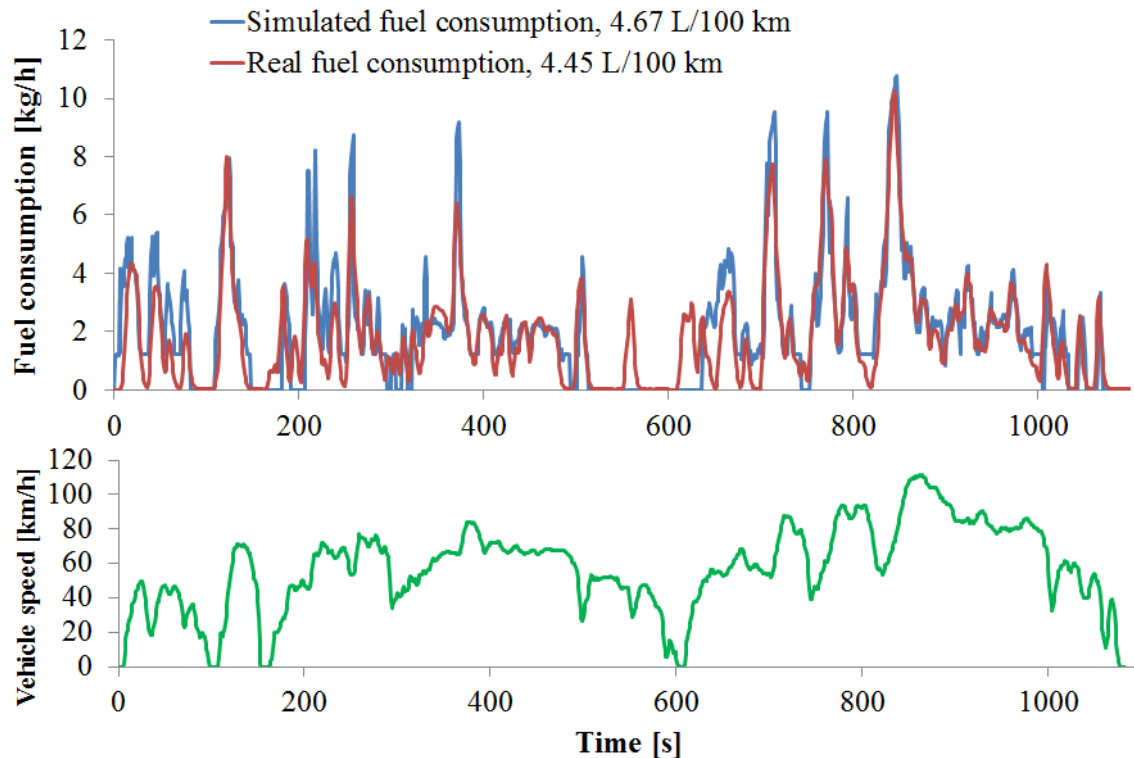


Figure 126: Simulation-Measurement Comparison Toyota Prius III Plugin – Artemis Road

3.3.9.4.5. Summary

Main differences between simulation and measurement are always visible at the start of the simulation (up to 100s). This may be caused by the fact that the initial state of charge of the battery is different, or that after starting the engine the real control has some lead time in which it reacts differently compared to the standard behavior. This effect is especially visible in the WLTC and the Artemis Urban cycles where in the measurement initially an area with constant fuel consumption can be observed. This indicates that there is an area where the ICE is probably running at constant speed/constant load condition.

The second visible difference is typically in areas with low power requirement of the vehicle (low speeds, low accelerations). During this areas the start and stop of the ICE is mainly controlled by the available battery charge.

The visible differences show the importance of having an accurate control model on accuracy of the simulation results. However the OEMs are typically not willing to disclose this know-how. Reverse engineering of the control is partly possible but requires significant effort on the measurement side which was not feasible in the project.

Figure 127 shows the summary of the total fuel consumption for all 4 compared driving cycles. Considering that because of lack of data the control is a very coarse one a maximum difference of 6% is acceptable.

			Measurement	Simulation	Difference to Measurements	
					Relative	Absolute
			l/100km	l/100km	%	l/100km
Toyota Prius III Plugin	Plugin HEV	NEDC	5.18	4.89	5.6%	-0.29
		WLTC	4.87	4.85	0.4%	-0.02
		Artemis Urban	6.86	6.44	6.1%	-0.42
		Artemis Road	4.45	4.67	4.9%	0.22

Figure 127: Validation Results Toyota Prius III Plugin

3.4. OVERALL PICTURE OF CHASSIS DYNAMOMETER VALIDATION RESULTS

The overall conclusion of the comparison between the simulated and the measured consumption over the chassis dyno is that the simulated models can on average satisfactorily approach the consumption over a complete driving cycle. The mean difference for all vehicles and driving cycles tested was -0.7% (simulated-measured) and the standard deviation of the difference was 3.8%. This narrow band shows good precision and an unbiased result. Of course, individual differences can be higher. The maximum difference for one vehicle over a single cycle has been 8.9%, however this was rather an outlier, as most of the differences were below 6%. Further improvement of the models is always possible, however perfectly matching the individual vehicles tested was never the intention. The intention of this task was to explore whether the micro simulation emission model selected has the potential to be used in the simulations with generic vehicle models and not to perfectly match specific vehicle models. The results obtained indicate that this is indeed the case, as in several vehicles and driving cycles, the model produces overall unbiased results.

The quality of the microsimulations also depend on how the model behaves on a second by second basis, as several of the microevents have an impact on the instantaneous consumption and emission levels. The graphs presented for the five vehicle models simulated show that the simulation closely follow the cycle speed pattern. Summarizing the results in single arithmetic values is more difficult for the thousand instantaneous values simulated. But some specific quality characteristics can be outlined:

- Engine shut off events were satisfactorily simulated for vehicle with start and stop systems, also including the PHEV. This shows that the operation algorithms can be satisfactorily approached.
- Gradients in fuel consumption during engine load and speed changes were also represented with good fidelity showing that the model adequately responds to changes in driving conditions.
- Overall levels during peaks and plateaus in fuel consumption were consistent between the measurements and the simulations. This shows that not only average, but also individual operation modes are precisely estimated.

These results show that the micro emission and consumption model is appropriate for use even in driving situations which are slightly differentiated, as may be the case with some of the ICT measures to be examined.

4 Model validation by real-world on-board measurements

4.1. INTRODUCTION

Real world on board measurements have been performed in Madrid, Turin and Rome in order to validate the simulated fuel consumption accuracy under daily routine conditions.

Investigation of these results is completed for all three city case studies. The analysis of the results is presented below.

4.1.1. VEHICLES

Two petrol (FIAT Punto 1.2) and one diesel (FIAT Punto 1.3) vehicles were used for the real world measurements. Their specifications, provided by CRF and implemented in CRUISE, are shown in Table 12 and Table 13. The same diesel vehicle was used in Madrid and Rome, while the petrol vehicle used in Madrid was different than the one used in Turin as regards the transmission system and the engine map. The average difference in terms of fuel consumption between these two petrol models was found to be approximately 23%, when comparing the derived simulations with respective measurements. The biggest part of the discrepancy was found to be attributed to the different engine map that has been used. Also, minor deviations, in these two cases, can be explained from not using the exact weight of the vehicles, from deviations in the rolling resistance, from data acquisition errors etc. Therefore, in addition to the transmission system, we modified the delivered engine map so the gap of the 23% was eliminated.

Table 12: FIAT Punto 1.2 gasoline specifications.

Component	Data	Value
Vehicle	Wheel Base [m]	2.5
	Weight [kg]	1086
	Frontal Area [m ² , drag coefficient]	2.06, 0.39
Engine	Inertia [kg*m ²]	0.19
	Displacement [L]	1.242
	Cyl Nr	4
	Maximum Speed	From full load curve
	Idle Speed	From full load curve
	Fuel Type	Gasoline
	Fuel Consumption Map, Full Load Curve	Analytical
Transmission	Transmission Ratios (Madrid)	1st: 3.91, 2nd: 2.16, 3rd: 1.48, 4th: 1.12, 5th: 0.9
	Transmission Ratios (Turin)	1st: 3.909, 2nd: 2.158, 3rd: 1.345, 4th: 0.974, 5th: 0.829
	Efficiency or Torque Loss	Global trasmission efficiency: 0.93
Final Drive	Transmission Ratio or Nr of Teeth	3.44
Wheels	Inertia [kg*m ²]	0.9
	Dynamic Radius [mm]	283
	Rolling Resistance Function [kg/ton]	10.7

Table 13: FIAT Punto 1.3 diesel specifications.

Component	Data	Value
Vehicle	Wheel Base [m]	2.5
	Weight [kg]	1090
	Frontal Area [m ² , drag coefficient]	2.14, 0.35
Engine	Inertia [kg*m ²]	0.16
	Displacement [L]	1.3
	Cyl Nr	4
	Maximum Speed	From full load curve
	Idle Speed	From full load curve
	Fuel Type	Diesel
	Fuel Consumption Map, Full Load Curve	Analytical
Transmission	Transmission Ratios or Nr of Teeth	1st: 3.909, 2nd: 2.238, 3rd: 1.444, 4th: 1.029, 5th: 0.767
	Efficiency or Torque Loss	Global trasmission efficiency: 0.93
Final Drive	Transmission Ratio or Nr of Teeth	3.563
Wheels	Inertia [kg*m ²]	0.77
	Dynamic Radius [mm]	296
	Rolling Resistance Function [kg/ton]	$8.8 + 0.00031 \cdot V^2$

4.1.2. MEASUREMENT LOCATIONS

Measurements have been conducted in Madrid during both periods foreseen for the second survey (2 weeks in March and 2 in April 2013). Specifically the route considered was the section “Arroyofresno - San Pol de Mar” in the west section of the ring road M-30 equipped with variable speed control limits ICT systems.

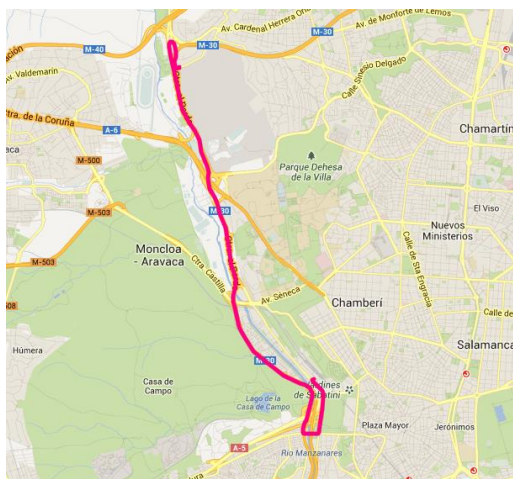
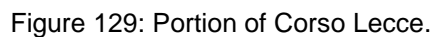


Figure 128: Madrid section and VMS panel.

As regards the Turin measurements, the section which fulfilled the same criteria as in Madrid was Corso Lecce between the intersection with Corso Regina Margherita and the intersection with Via Lera (total length about 1700 m, Figure 129).



For each vehicle, the trips were filtered rejecting missions with erroneous values. After this first filter, the final selection was based on different levels of service, ranging from free flow to congested and including trips with the variable speed limits activated.

Each floating car was equipped with an OBDKey device provided by CRF, which allows to measure speed and fuel consumption retrieving these values from the internal CAN bus and sending them to an Android based smartphone. The measurements were therefore available as csv files easily transferable to a PC for further processing.

- Data and time
- Latitude
- Longitude

- Altitude
- Number of satellites
- Speed
- Engine revolution
- Fuel consumption

4.3. RESULTS AND DISCUSSION

The simulation results are reported in Figure 130.

Location	Trip log	Vehicle type	Simulated FC [l/100 km]
Madrid	130304181441	Diesel	4.1
Madrid	130312182257	Diesel	4.6
Madrid	130313104802	Diesel	3.9
Madrid	130408181750	Diesel	4.2
Madrid	130411183847	Diesel	4.1
Madrid	130301140551	Petrol	4.9
Madrid	130305182847	Petrol	4.6
Madrid	130313095737	Petrol	4.9
Madrid	130408183658	Petrol	4.9
Madrid	130416180828	Petrol	4.9
Rome	130410074158	Diesel	5.6
Rome	130410130808	Diesel	4.5
Rome	130411123230	Diesel	3.9
Rome	130411085334	Diesel	4.8
Rome	130411074441	Diesel	5.1
Turin	121106110606	Petrol	8.1
Turin	121106110606	Petrol	9.3
Turin	121115115807	Petrol	8.8
Turin	121107110628	Petrol	9.0
Turin	121107110628	Petrol	9.3

Figure 130: Simulated fuel consumption.

In last column, the results obtained by the refined data input (called ‘physical’ data) are reported. Overall the fuel consumption provided by the simulations is in line with the expectations, considering the supplied vehicle data. In Figure 131, the overall percentage difference (simulation vs. collected data) is also reported. The considered simulations are the ones obtained by AVL Cruise fed with ‘physical data’. Negative values represent simulations the consumptions of which are lower than real ones. Both simulated vehicles (gasoline/diesel) are charted together.

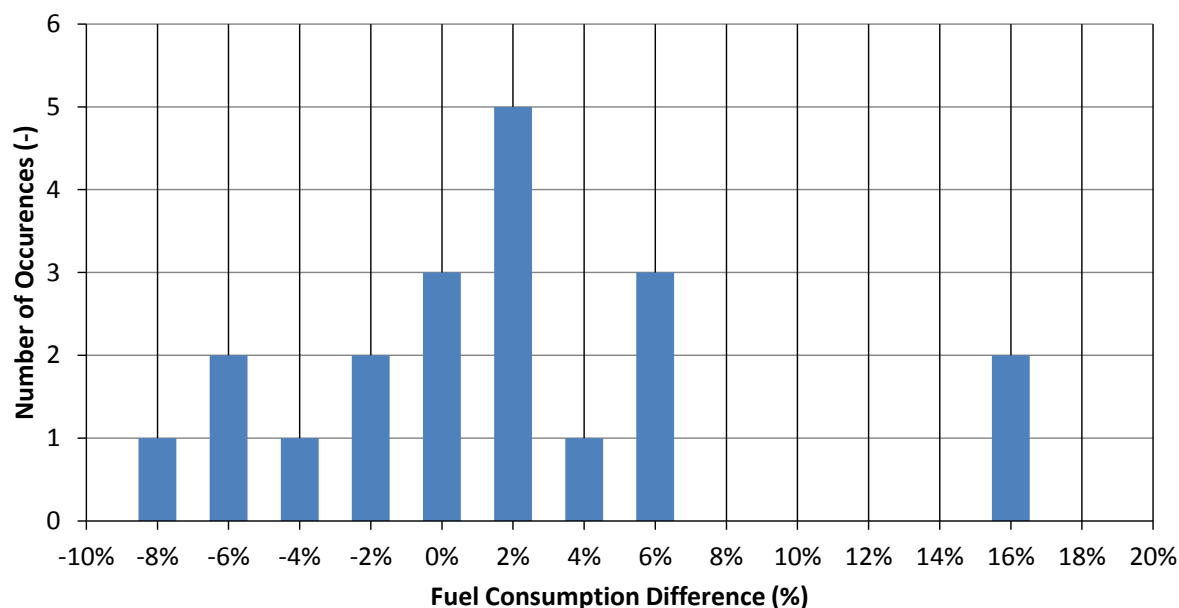


Figure 131: Histogram of the fuel consumption difference between measured and simulated results.

The obtained accuracy from all trips is within $\pm 5\%$ difference, at 75% confidence level as Figure 132 shows (the box and whiskers chart difference is shown for all trips). These results are in line with the expectations considering:

- the CAN-B “fuel consumption” collected on the cars used in the test site;
- the ‘general purpose’ nature of the data used to feed the Cruise model.

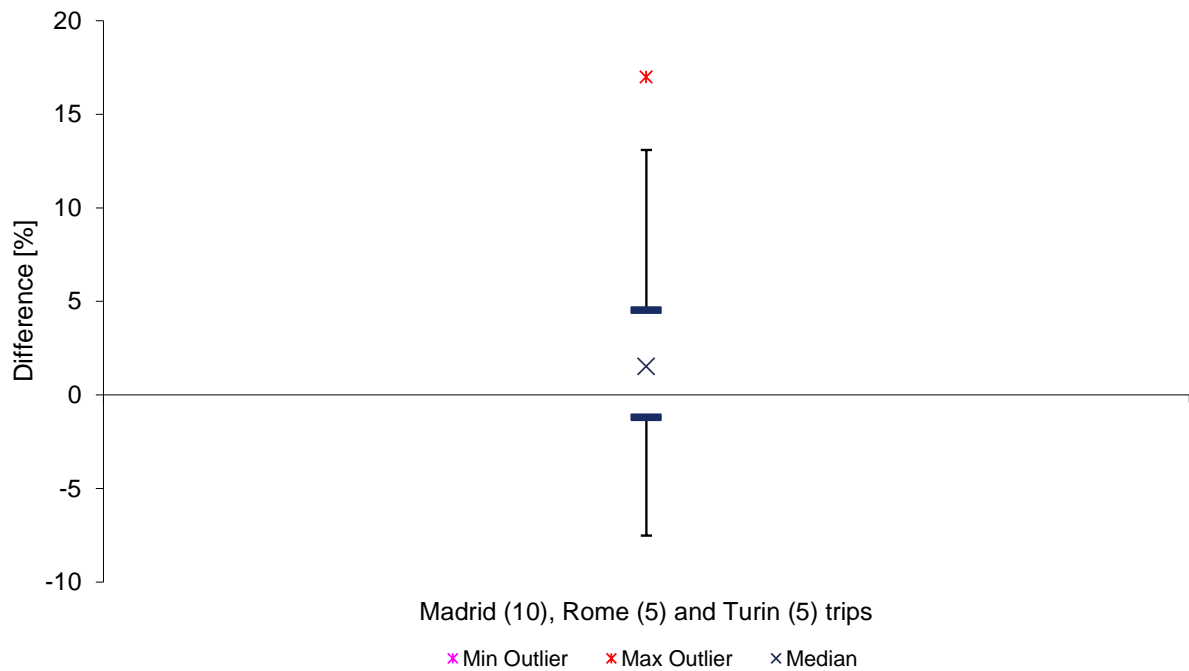


Figure 132: Box and whiskers plot for the measured-simulated difference of Madrid, Rome and Turin trips. The bold blue horizontal lines indicate the 75% confidence level, while the smaller blue horizontal lines indicate the 99% confidence level.

References

1. Mellios, G., Hausberger, S, Keller, M., Samaras, C., Ntziachristos, L., Dilara, P., Fontaras, G. 2011 Parameterisation of fuel consumption and CO2 emissions of passenger cars and light commercial vehicles for modelling purposes, European Commission, Joint Research Centre, Institute for Energy and Transport, JRC 66088, doi :10.2788/58009.
2. European Environment Agency, 2013. Monitoring CO2 emissions from new passenger cars in the EU: summary of data for 2012, Copenhagen, Denmark.
3. Mock, P., German, J., Bandivadekar, A., Riemersma, I., 2012. Discrepancies between typw-approval and « real-world » fuel-consumption and CO2 values. ICCT Working paper 2012-02, Washington, Berlin, San Francisco.
4. Smit, R., Ntziachristos, L., Boulter, P. 2010. Validation of road vehicle and traffic emission models – A review. Atmospheric Environment, 44, 2943–2953.

Abbreviations

Abbreviation	Explanation
AER	All Electric Range
AMT	Automated Manual Transmission
AT	Automatic Transmission
AWD	All Wheel Driven
CVT	Continuously Variable Transmission
DCT	Double Clutch Transmission
EV	Electric Vehicle
FWD	Front Wheel Driven
HEV	Hybrid Electric Vehicle
ICE	Internal Combustion Engine
LPM	Load Point Moving
REX	Range Extender
RWD	Rear Wheel Driven
SOC	State of Charge